

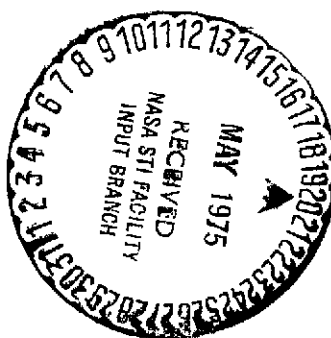
(NASA-CR-142703) THE DYNAMICS OF SPIN
STABILIZED SPACECRAFT WITH MOVABLE
APPENDAGES, PART 1 Final Report (Howard
Univ.) 121 p HC \$5.25

CSSL 22B

N75-22367

Unclas
20362

G3/18



N 75 22367

HOWARD UNIVERSITY
SCHOOL OF ENGINEERING
DEPARTMENT OF MECHANICAL ENGINEERING
WASHINGTON, D.C. 20059

FINAL REPORT

NASA GRANT: NGR-09-011-053 (Supplement No. 1)

THE DYNAMICS OF SPIN STABILIZED SPACECRAFT WITH
MOVABLE APPENDAGES

(PART I)

by

Peter M. Bainum
Professor of Aerospace Engineering
Principal Investigator

and

R. Sellappan
Graduate Research Assistant

May 1975

REPRODUCED BY
NATIONAL TECHNICAL
INFORMATION SERVICE
U.S. DEPARTMENT OF COMMERCE
SPRINGFIELD, VA. 22161

ABSTRACT

The motion and stability of spin stabilized spacecraft with movable external appendages are treated both analytically and numerically. The two basic types of appendages considered are: (1) a telescoping type of varying length and (2) a hinged type of fixed length whose orientation with respect to the main part of the spacecraft can vary. Two classes of telescoping appendages are considered: (a) where an end mass is mounted at the end of an (assumed) massless boom; and (b) where the appendage is assumed to consist of a uniformly distributed homogeneous mass throughout its length.

For the telescoping system Eulerian equations of motion are developed. During all deployment sequences it is assumed that the transverse component of angular momentum is much smaller than the component along the major spin axis. Closed form analytical solutions for the time response of the transverse components of angular velocities are obtained when the spacecraft hub has a nearly spherical mass distribution. For the more general case, a series solution is obtained and this solution is limited by its radius of convergence. The comparison of the different approximate analytical methods with numerical integration results are studied and it is observed that the oscillatory nature of the responses of the transverse angular velocity components reduces rapidly with faster extension rates.

As an application for spacecraft rescue and recovery, booms are extended along all principal axes to (a) detumble a symmetrical

spacecraft, and (b) achieve a desired final spin about one of the principal axes. From an application of Lyapunov's second method boom extension maneuvers can be determined. Numerical examination of detumbling for asymmetrical hubs also is considered. The use of telescoping systems for detumbling a randomly spinning spacecraft to achieve a desired final state in a time optimal manner is studied and it is found that simple boom extension maneuvers alone can not be used to achieve the desired state in minimum time.

The equations of motion for the hinged system are developed using the Quasi-Lagrangian and the general Lagrangian formulation. In this formulation there is no restriction on the location of the hinge points.

TABLE OF CONTENTS

	PAGE
ABSTRACT	ii
NOMENCLATURE	vi
LIST OF ILLUSTRATIONS	ix
 I. INTRODUCTION	 1
II. MOTION DURING DEPLOYMENT OF TELESCOPING SYSTEM	5
1. General Considerations	5
2. End Mass Moving	7
a. Analytical Solution for Asymmetrical Deployment	7
b. Series Solution	13
c. Numerical Results	17
3. Uniformly Distributed Mass Moving	20
a. Analytical Solution for Asymmetrical Deployment	20
b. Numerical Results	24
III. USE OF TELESCOPING SYSTEM FOR DETUMBLING	38
1. General Considerations	38
2. End Mass Moving	38
a. Development of Kinetic Energy	38
b. Achieve Zero Inertial Angular Rate	39
1. Lyapunov Function-Kinetic Energy	39
2. Analytical Solution	41
3. Numerical Results	43

TABLE OF CONTENTS

	PAGE
c. Achieve Final Spin About One of the Principal Axes	44
1. Lyapunov Function-Modified Kinetic Energy ..	44
2. Analytical Solution	46
3. Numerical Results	48
3. Uniformly Distributed Mass Moving	50
a. Achieve Zero Inertial Angular Rate	50
1. Analytical Solution	50
b. Achieve Final Spin About One of the Principal Axes	51
1. Analytical Solution	51
IV. TIME OPTIMAL CONTROL	67
1. Combination of Booms and Control Jets (Norm Invariant Principle).....	67
2. Extension of End Masses	70
V. HINGED SYSTEM	75
1. Derivation of Kinetic Energy	75
2. Development of Equations of Motion	79
3. Numerical Results	82
VI. CONCLUDING COMMENTS	85
VIII. FUTURE WORK - PART II	88
TABLE I - TWO YEAR PLAN OF STUDY	92
REFERENCES	94
COMPUTER PROGRAMS	96

NOMENCLATURE

a_x	=	offset of hinge point(s) from the '2' axis
$a_1(t), a_2(t)$	=	time varying coefficients in the approximate equations for h_1, h_2
a_n	=	coefficients in the series solution for $h_1(t)$
$b(t)$	=	for deployment when '3' axis is a symmetry axis, $b(t) = a_1(t) = a_2(t)$
b_n	=	coefficients in the series solution for $h_2(t)$
C, D, E, F	=	constants appearing in the approximate analytical solutions for h_1, h_2 for the case of a nearly spherical hub
c	=	boom extension rate
h_1, h_2, h_3	=	components of the angular momentum vector along the principal axes
h_0	=	assumed constant value of h_3 during nominal deployment maneuver
I_1, I_2, I_3	=	instantaneous values of principal moments of inertia
I_1^*, I_2^*, I_3^*	=	hub principal moments of inertia
$\bar{I}_1^*, \bar{I}_2^*, \bar{I}_3^*$	=	moments of inertia at the switching time T_{3f} in the recovery sequence to achieve final spin about the '3' axis
J	=	$\int_0^{T_f} dt = T_f$, cost functional for time optimal control
K	=	$2\rho c^3$
ℓ	=	constant length of hinged appendages
$\ell(t)$	=	time varying length of telescopic appendages
M	=	mass of the main part of the spacecraft
m	=	boom end mass

m^*	=	constraint on the control vector such that, $ \bar{u} \leq m^*$
P	=	$2 mc^2$
R_1, R_2	=	Constants appearing in the solutions for $\omega_1(t)$ for the asymmetrical deployment of booms with uniformly distributed mass
r_0	=	offset of the hinge point(s) from the '3' axis
t	=	time
T	=	kinetic energy
T_{3f}	=	switching time in the recovery sequence to achieve final spin about the '3' axis
$\bar{u}(t)$	=	control vector
V	=	Lyapunov function
\bar{V}_i	=	inertial velocity of the i^{th} mass of the (hinged) system
\bar{V}_M/cm	=	velocity of the main part of the spacecraft with respect to the system center of mass
\bar{V}_M/o	=	velocity of the main part of the spacecraft with respect to the center of the coordinate system (o)
$\bar{V}_{mi}/o = \dot{\bar{r}}_i$	=	velocity of the i^{th} mass in the system with respect to the center of the coordinate system
\bar{V}_o/cm	=	velocity of point 'o' with respect to the system center of mass
$\bar{X}(t)$	=	State vector
$\bar{X}^*(t)$	=	solution of controllable norm-invariant system under unique time optimal control $\bar{u}^*(t)$
α_1, α_2	=	coordinates describing the orientation of the hinged appendages relative to the hub

ω_0	= constant value of ω_3 when two pairs of booms are extended (symmetrically) parallel to the '3' axis
$\omega_1, \omega_2, \omega_3$	= angular velocity components along the principal axis
Ω	= desired final value of ω_3 (ω_{3f})
ρ	= mass density per unit boom length
ψ_0^*, ψ_0	= phase angles appearing in the solutions for $\omega_1(t)$, $\omega_2(t)$ and determined from conditions at $t = 0$, $t = T_{3f}$, respectively
τ	= $\int b(t)dt$
$\tau_i(t)$	= elements of control torque vector \bar{u}
$\dot{}$	= indicates time differentiation
(0)	= indicates initial conditions
$ $	= indicates norm of a vector quantity

LIST OF ILLUSTRATIONS

FIGURE		PAGE
2.1.	TWO TYPES OF TELESCOPING APPENDAGES	26
2.2.	COMPARISON OF ANALYTICAL, NUMERICAL INTEGRATION AND SERIES SOLUTION RESULTS FOR A NEARLY SPHERICAL HUB WITH EXTENSION RATE $c = 4$ ft/sec. (END MASS MOVING).....	27
2.3.	COMPARISON OF ANALYTICAL, NUMERICAL INTEGRATION AND SERIES SOLUTION RESULTS FOR A NEARLY SPEHRICAL HUB WITH EXTENSION RATE $c = 1$ ft/sec. (END MASS MOVING)	28
2.4.	COMPARISON OF ANALYTICAL AND NUMERICAL INTEGRATION RESULTS FOR A SPEHRICAL HUB WITH EXTENSION RATE $c = 1$ ft/sec. (END MASS MOVING)	29
2.5.	COMPARISON OF ANALYTICAL AND NUMERICAL INTEGRATION RESULTS FOR A NEARLY SPHERICAL HUB WITH EXTENSION RATE $c = 1$ ft/sec. WITH THE INITIAL CONDITIONS DIFFERENT FROM FIG. 2.3 (END MASS MOVING)	30
2.6.	EFFECT OF VARIATION OF I_3^* FOR FIXED INITIAL CONDITIONS WITH EXTENSION RATE $c = 1$ ft/sec. (END MASS MOVING) - NUMERICAL INTEGRATION	31
2.7.	EFFECT OF VARYING END MASS FOR FIXED INITIAL CONDITIONS WITH EXTENSION RATE $c = 1$ ft/sec. (END MASS MOVING) - NUMERICAL INTEGRATION	33
2.8.	COMPARISON OF ANALYTICAL AND NUMERICAL INTEGRATION RESULTS WITH EXTENSION RATE $c = 4$ ft/sec. (UNIFORMLY DISTRIBUTED MASS MOVING)	34
2.9.	COMPARISON OF ANALYTICAL AND NUMERICAL INTEGRATION RESULTS WITH EXTENSION RATE $c = 1$ ft/sec. (UNIFORMLY DISTRIBUTED MASS MOVING)	35
2.10.	COMPARISON OF BOTH TYPES OF TELESCOPING SYSTEMS WITH EXTENSION RATE $c = 1$ ft/sec. - NUMERICAL INTEGRATION	36
3.1.	SYSTEM GEOMETRY FOR END MASS EXTENSION MANEUVER USED TO RECOVER A TUMBLING SPACECRAFT.....	53

LIST OF ILLUSTRATIONS

FIGURE		PAGE
3.2.	DYNAMICS OF UNCONTROLLED MOTION-SLOW TUMBLING	54
3.3.	RECOVERY DYNAMICS FOR INITIAL SLOW TUMBLING WITH EXTENSION RATE $c_j = 4$ ft/sec.	55
3.4.	DYNAMICS OF UNCONTROLLED MOTION-FAST TUMBLING.....	56
3.5.	RECOVERY DYNAMICS FOR INITIAL FAST TUMBLING WITH EXTENSION RATE $c_j = 4$ ft/sec.....	57
3.6.	EFFECT OF BOOM EXTENSION RATE ON RECOVERY (INITIAL FAST TUMBLING).....	58
3.7.	COMPARISON OF RECOVERY DYNAMICS OF ASYMMETRICAL SPACECRAFT WITH SYMMETRICAL SPACECRAFT (EXTENSION RATE $c_j = 4$ ft/sec).....	61
3.8.	RECOVERY MANEUVER TO ACHIEVE FINAL SPIN ALONG '3' AXIS WITH EXTENSION RATE $c_j = 4$ ft/sec.....	63
3.9.	RECOVERY MANEUVER TO ACHIEVE FINAL SPIN ALONG '3' AXIS WITH EXTENSION RATE $c_j = 1$ ft/sec.....	64
3.10.	COMPARISON OF RECOVERY MANEUVER OF ASYMMETRICAL SPACECRAFT WITH SYMMETRICAL SPACECRAFT TO ACHIEVE FINAL SPIN ALONG '3' AXIS (EXTENSION RATE $c_j = 4$ ft/sec).....	65
4.1.	EXTENSION OF END MASSES ALONG '3' AXIS.....	74
5.1.	HINGED DEPLOYMENT SYSTEM.....	83
5.2.	COORDINATE SYSTEM FOR FIG. 5.1.....	83
5.3.	MORE GENERAL CASE OF HINGED DEPLOYMENT SYSTEM.....	84

I. INTRODUCTION

A number of spin stabilized spacecraft have long appendages which nominally lie in the plane of rotation perpendicular to the desired spin axis. These appendages might be on-board antennas which must be extended in orbit after the initial injection sequence. The extension of on-board antenna booms is usually done with the use of motors located in the central hub of the spacecraft. The dynamical aspects of such spacecraft have been discussed in the recent literature.¹

Of special interest is the stability of the system during the initial extension of boom-type telescoping appendages. An early investigation considers this problem for the case of telescoping type appendages consisting of two end masses at the ends of massless rods.² It is assumed that the extension maneuver is restricted to a plane which is perpendicular to the nominal spin axis and that both the system angular momentum and kinetic energy are conserved during this maneuver. In addition the transverse components of angular velocities are assumed to be zero during extension. Under these assumptions it is seen that the resulting Lagrange equations of motion will yield an approximate analytical solution for limiting values of initial to final moment of inertia ratios.² A more recent treatment using an Eulerian formulation considers the extension of rigid booms where the transverse component of angular momentum remains less than the polar component throughout extension. For the special case where the spin axis is an axis of symmetry the linearized equations can be solved

analytically.³ A similar approximate solution has also been obtained previously under the same type of assumptions.⁴

The first phase of the current study will examine the three dimensional motion of a general spinning spacecraft system with movable telescoping appendages during the initial deployment maneuver. During all initial (nominal) deployment sequences, in accordance with actual practice, it will be assumed that the transverse component of angular momentum is much smaller than the component along the major spin axis. The dynamics of such a system will be studied using a variety of analytical techniques for special cases and numerical methods for the general case.

It is thought that by using movable and/or extendible booms the recovery of a tumbling spacecraft by passive means may be feasible. Methods of recovering spinning satellites to a flat-spin condition using spin-up thrusters and multiple combinations of thrusters were examined in a recent paper.⁵ It was concluded that the use of such thrusters for the recovery operation are often limited by the weight and propellant capacity of the thruster system, and also the reliability problems associated with multiple thrusters in sequence. Kaplan describes an alternate recovery system which utilizes a movable-mass control device that is internal to the spacecraft and can move along a fixed direction track.⁶ This device is activated upon initiation of tumble and is programmed via a control law to quickly stabilize⁷ motion about the major principal axis. In a recent related paper⁷ it

was concluded that the mass track should be placed as far as possible from the vehicle center of mass and be oriented parallel to the maximum inertia axis; in addition the performance of the control system can be improved through larger mass amplitudes along the track and also larger mass sizes.

It is apparent that the location and displacement amplitude of any internal control mass will be limited by the physical dimensions of the space vehicle. Externally movable appendages could allow for a greater range of location and displacement amplitudes of such a system; however, as the size of the appendages increases the flexibility problems associated with such structures would have to be considered.

Of interest in this study will be the consideration of the detumbling dynamics of a spacecraft system with extensible boom-type appendages along the principal axes. The recovery maneuver from an initial tumble is designed to reach either of two final states: (1) close to a zero inertial angular velocity vector and (2) to approximate a final spin about a principal axis. (It is thought that small terminal residual angular rates could then be removed by temporarily activating on-board damping systems). A key advantage of this type of system would be its potential reuse for subsequent detumbling recovery operations as the need arises.

For the case of time optimal three-axis control of the nonlinear norm invariant system it is an established fact that the control

torques about each axis must be proportional to the instantaneous angular momentum components about each axis, respectively;^{8,9} it is doubtful that such a time-optimal control torque could be generated only by boom extension techniques. However it may be possible to consider a combination of movable end masses and optimal control jets for three-axis control of a tumbling spacecraft. In the event of jet failure the movable end masses could certainly be used as a back-up re-usable system for detumbling (even if they cannot effect time-optimal recovery).

Other types of spacecraft employ fixed length appendages (hinged systems) whose orientation relative to the main spacecraft is changed during the deployment maneuver. The dynamics of this type of fixed length appendages during the deployment maneuver with rigid appendages have been studied only for the case where the transverse components of the angular velocity vector are assumed to be zero throughout deployment² and where the hinge points are located on the hub's principal transverse axes.² The general three dimensional deployment dynamics of such a hinged system will be considered here without any restriction on the location of the hinge points.

II. MOTION DURING DEPLOYMENT OF TELESCOPING SYSTEM

1. General Considerations

The motion and stability of spin stabilized spacecraft with telescoping appendages are studied both analytically and numerically. The telescoping appendages considered here are of varying length and could represent extensible antennas or a tether connected to the main part of spacecraft. Two types of telescoping appendages are considered (Fig. 2.1): (a) the case where an end mass is mounted at the end of an (assumed) massless boom (end mass moving) and (b) where the appendage is assumed to consist of a uniformly distributed, homogeneous mass throughout its length (uniformly distributed mass moving).

The torque free equations for a spacecraft with varying moments of inertia are:

$$\begin{aligned}\dot{h}_1 &= \omega_3 h_2 - \omega_2 h_3 \\ \dot{h}_2 &= \omega_1 h_3 - \omega_3 h_1 \\ \dot{h}_3 &= \omega_2 h_1 - \omega_1 h_2\end{aligned}\tag{2.1}$$

$$\text{where } h_i(t) = I_i(t) \omega_i(t)\tag{2.2}$$

Making the approximation:

$$|h_1|, |h_2| \ll |h_3|$$

$$\text{and } h_3 = h_0 = \text{const.}$$

the equations for h_1 and h_2 become

$$\dot{h}_1 = -a_2(t) h_2 \quad (2.3)$$

$$\dot{h}_2 = a_1(t) h_1 \quad (2.4)$$

Here $a_1(t)$ and $a_2(t)$ are defined as:

$$a_1(t) = \frac{(I_3(t) - I_1(t))}{I_3(t) I_1(t)} h_0 \quad (2.5)$$

$$a_2(t) = \frac{(I_3(t) - I_2(t))}{I_3(t) I_2(t)} h_0 \quad (2.6)$$

As a special case when the spin axis is an axis of symmetry ($a_1(t) = a_2(t) = b(t)$) during deployment, Eqs. (2.3) and (2.4) become:

$$\dot{h}_1 + b(t) h_2 = 0 \quad (2.7)$$

$$\dot{h}_2 - b(t) h_1 = 0 \quad (2.8)$$

Introducing $\tau = \int b(t) dt$ the above equations reduce to,

$$\frac{dh_1}{d\tau} + h_2 = 0 \quad (2.9)$$

$$\frac{dh_2}{d\tau} - h_1 = 0 \quad (2.10)$$

The solutions to Eqs. (2.9) and (2.10) can be written as

$$h_1(t) = q_0^* \cos \tau = q_0^* \cos \left(\int_0^t b(t) dt + \psi_0^* \right) \quad (2.11)$$

$$h_2(t) = q_0^* \sin \tau = q_0^* \sin \left(\int_0^t b(t) dt + \psi_0^* \right) \quad (2.12)$$

The solutions given by Eqs. (2.11) and (2.12) are identical with those given in Ref. 3.

For the general case where there is no axis of symmetry during deployment the following approach is taken. Differentiating Eq. (2.3) with respect to time and using Eq. (2.4), the resulting equation for h_1 is:

$$\ddot{h}_1 - \frac{\dot{a}_2(t)}{a_2(t)} \dot{h}_1 + a_1(t) a_2(t) h_1 = 0 \quad (2.13)$$

Similarly the equation for h_2 results as:

$$\ddot{h}_2 - \frac{\dot{a}_1(t)}{a_1(t)} \dot{h}_2 + a_1(t) a_2(t) h_2 = 0 \quad (2.14)$$

Eqs. (2.13) and (2.14) will be extensively used in the following sections.

2. End Mass Moving

a. Analytical Solution for Asymmetrical Deployment

The telescoping system, where the end masses are attached at the end of massless rods along the '2' axis, is shown in Fig. 2.1(a). The extension of the masses is assumed to originate from the center

of the spacecraft hub. The moments of inertia about the three principal axes during the extension are

$$\begin{aligned} I_1 &= I_1^* + 2m\ell^2 \\ I_2 &= I_2^* \\ I_3 &= I_3^* + 2m\ell^2 \end{aligned} \quad (2.15)$$

For a uniform extension rate, $\ell = ct$, and introducing $P = 2mc^2$ Eqs. (2.15) become:

$$\begin{aligned} I_1 &= I_1^* + Pt^2 \\ I_2 &= I_2^* \\ I_3 &= I_3^* + Pt^2 \end{aligned} \quad (2.16)$$

From Eq. (2.6)

$$\frac{\dot{a}_2(t)}{a_2(t)} = \frac{I_2^2 \dot{I}_3 - I_3^2 \dot{I}_2}{I_3 I_2 (I_3 - I_2)} \quad (2.17)$$

Using Eqs. (2.16) and their derivatives, Eq. (2.17) can be written as:

$$\frac{\dot{a}_2(t)}{a_2(t)} = \frac{2I_2^* Pt}{(I_3^* + Pt^2)(I_3^* - I_2^* + Pt^2)} \quad (2.18)$$

From Eqs. (2.5) and (2.6) with Eq. (2.17), $a_1(t)$ $a_2(t)$ is obtained as:

$$a_1(t) a_2(t) = \frac{(I_3 - I_1)(I_3 - I_2)}{I_3^2 I_1 I_2} h_0^2 \quad (2.19)$$

$$= \frac{(I_3^* - I_1^*)(I_3^* + Pt^2 - I_2^*)}{(I_3^* + Pt^2)^2 (I_1^* + Pt^2) I_2^*} h_0^2 \quad (2.20)$$

Eqs. (2.18) and (2.20) are used in Eq. (2.13) to obtain the following second order ordinary differential equation for h_1 :

$$\ddot{h}_1 - \frac{2I_2^* Pt \dot{h}_1}{(I_3^* + Pt^2)(I_3^* + I_2^* + Pt^2)} + \frac{(I_3^* - I_1^*)(I_3^* - I_2^* + Pt^2) h_0^2 h_1}{(I_3^* + Pt^2)^2 (I_1^* + Pt^2) I_2^*} = 0 \quad (2.21)$$

From Eq. (2.5),

$$\frac{\dot{a}_1(t)}{a_1(t)} = \frac{I_1^2 \dot{I}_3 - I_3^2 \dot{I}_1}{I_3 I_1 (I_3 - I_1)} \quad (2.22)$$

The second order differential equation for h_2 is obtained in a procedure similar to that used for h_1 . Using Eqs. (2.22), (2.16) and (2.20) in Eq. (2.14) we obtain the result as:

$$\ddot{h}_2 + \frac{(I_1^* + I_3^* + 2Pt^2) 2Pt \dot{h}_2}{(I_3^* + Pt^2)(I_1^* + Pt^2)} + \frac{(I_3^* - I_1^*)(I_3^* - I_2^* + Pt^2) h_0^2 h_2}{(I_3^* + Pt^2)^2 (I_1^* + Pt^2) I_2^*} = 0 \quad (2.23)$$

It can be seen that Eqs. (2.21) and (2.23) contain time dependent coefficients with complex regular singular points for the case of positive boom extension rates ($P > 0$).

As a special case, for a nearly spherical hub ($I_1^* = I_2^* \approx I_3^* = I^*$) Eqs. (2.22) and (2.23) reduce to:

$$\ddot{h}_1 - \frac{2I^* Pt \dot{h}_1}{(I^* + Pt^2)(2I^* + Pt^2)} = 0 \quad (2.24)$$

$$\ddot{h}_2 + \frac{4Pt \dot{h}_2}{(I^* + Pt^2)} = 0 \quad (2.25)$$

Eq. (2.24) can be written as:

$$\begin{aligned} \frac{\ddot{h}_1}{\dot{h}_1} &= \frac{2I^* Pt}{(I^* + Pt^2)(2I^* + Pt^2)} \\ &= 2Pt \left[\frac{1}{I^* + Pt^2} - \frac{1}{2I^* + Pt^2} \right] \end{aligned} \quad (2.26)$$

Integrating with respect to time,

$$\dot{h}_1 = C \left[\frac{I^* + Pt^2}{2I^* + Pt^2} \right] \quad (2.27)$$

Integrating once again, we have,

$$h_1(t) = C \left[t - \sqrt{\frac{I^*}{2P}} \tan^{-1} \left(\frac{t}{\sqrt{2I^*/P}} \right) \right] + D \quad (2.28)$$

where C and D are constants which are determined from the initial conditions. From Eqs. (2.2), (2.16) and (2.28), the solution for $\omega_1(t)$ is given by:

$$\omega_1(t) = \frac{C[t - \sqrt{\frac{I^*}{2P}} \tan^{-1}(\frac{t}{\sqrt{2I^*/P}})] + D}{I^* + Pt^2} \quad (2.29)$$

$$\text{At } t = 0, \text{ from Eq. (2.29), } \omega_1(0) = D/I^* \quad (2.30)$$

$$\text{From Eq. (2.27), } \dot{h}_1(0) = I^* \dot{\omega}_1(0) = C/2 \quad (2.31)$$

Eqs. (2.30) and (2.31) are used in Eq. (2.29) to obtain the final expression for $\omega_1(t)$ as:

$$\omega_1(t) = \frac{\omega_1(0) + 2\dot{\omega}_1(0)[t - \sqrt{I^*/2P} \tan^{-1}(\frac{t}{\sqrt{2I^*/P}})]}{1 + \frac{Pt^2}{I^*}} \quad (2.32)$$

Eq. (2.25) can be written as,

$$\frac{\ddot{h}_2}{\dot{h}_2} = - \frac{4Pt}{(I^* + Pt^2)} \quad (2.33)$$

This is an exact differential equation and after integrating with respect to time,

$$\dot{h}_2 = \frac{E}{(I^* + Pt^2)} \quad (2.34)$$

Integrating once again, we get

$$h_2(t) = \frac{E}{P^2} \left[\frac{t}{2 \frac{I^*}{P} (t^2 + \frac{I^*}{P})} + \frac{1}{2 (\frac{I^*}{P})^{3/2}} \tan^{-1} \left(\frac{t}{\sqrt{I^*/P}} \right) \right] + F \quad (2.35)$$

where E and F are constants which are determined from the initial conditions. From Eqs. (2.2), (2.16) and (2.35), the solution for $\omega_2(t)$ is given by:

$$\omega_2(t) = \frac{1}{I^*} \left[\frac{E}{P^2} \left[\frac{t}{2 \frac{I^*}{P} (t^2 + \frac{I^*}{P})} + \frac{1}{2 (\frac{I^*}{P})^{3/2}} \tan^{-1} \left(\frac{t}{\sqrt{I^*/P}} \right) \right] + F \right] \quad (2.36)$$

$$\text{At } t = 0, \text{ from Eq. (2.36), } \omega_2(0) = F/I^* \quad (2.37)$$

$$\text{From Eq. (2.34), } \dot{h}_2(0) = I^* \dot{\omega}_2(0) = E/(I^*)^2 \quad (2.38)$$

Using Eqs. (2.37) and (2.38) in Eq. (2.36), the expression for $\omega_2(t)$ becomes

$$\omega_2(t) = \omega_2(0) + \dot{\omega}_2(0) \frac{I^*}{2P} \left[\frac{t}{(t^2 + \frac{I^*}{P})} + \frac{1}{\sqrt{I^*/P}} \tan^{-1} \left(\frac{t}{\sqrt{I^*/P}} \right) \right] \quad (2.39)$$

In general, for a symmetrical spacecraft, the initial conditions $\dot{\omega}_1(0)$ and $\dot{\omega}_2(0)$ can be related to $\omega_1(0)$ and $\omega_2(0)$ from the torque-free precession before the extension begins. However, it should be noted that such initial angular accelerations may also be caused by other

types of external perturbations.

b. Series Solution

As Eqs. (2.21) and (2.23) cannot be solved in closed form except for the special case of a nearly spherical hub, a series solution is developed for $h_1(t)$ and $h_2(t)$. A similar type of series solution has been previously used to predict the planar librational motion of a gravity-gradient satellite during boom deployment. Here $t = 0$ is an ordinary point of Eqs. (2.21) and (2.23), and the radius of convergence R is the smallest value of:

$$\sqrt{\frac{I_3^*}{P}} \quad \text{or} \quad \sqrt{\frac{I_1^*}{P}}$$

The series solution for h_1 may be expanded about $t = 0$ in the form:

$$h_1 = \sum_{n=0}^{\infty} a_n t^n \quad (2.40)$$

Substituting this into Eq. (2.21), we have:

$$\begin{aligned} \sum_{n=0}^{\infty} a_n \cdot n \cdot (n-1) t^{n-2} - \frac{2I_2^* P t \sum_{n=0}^{\infty} a_n \cdot n \cdot t^{n-1}}{(I_3^* + P t^2)(I_3^* + I_2^* + P t^2)} \\ + \frac{(I_3^* - I_1^*)(I_3^* - I_2^* + P t^2) h_0^2}{(I_3^* + P t^2)^2 (I_1^* + P t^2) I_2^*} \sum_{n=0}^{\infty} a_n t^n = 0 \end{aligned} \quad (2.41)$$

Rearranging and collecting terms in Eq. (2.41), after a number of algebraic manipulations, we get,

$$\begin{aligned}
& D_1 \sum_{n=0}^{\infty} a_n (n-1) t^{n-2} + \sum_{n=2}^{\infty} [E_1 (n-2)(n-3) - Q_1 (n-2) + L_1] a_{n-2} t^{n-2} \\
& + \sum_{n=4}^{\infty} [F_1 (n-4) (n-5) - J_1 (n-4) + M_1] a_{n-4} t^{n-2} \\
& + \sum_{n=6}^{\infty} [G_1 (n-6) (n-7) - K_1 (n-6) + N_1] a_{n-6} t^{n-2} \\
& + H_1 \sum_{n=8}^{\infty} (n-8) (n-9) a_{n-8} t^{n-2} = 0 \quad (2.42)
\end{aligned}$$

where $D_1 = I_1^* I_2^* (I_3^*)^2 (I_2^* + I_3^*)$

$$E_1 = I_2^* P [(I_3^*)^2 (I_1^* + I_2^* + I_3^*) + 2 I_1^* I_3^* (I_2^* + I_3^*)]$$

$$F_1 = I_2^* P^2 [(I_3^*)^2 + I_1^* (I_2^* + I_3^*)]$$

$$G_1 = I_2^* P^3 [I_1^* + I_2^* + 3 I_3^*]$$

$$H_1 = I_2^* P^4 ; \quad Q_1 = 2 I_1^* I_3^* (I_2^*)^2 P$$

$$J_1 = 2(I_1^* + I_3^*)(I_2^*)^2 P^2 ; \quad K_1 = 2(I_2^*)^2 P^3$$

$$L_1 = h_0^2 (I_3^* - I_1^*) [(I_3^*)^2 - (I_2^*)^2]$$

$$M_1 = 2h_0^2 I_3^* (I_3^* - I_1^*) P ; \quad N_1 = h_0^2 (I_3^* - I_1^*) P^2$$

From Eq. (2.42),

when $n = 0$, $D_1 a_0 (0)(-1) = 0$; i.e. $a_0 \neq 0$ in general;

when $n = 1$, $D_1 a_1 (1)(0) = 0$; i.e. $a_1 \neq 0$, in general;

when $n = 2$, $D_1 a_2 (2)(1) + L_1(a_0) = 0$, and

$$a_2 = - \frac{L_1}{D_1 \cdot 2 \cdot 1} a_0 \quad (2.43)$$

Similarly,

$$a_3 = - \frac{(-Q_1 + L_1)}{D_1 \cdot 3 \cdot 2} a_1 \quad (2.44)$$

$$a_4 = - \frac{[(2 \cdot 1 \cdot E_1 - 2Q_1 + L_1)a_2 + M_1 a_0]}{D_1 \cdot 4 \cdot 3} \quad (2.45)$$

$$a_5 = - \frac{[(3 \cdot 2 \cdot E_1 - 3Q_1 + L_1)a_3 + (-J_1 + M_1) a_1]}{D_1 \cdot 5 \cdot 4} \quad (2.46)$$

The general form for the first ten terms can be written as (where it is understood $a_j = 0$ for $j < 0$):

$$\begin{aligned} a_n = & - \{ \{ (n-2)(n-3)E_1 - (n-2)Q_1 + L_1 \} a_{n-2} \\ & + \{ (n-4)(n-5)F_1 - (n-4)J_1 + M_1 \} a_{n-4} \\ & + \{ (n-6)(n-7)G_1 - (n-6)K_1 + N_1 \} a_{n-6} \\ & + (n-8)(n-9) H_1 a_{n-8} \} / [D_1 \cdot n \cdot (n-1)] \end{aligned} \quad (2.47)$$

It is seen that the odd coefficients can be related to a_1 and the even coefficients to a_0 . The solution for $h_1(t)$ is written as

$$\begin{aligned} h_1(t) &= \sum_{n=0}^{\infty} a_n t^n \\ &= a_0 [F_1(t)] + a_1 [G_1(t)] \end{aligned} \quad (2.48)$$

where $F_1(t)$ contains the even coefficients and $G_1(t)$ the odd coefficients. The constants a_0 and a_1 are determined from the initial conditions as follows:

$$a_0 = h_1(0) = I_1^* \omega_1(0) \quad (2.49)$$

$$a_1 = \dot{h}_1(0) = I_1^* \dot{\omega}_1(0) \quad (2.50)$$

The expression for $\omega_1(t)$ is given by:

$$\omega_1(t) = \frac{h_1(t)}{I_1^* + p t^2} \quad (2.51)$$

In a similar way, the series solution for $h_2(t)$ can be written as:

$$\begin{aligned} h_2(t) &= \sum_{n=0}^{\infty} b_n t^n \\ &= b_0 [F_2(t)] + b_1 [G_2(t)] \end{aligned} \quad (2.52)$$

where $F_2(t)$ and $G_2(t)$ are similar to $F_1(t)$ and $G_1(t)$. The constants

are related to the initial conditions according to:

$$b_0 = h_2(0) = I_2^* \omega_2(0) \quad (2.53)$$

$$b_1 = \dot{h}_2(0) = I_2^* \dot{\omega}_2(0) \quad (2.54)$$

The solution for $\omega_2(t)$ is then given by

$$\omega_2(t) = h_2(t)/I_2^* \quad (2.55)$$

The expression for $\omega_3(t)$ results directly from the conservation of $h_3(h_0)$:

$$\omega_3(t) = \frac{h_0}{I_3^* + P t^2} \quad (2.56)$$

c. Numerical Results.

In this section the results of numerical integration of the nonlinear differential equations of motion for the most general case are presented. The purpose of the numerical investigation is twofold: first, to verify the analytical results obtained and, second, to compare the motion for different cases considered. The numerical integration is carried out using the IBM 1130 electronic computer. The RKGS and RKSCS subroutines are used to integrate three nonlinear equations with time varying coefficients. The subroutine RKGS¹² uses the Runge-Kutta method for the solution of initial value problems. The purpose of the Runge-Kutta method is to obtain an approximate solution of a system of first order ordinary differential equations

with given initial values. It is a fourth order integration procedure which is stable and self starting; that is, only the functional values at a single previous point are required to obtain the functional values ahead. For this reason it is easy to change the step size at any step in the calculations. The entire input of the procedure is: (1) lower and upper bound of the integration interval, initial increment of the independent variable, upper bound of the local truncation error; (2) initial values of the dependent variables and weights for the local truncation errors in each component of the dependent variables; (3) the number of differential equations in the system; (4) as external subroutine sub-programs, the computation of the right-hand side of the system of differential equations; for flexibility in output, an output subroutine. The subroutine RKSCS establishes weighting factors for the error function.

A typical time response of the components of transverse angular velocity for a nearly spherical hub is shown in Figs. 2.2 and 2.3. End mass extension rates of $c = 4$ and $c = 1$ ft/sec respectively are considered where extension is assumed to occur only along the '2' axis. For numerical integration Eqs. (2.1) and (2.16) are used to obtain the results. The approximate analytical solution given by Eqs. (2.32) and (2.39) and the series solution, given by Eqs. (2.51) and (2.55) with ten terms present, are compared with numerical integration results. It is observed that the analytical solution corresponds more closely with numerical integration results when the extension rate is

increased. The series solution can be used only in the initial part of the extension where the analytical solution also gives essentially the same result. The series solution is limited by its radius of convergence as shown for each case. Fig. 2.4 shows the case of Fig. 2.3 where the hub is spherical (analytical and numerical integration results are the same) and the same initial angular velocity components. Fig. 2.5 is a comparison of the analytical and numerical integration results for different initial conditions than those shown in Fig. 2.3. It can be seen with the numerical integration results that even though the final magnitudes of the angular velocities are small, the responses differ predominantly for the intermediate time ranges.

In Figs. 2.6(a) and (b), the effect of varying the hub spin-axis moment of inertia is shown using numerical integration. It is observed that when the hub spin axis moment of inertia (I_3^*) is increased from a spherical one ($I_3^* = I_1^* = I_2^* = 5 \text{ slug-ft}^2$), the transverse angular responses tend to become more oscillatory in nature during the full deployment time.

The effect of varying the end mass is considered next and it is seen (Fig. 2.7) that the transverse angular velocity amplitudes tend to decay more rapidly when the end mass is increased. This type of response is due to the increase in moment of inertia when the end mass is increased.

3. Uniformly Distributed Mass Moving

a. Analytical Solution for Asymmetrical Deployment

The telescoping system with the uniformly distributed mass moving along the '2' axis is shown in Fig. 2.1(b). The extension of the telescoping system is considered to originate from the center of the spacecraft hub. The moments of inertia during this deployment can be expressed by,

$$\begin{aligned} I_1 &= I_1^* + \frac{2}{3} \rho \ell^3 \\ I_2 &= I_2^* \end{aligned} \tag{2.57}$$

$$I_3 = I_3^* + \frac{2}{3} \rho \ell^3$$

where ρ = linear density = mass/unit length.

With $\ell = ct$ and $K = 2\rho c^3$, Eq. (2.57) can be written as:

$$\begin{aligned} I_1 &= I_1^* + \frac{K}{3} t^3 \\ I_2 &= I_2^* \end{aligned} \tag{2.58}$$

$$I_3 = I_3^* + \frac{K}{3} t^3$$

Following the same procedure as used for the case of the moving end mass the angular momentum equations for h_1 and h_2 , from Eqs. (2.13) and (2.14), can be developed to yield the following:

$$\ddot{h}_1 - \frac{I_2^* K t^2}{(I_3^* + \frac{K t^3}{3})(I_3^* - I_2^* + \frac{K t^3}{3})} \dot{h}_1 + \frac{(I_3^* - I_1^*)(I_3^* - I_2^* + \frac{K t^3}{3})}{(I_3^* + \frac{K t^3}{3})^2 (I_1^* + \frac{K t^3}{3}) I_2^*} h_0^2 h_1 = 0 \quad (2.59)$$

$$\ddot{h}_2 + \frac{(I_1^* + I_3^* + \frac{2K t^3}{3}) K t^2}{(I_3^* + \frac{K t^3}{3})(I_1^* + \frac{K t^3}{3})} \dot{h}_2 + \frac{(I_3^* - I_1^*)(I_3^* - I_2^* + \frac{K t^3}{3})}{(I_3^* + \frac{K t^3}{3})^2 (I_1^* + \frac{K t^3}{3}) I_2^*} h_0^2 h_2 = 0 \quad (2.60)$$

As a special case, for the nearly spherical hub
 $(I_1^* = I_2^* = I_3^* = I^*)$, the above equations can be approximated by:

$$\ddot{h}_1 - \frac{3 I^* \dot{h}_1}{(I^* + \frac{K t^3}{3}) t} = 0 \quad (2.61)$$

$$\ddot{h}_2 + \frac{2 K t^2 \dot{h}_2}{(I^* + \frac{K t^3}{3})} = 0 \quad (2.62)$$

Eq. (2.61) can be written as

$$\frac{\ddot{h}_1}{\dot{h}_1} = \frac{3 a^3}{(a^3 + t^3) t} \quad (2.63)$$

$$\text{where } a^3 = \frac{3 I^*}{K} \quad (2.64)$$

Integrating Eq. (2.63)

$$\dot{h}_1 = R_1 \frac{t^3}{a^3 + t^3} \quad (2.65)$$

where R_1 is a constant. Integrating again and introducing the initial

conditions the solution for $\omega_1(t)$ can be obtained as:

$$\omega_1(t) = \frac{\omega_1(0) + \frac{R_1}{I^*} \left[t - \frac{a}{6} \ln \left\{ \frac{(t+a)^2}{t^2 - at + a^2} \right\} - \frac{a}{\sqrt{3}} \left(\tan^{-1} \left(\frac{2t-a}{a\sqrt{3}} \right) + \frac{\pi}{6} \right) \right]}{1 + t^3/a^3} \quad (2.66)$$

The constant R_1 cannot be determined from the initial conditions using Eq. (2.66), since at $t = 0$, R_1 is indeterminate. A series solution (about the ordinary point $t = 0$) of Eq. (2.61) can be developed to yield:

$$\omega_1(t) = \frac{\omega_1(0) + R_2 t^4 \left[1 - \frac{4}{7} \frac{t^3}{a^3} + \frac{4}{10} \frac{t^6}{a^6} - \dots \right]}{1 + t^3/a^3} \quad (2.67)$$

Here also the constant R_2 cannot be determined from the initial conditions using Eq. (2.67).

A different approach is now adopted using the parent equations of Eqs. (2.59), (2.60), i.e. Eqs. (2.3) and (2.4), to evaluate R_1 in Eq. (2.66). The equation for \dot{h}_1 is obtained from Eqs. (2.3), (2.6), and (2.58) as below:

$$\begin{aligned} \dot{h}_1 &= -a_2(t)h_2 \\ &= - \frac{(I_3^* + \frac{Kt^3}{3} - I_2^*)}{(I_3^* + \frac{Kt^3}{3}) I_2^*} h_0 h_2 \end{aligned} \quad (2.68)$$

For the case of a nearly spherical hub, Eq. (2.68) reduces to the following equation, using Eq. (2.64),

$$\ddot{h}_1 = - \frac{t^3}{I^*(a^3 + t^3)} h_0 h_2 \quad (2.69)$$

Equating Eqs. (2.65) and (2.69) we obtain:

$$R_1 = -h_0 h_2 / I^* \quad (2.70)$$

Using the initial condition, $h_2(0)$, and recalling that $h_0 = I_3^* \omega_3(0) = I^* \omega_3(0)$, the constant may be evaluated by,

$$R_1 = - I^* \omega_3(0) \omega_2(0) \quad (2.71)$$

Using Eq. (2.71) in Eq. (2.66), the solution, $\omega_1(t)$, results as:

$$\omega_1(t) = \frac{\omega_1(0) - \omega_3(0)\omega_2(0) \left[t - \frac{a}{6} \ln \left\{ \frac{(t+a)^2}{t^2 - at + a^2} \right\} - \frac{a}{\sqrt{3}} \left\{ \tan^{-1} \left(\frac{2t-a}{a\sqrt{3}} \right) + \frac{\pi}{6} \right\} \right]}{1 + t^3/a^3} \quad (2.72)$$

Eq. (2.62) can be written as

$$\frac{\ddot{h}_2}{\dot{h}_2} = - \frac{2 K t^2}{(I^* + \frac{K t^3}{3})} \quad (2.73)$$

Integrating Eq. (2.73), we get

$$\dot{h}_2 = \frac{S_1}{(I^* + \frac{K t^3}{3})^2} \quad (2.74)$$

where S_1 is a constant.

Integrating again, and introducing the initial conditions, the solution for $\omega_2(t)$ results as:

$$\begin{aligned} \omega_2(t) = \omega_2(0) + \frac{\dot{\omega}_2(0)}{3} \left[\frac{a^3 t}{a^3 + t^3} + \frac{a}{3} \ln \left\{ \frac{(a+t)^2}{a^2 - at + t^2} \right\} \right. \\ \left. + \frac{2a}{\sqrt{3}} \left\{ \tan^{-1} \left(\frac{2t - a}{\sqrt{3} a} \right) + \frac{\pi}{6} \right\} \right] \end{aligned} \quad (2.75)$$

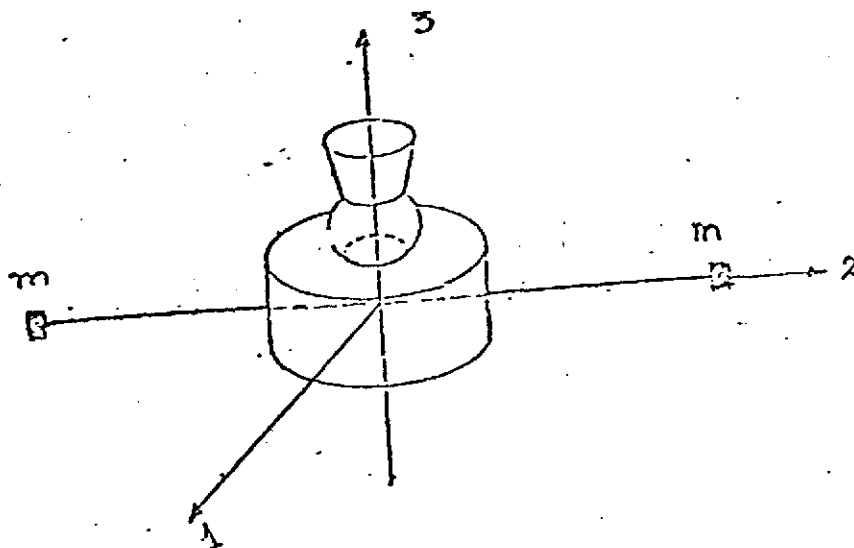
b. Numerical Results

Figs. (2.8) and (2.9) represent a typical comparison of analytical with numerical results. Extension rates $c = 4$ and 1 ft/sec, respectively, are assumed for an asymmetrical deployment only along the '2' axis. The analytical result is obtained using Eqs. (2.72) and (2.75). Numerical integration results are obtained using Eqs. (2.1) and (2.58). The analytical approximation improves with the faster deployment rate for the case of the nearly spherical hub. (The same type of improvement with faster deployment has previously been noted for the case of the moving end mass, Fig. 2.2). Because of the very limited radius of convergence of the series solution, a comparison with this method of solution was not performed for the case of uniformly distributed mass along the boom.

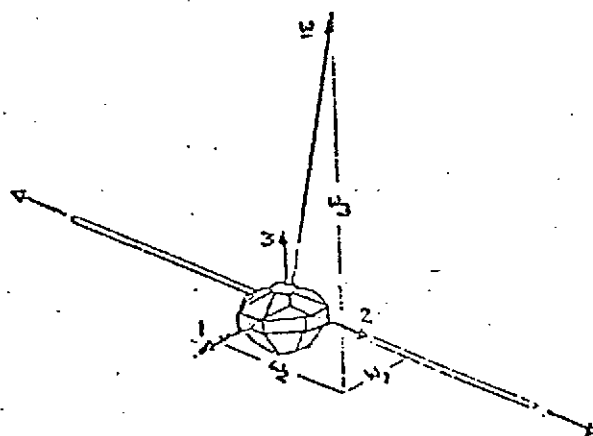
The response of both types of telescoping systems, when the uniformly distributed mass is replaced by an equivalent end mass, is shown in Figs. 2.10(a) and (b). It is seen that initially both types yield approximately the same responses but the amplitudes of transverse angular velocities are rapidly reduced for the end mass system.

This shows the effect of increased moment of inertia, as time increases, due to the total mass being placed at the end of the boom.

The total computer time for numerical integration of the general torque free equations with step size of $\Delta t = 1$ sec varied from 135 to 145 secs for both the moving end mass and uniformly distributed mass cases. The extension rates considered were $c = 4$ and 1 ft/sec for a total boom length of 60 ft. The computer time for the evaluation of each analytical solution for the above cases considered was about 20 to 25 secs.



a. END MASS MOVING



b. UNIFORMLY DISTRIBUTED MASS MOVING

ORIGINAL PAGE IS
OF POOR QUALITY

FIG. 2.1. TWO TYPES OF TELESCOPING APPENDAGES

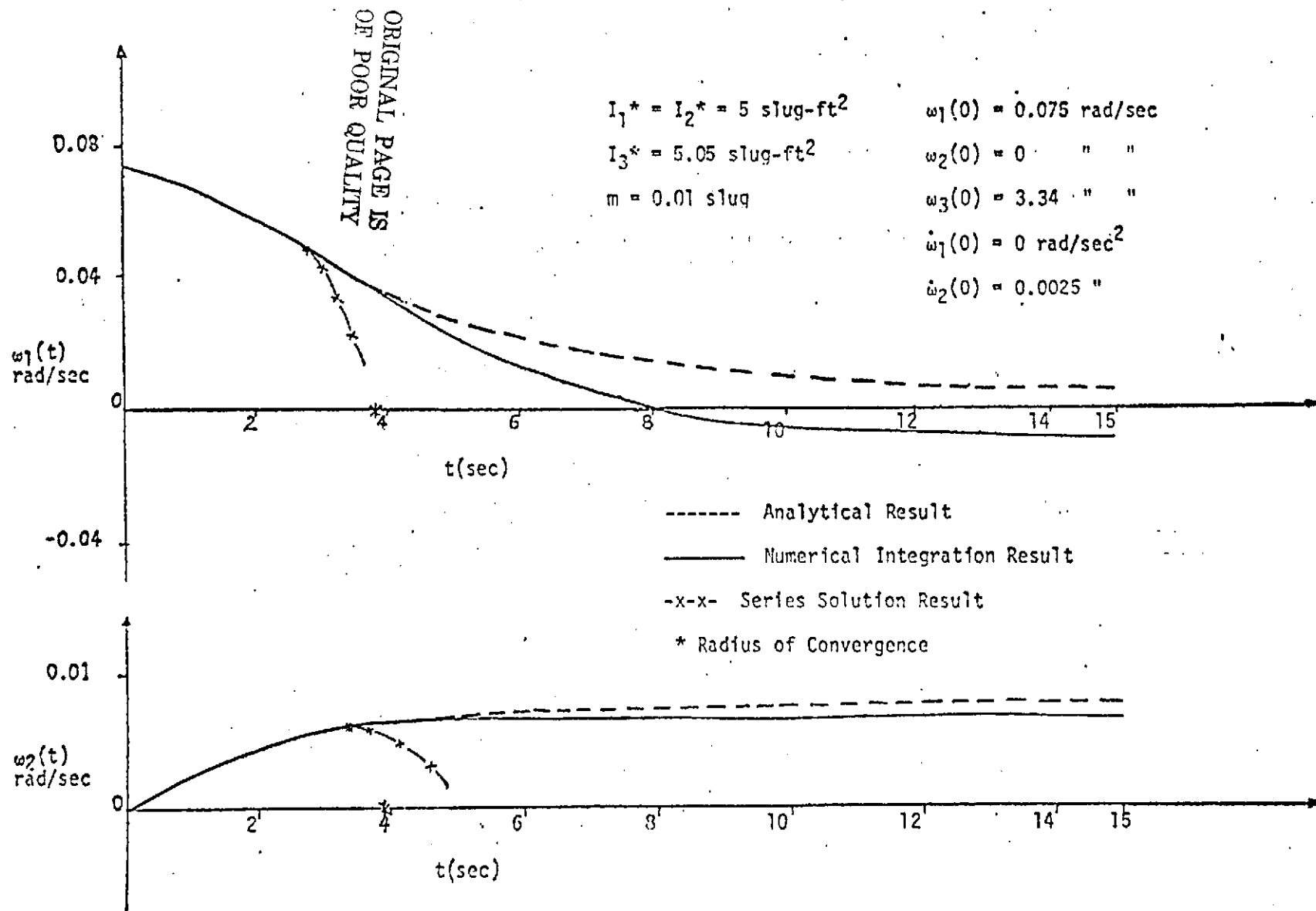


FIG. 2.2. COMPARISON OF ANALYTICAL, NUMERICAL INTEGRATION AND SERIES SOLUTION RESULTS FOR A NEARLY SPHERICAL HUB WITH EXTENSION RATE $c = 4 \text{ ft/sec}$. (END MASS MOVING)

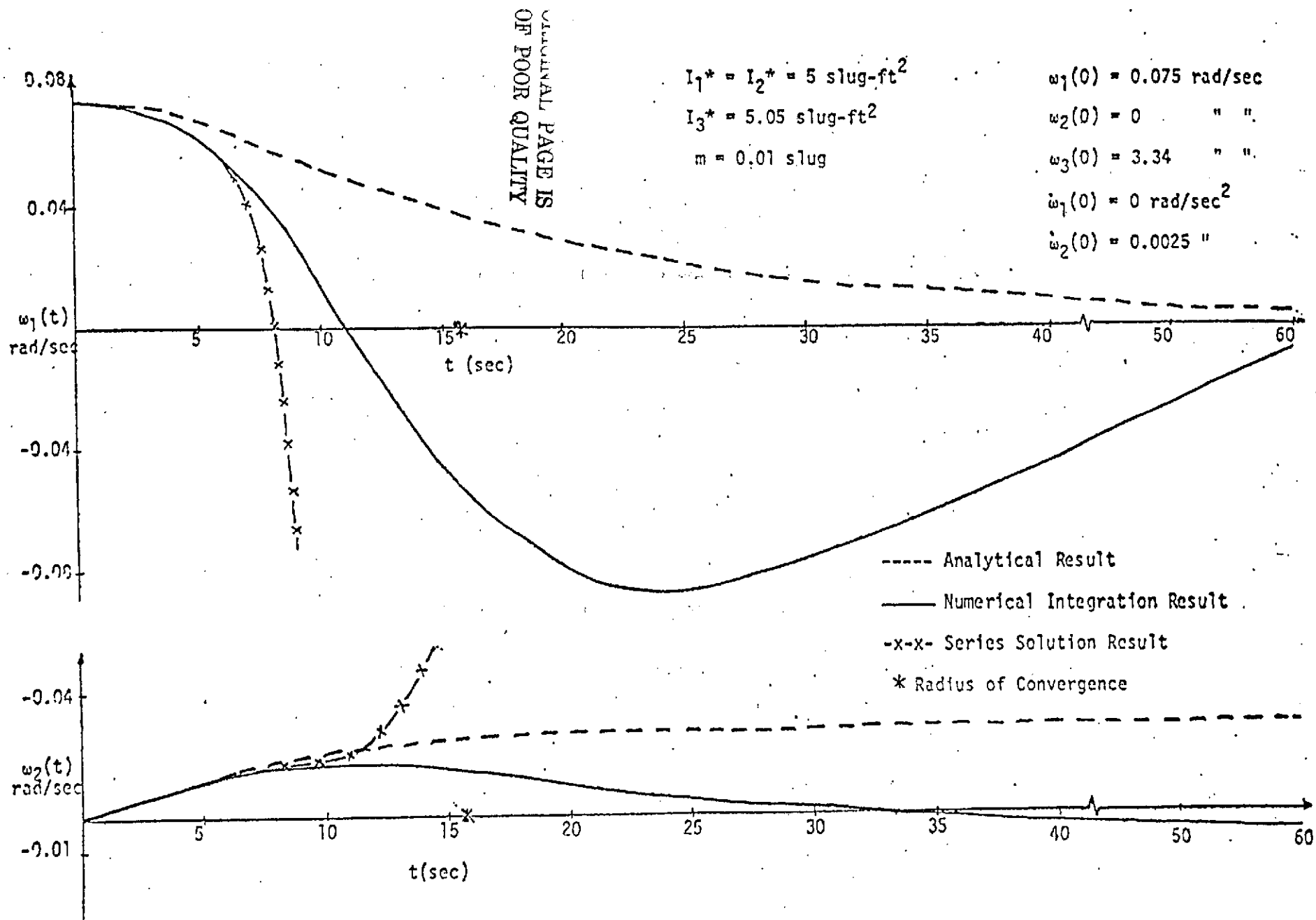


FIG. 2.3. COMPARISON OF ANALYTICAL, NUMERICAL INTEGRATION AND SERIES SOLUTION RESULTS FOR A NEARLY SPHERICAL HUB WITH EXTENSION RATE $c = 1 \text{ ft/sec}$. (END MASS MOVING)

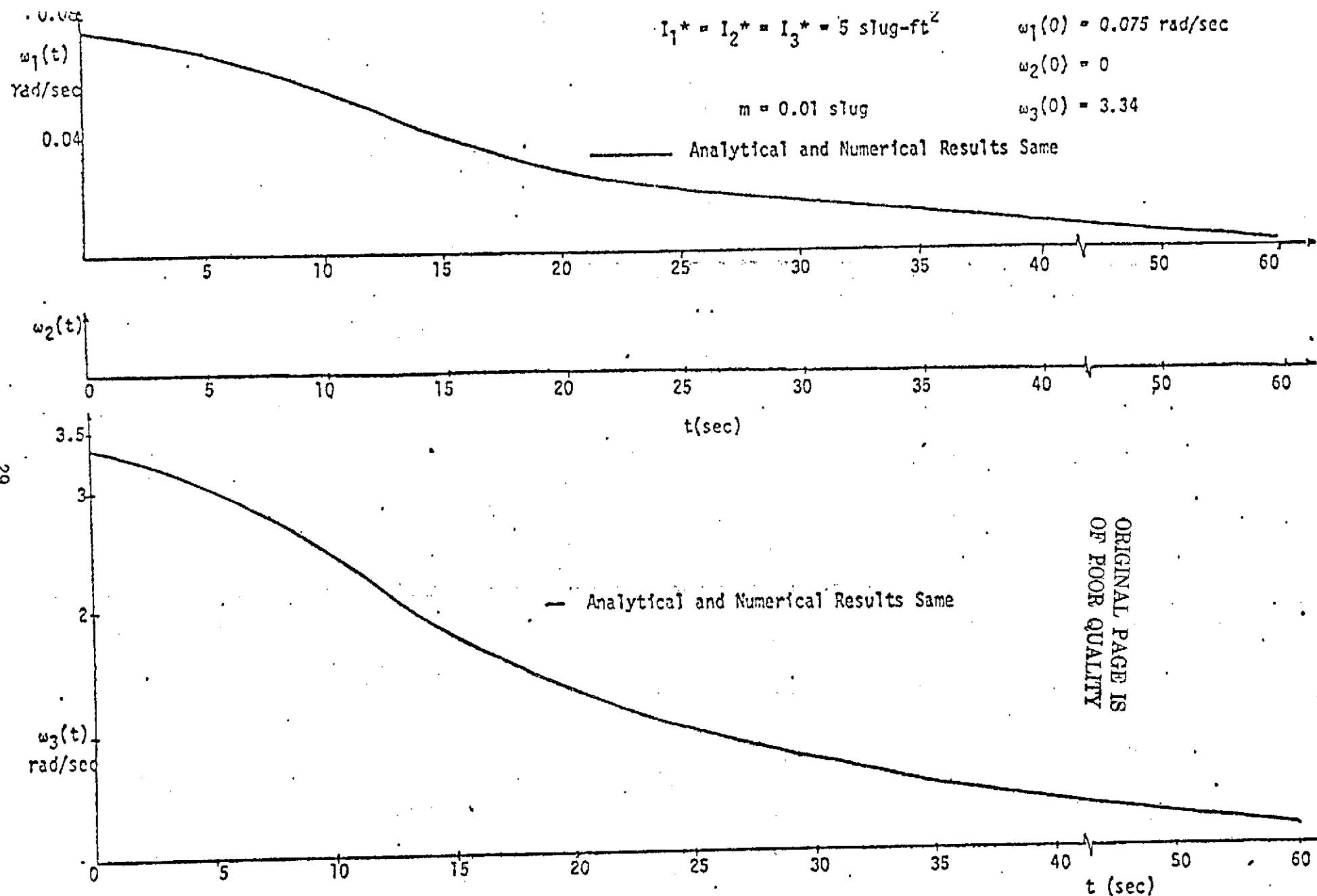


FIG. 2.4. COMPARISON OF ANALYTICAL AND NUMERICAL INTEGRATION RESULTS FOR A SPHERICAL HUB WITH EXTENSION RATE $c = 1 \text{ ft/sec}$. (END MASS MOVING)

$$I_1^* = I_2^* = 5 \text{ slug-ft}^2$$

$$I_3^* = 5.05 \text{ slug-ft}^2$$

$$m = 0.01 \text{ slug}$$

$$\omega_1(0) = 0.06495 \text{ rad/sec}$$

$$\omega_2(0) = 0.0375 \text{ " "}$$

$$\omega_3(0) = 3.34 \text{ " "}$$

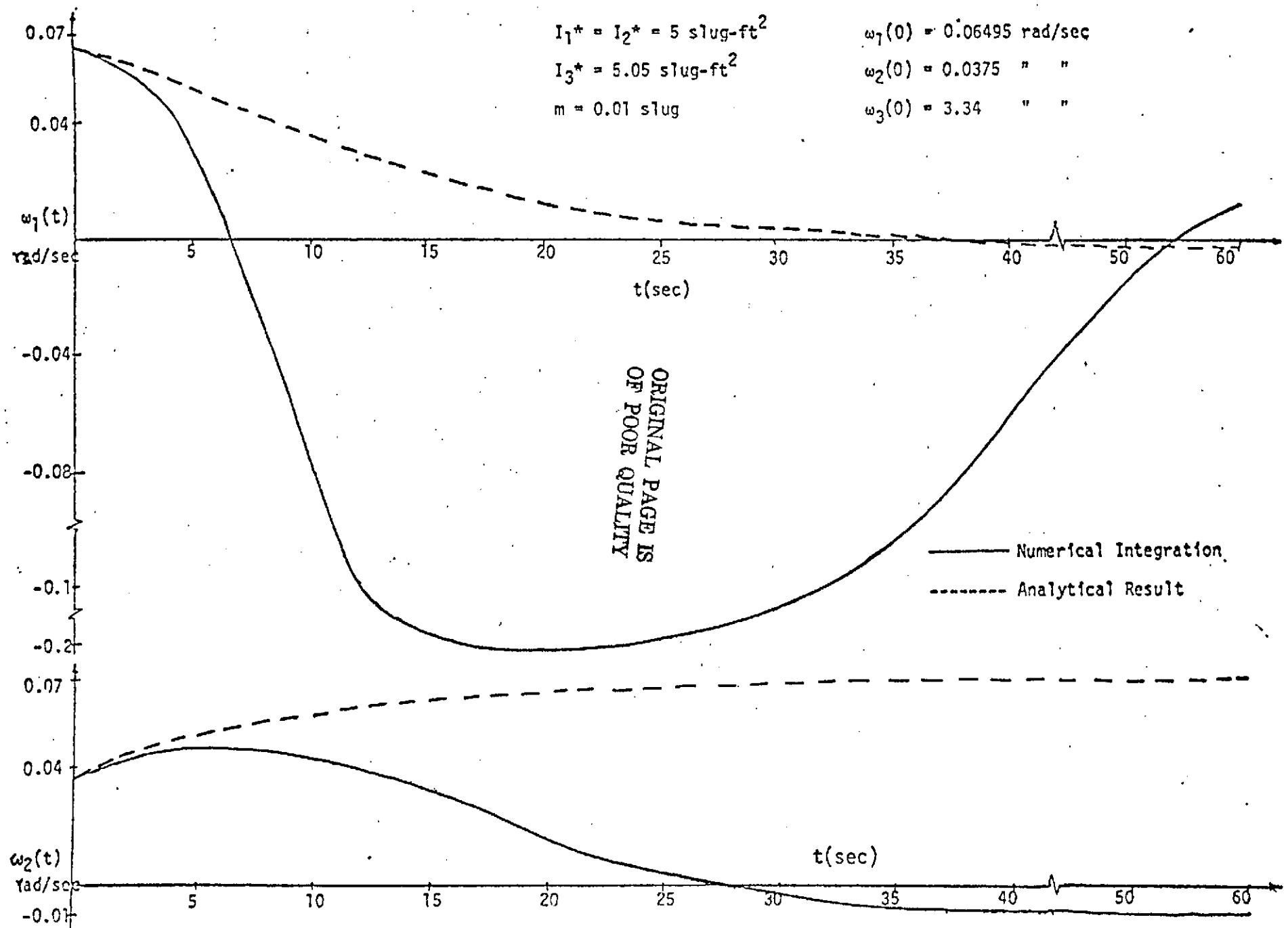


FIG. 2.5. COMPARISON OF ANALYTICAL AND NUMERICAL INTEGRATION RESULTS FOR A NEARLY SPHERICAL HUB WITH EXTENSION RATE $c = 1$ ft/sec WITH THE INITIAL CONDITIONS DIFFERENT FROM FIG. 2.3. (END MASS MOVING)

ORIGINAL PAGE IS
OF POOR QUALITY

$$I_1^* = I_2^* = 5 \text{ slug-ft}^2$$

$$m = 0.01 \text{ slug}$$

$$\omega_1(0) = 0.075 \text{ rad/sec}$$

$$\omega_2(0) = 0.0 \text{ rad/sec}$$

$$\omega_3(0) = 3.34 \text{ rad/sec}$$

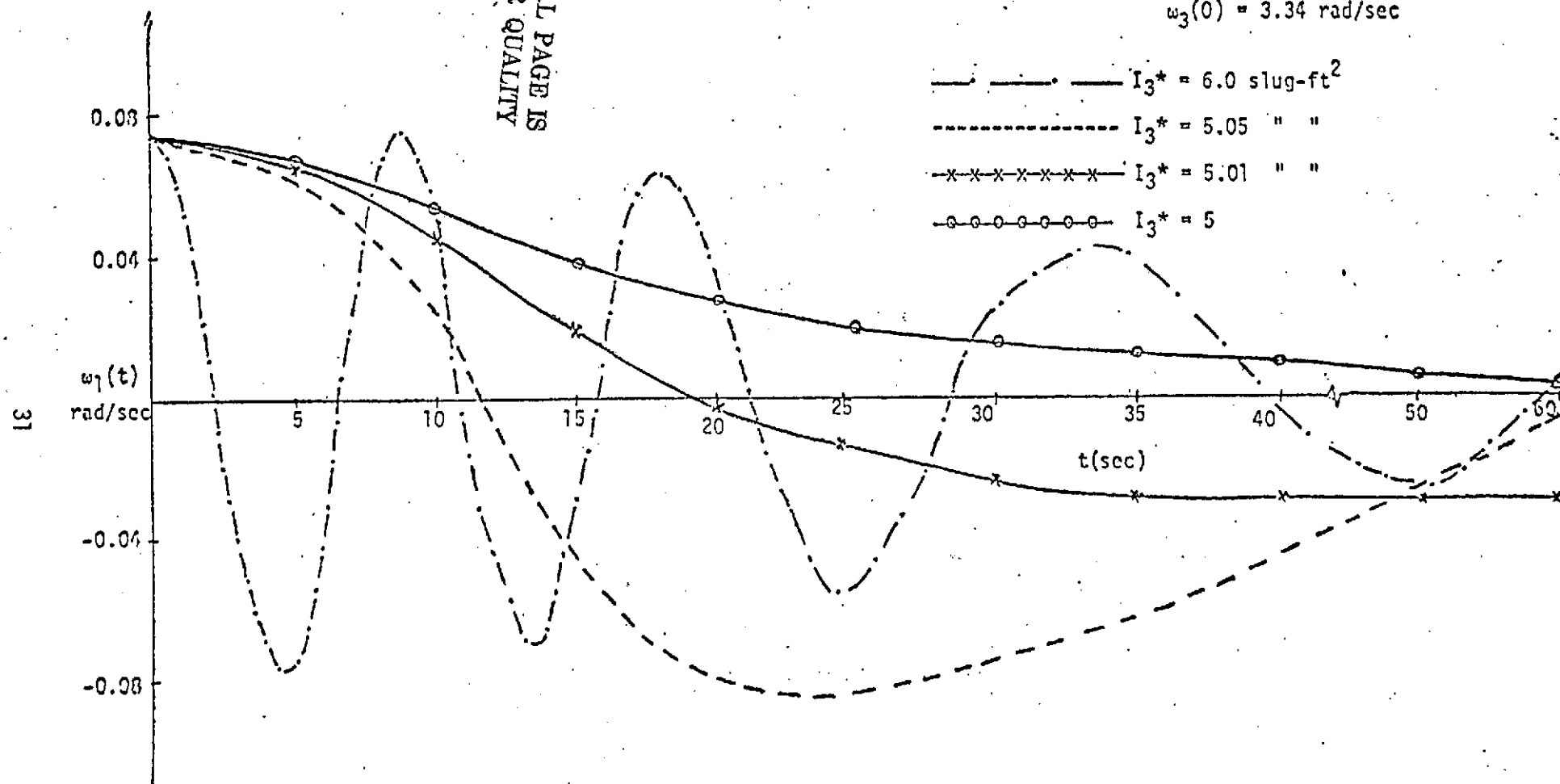


FIG. 2.6(a). EFFECT OF VARIATION OF I_3^* FOR FIXED INITIAL CONDITIONS WITH EXTENSION RATE $c = 1 \text{ ft/sec}$ (END MASS MOVING)-NUMERICAL INTEGRATION.

$$I_1^* = I_2^* = 5 \text{ slug-ft}^2$$

$$m = 0.01 \text{ slug}$$

$$\omega_1(0) = 0.075 \text{ rad/sec}$$

$$\omega_2(0) = 0.0 \text{ rad/sec}$$

$$\omega_3(0) = 3.34 \text{ rad/sec}$$

$$I_3^* = 6.0 \text{ slug-ft}^2$$

$$I_3^* = 5.05 \text{ " "}$$

$$I_3^* = 5.01 \text{ " "}$$

$$I_3^* = 5.00 \text{ " "}$$

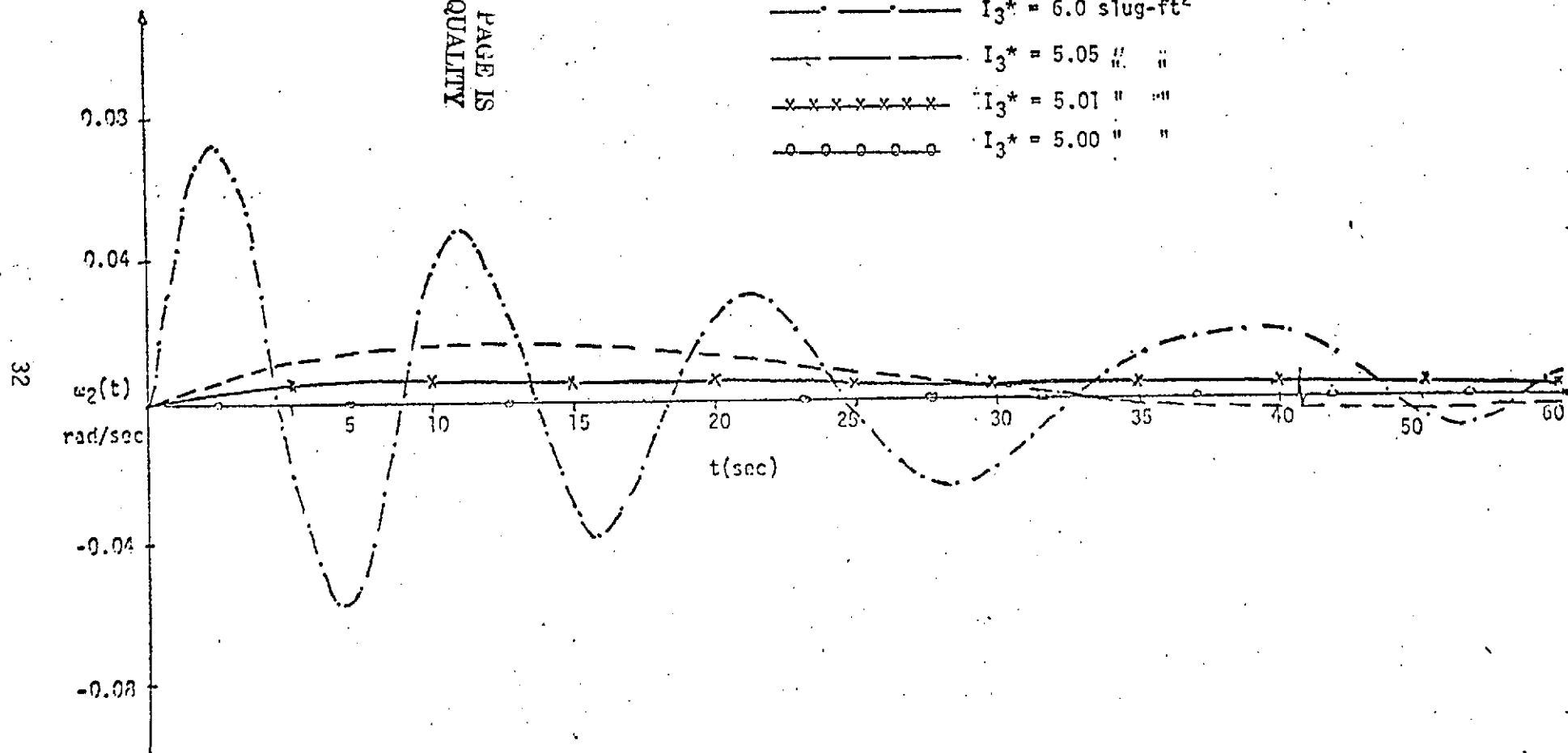


FIG. 2.6(b). EFFECT OF VARIATION OF I_3^* FOR FIXED INITIAL CONDITIONS WITH EXTENSION RATE $c = 1 \text{ ft/sec}$ (END MASS MOVING) - NUMERICAL INTEGRATION.

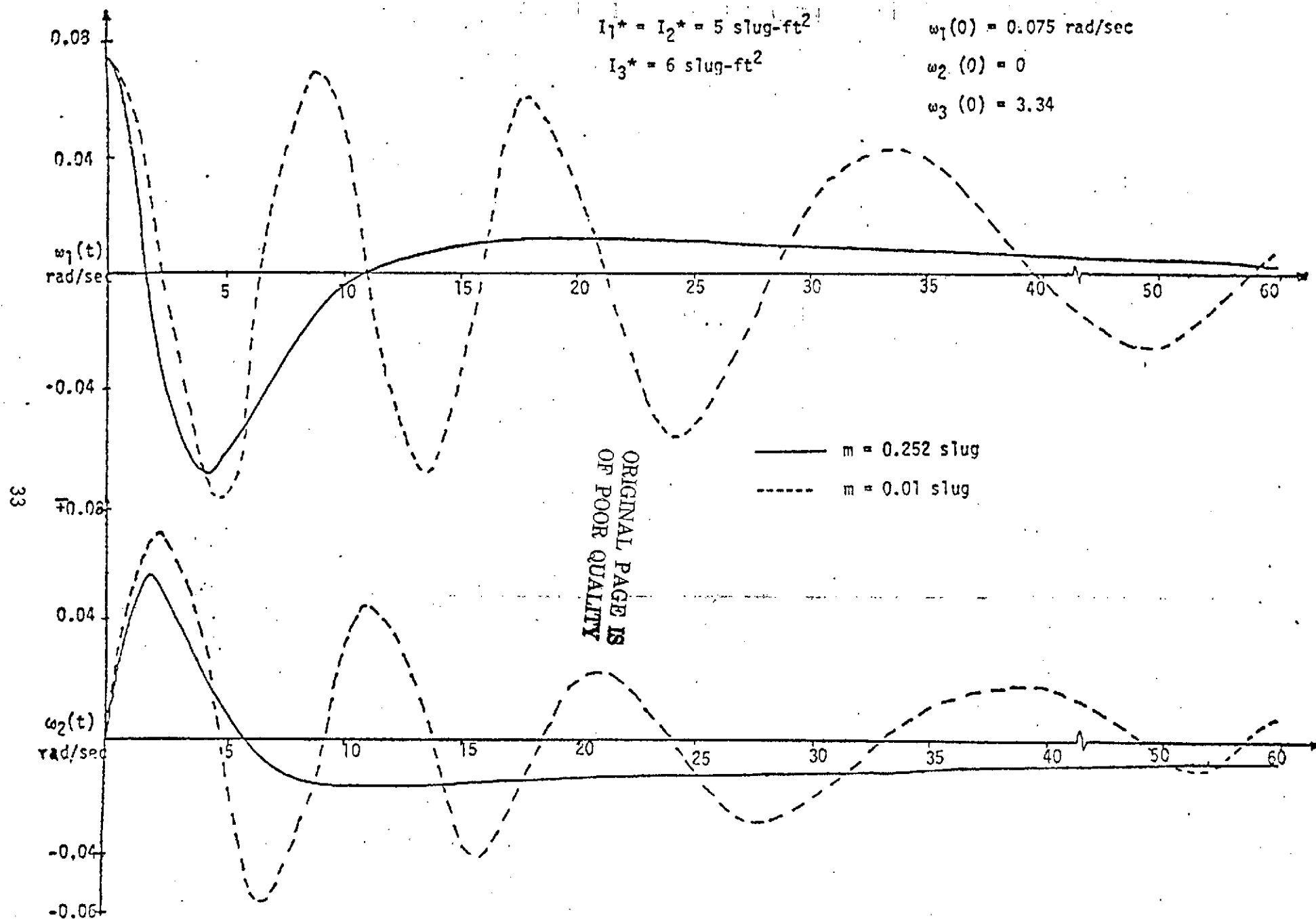


FIG. 2.7. EFFECT OF VARYING END MASS FOR FIXED INITIAL CONDITIONS WITH EXTENSION RATE
 $c = 1 \text{ ft/sec}$ (END MASS MOVING) - NUMERICAL INTEGRATION.

ORIGINAL PAGE IS
OF POOR QUALITY

$$I_1^* = I_2^* = 5 \text{ slug ft}^2$$

$$I_3^* = 5.05 \text{ slug-ft}^2$$

$$\text{Density} = 0.0042 \text{ slug/ft}$$

$$\omega_1(0) = 0.075 \text{ rad/sec}$$

$$\omega_2(0) = 0.0 \text{ " "}$$

$$\omega_3(0) = 3.34 \text{ " "}$$

$$\dot{\omega}_1(0) = 0 \text{ rad/sec}^2$$

$$\dot{\omega}_2(0) = 0.0025 \text{ "}$$

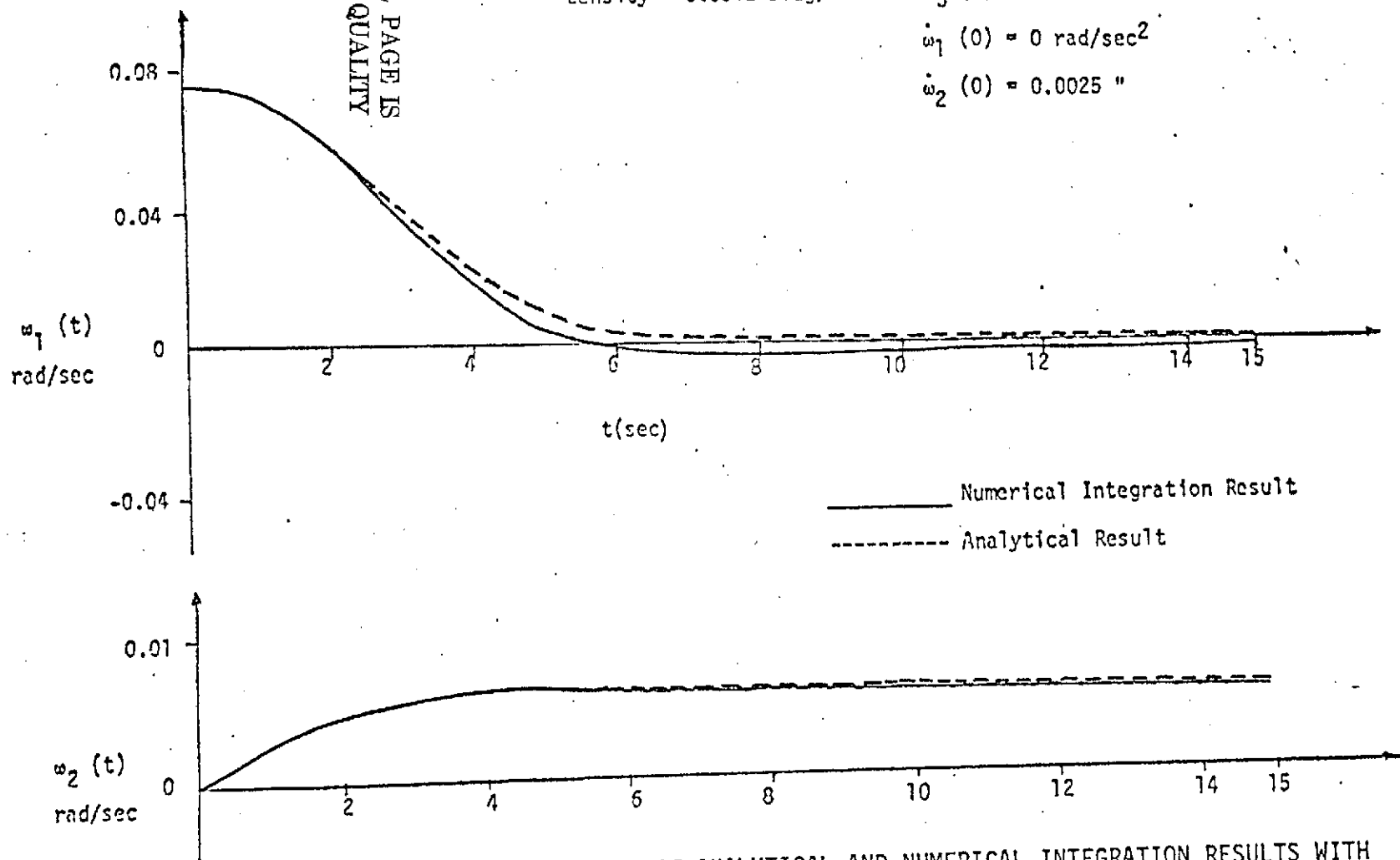


FIG. 2.8. COMPARISON OF ANALYTICAL AND NUMERICAL INTEGRATION RESULTS WITH EXTENSION RATE $c = 4 \text{ ft/sec}$ (UNIFORMLY DISTRIBUTED MASS MOVING)

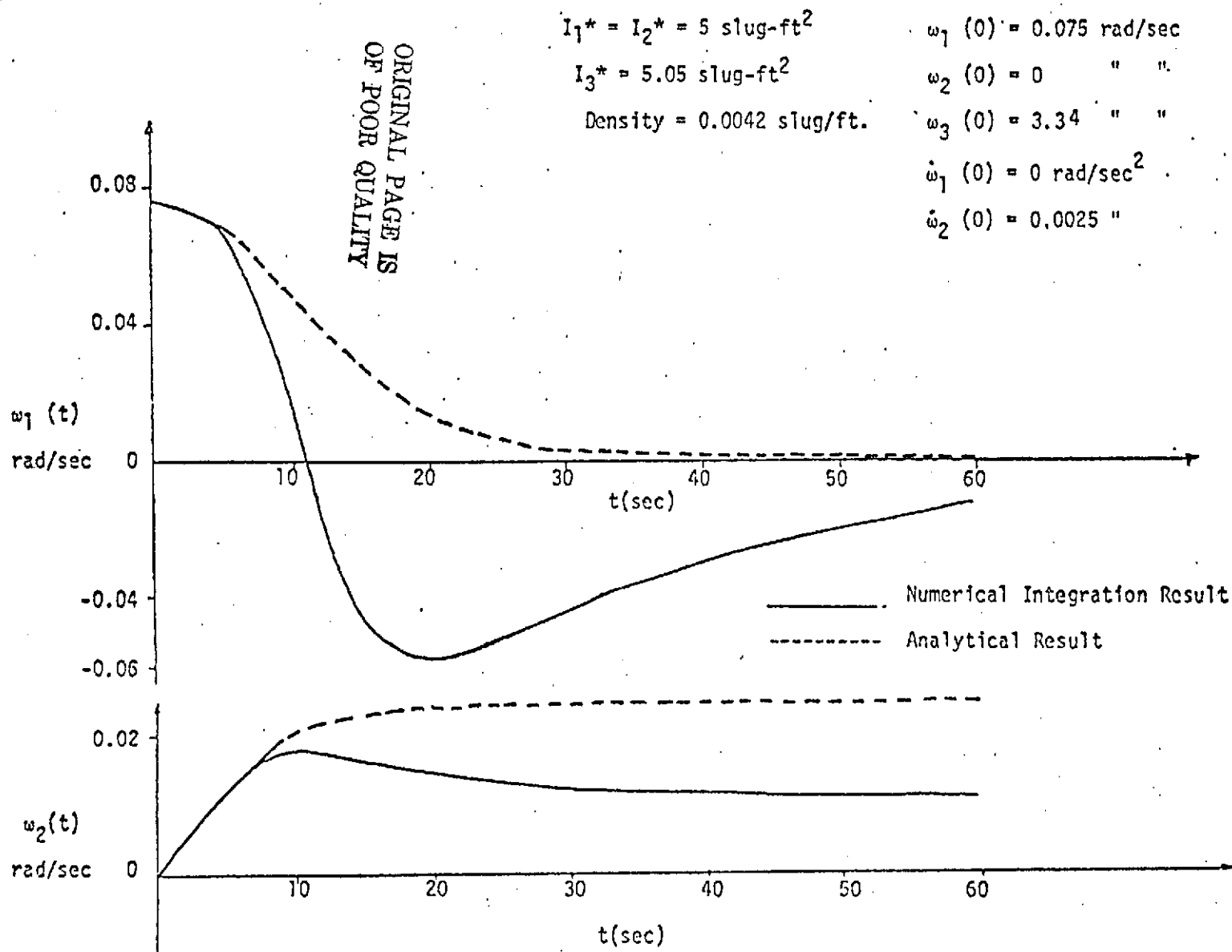


FIG. 2.9. COMPARISON OF ANALYTICAL AND NUMERICAL INTEGRATION RESULTS WITH EXTENSION RATE $c = 1 \text{ ft/sec}$ (UNIFORMLY DISTRIBUTED MASS MOVING).

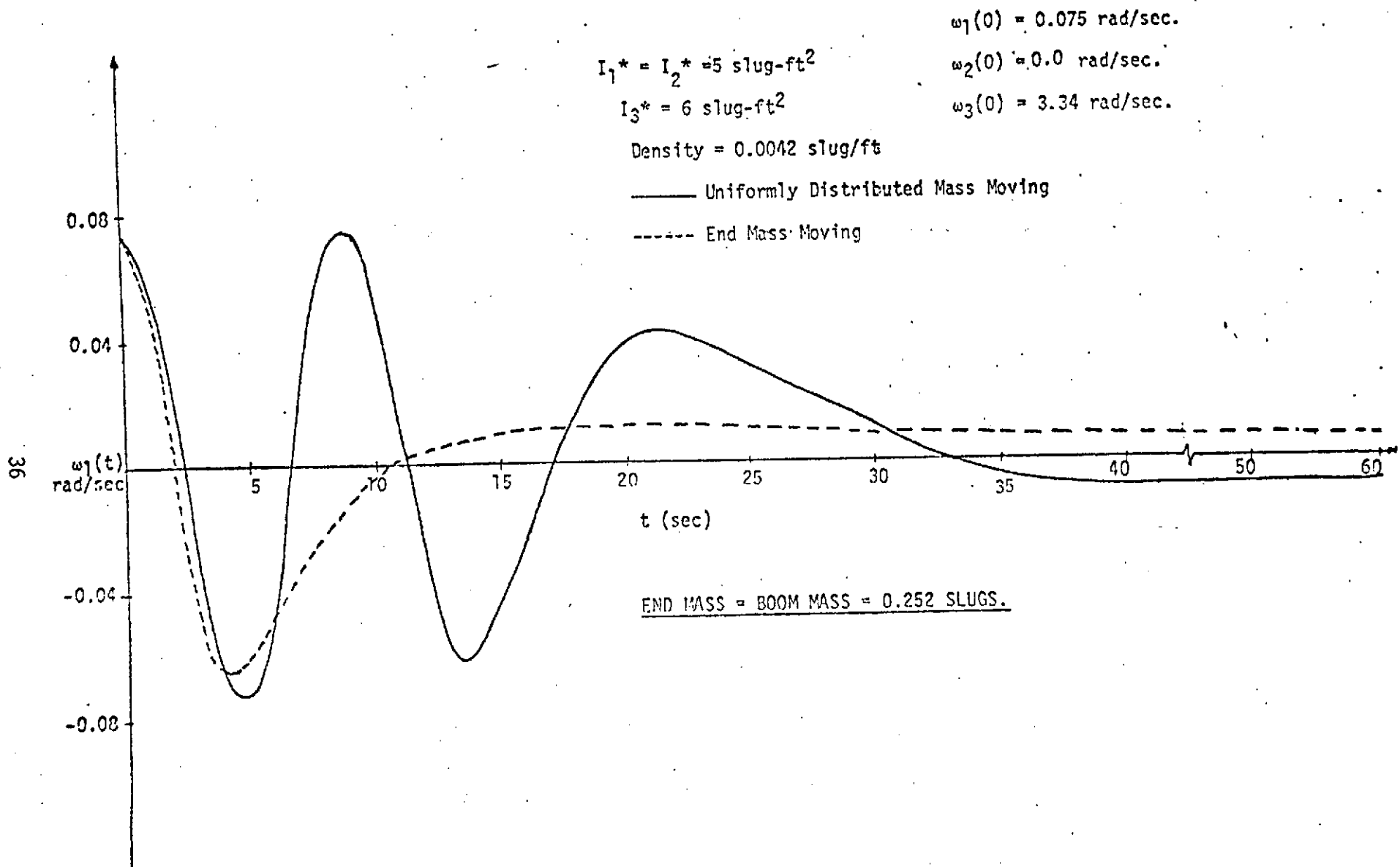


FIG. 2.10(a). COMPARISON OF BOTH TYPES OF TELESCOPING SYSTEMS WITH EXTENSION RATE $c = 1 \text{ ft/sec}$ - NUMERICAL INTEGRATION.

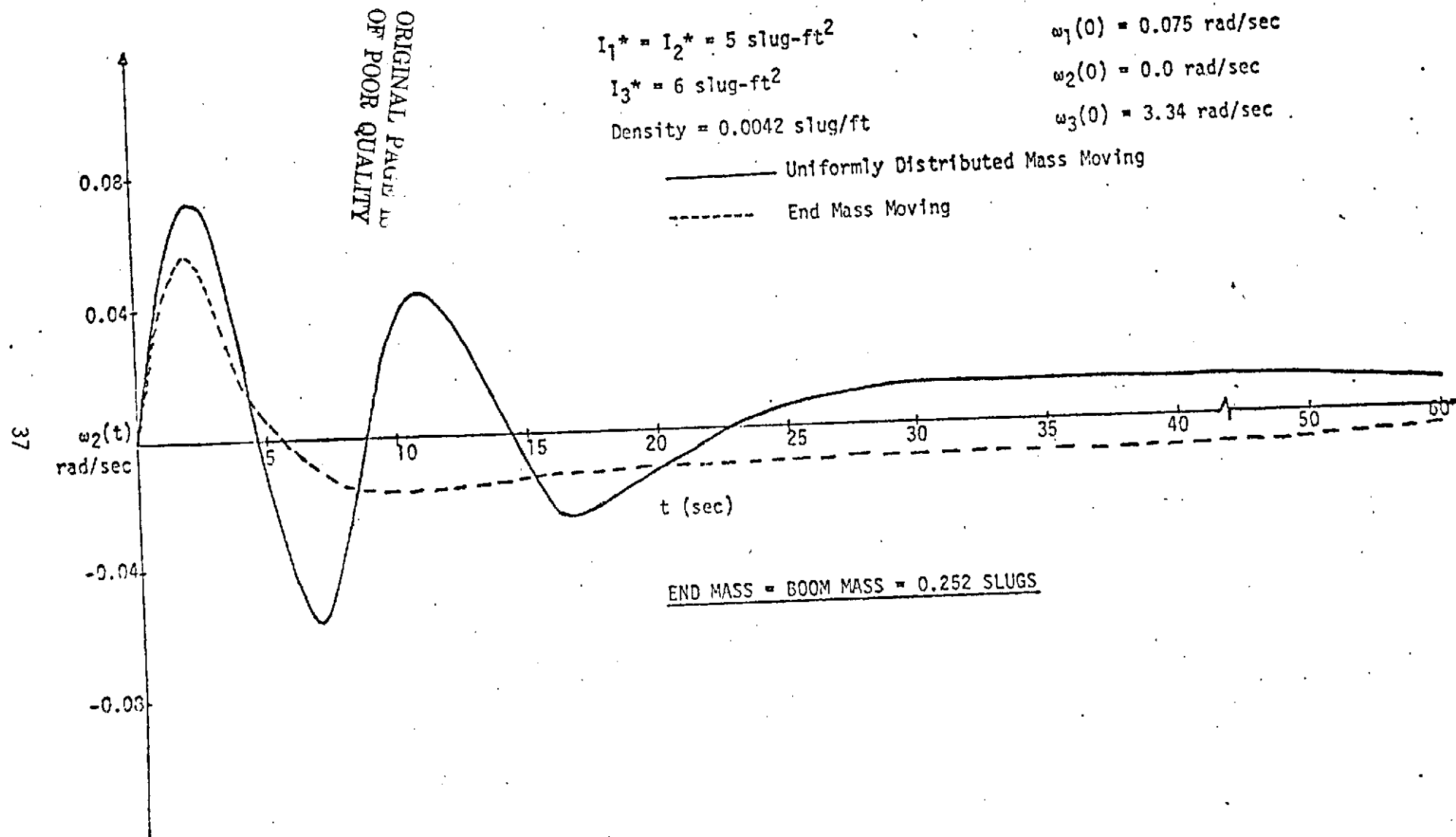


FIG. 2.10(b). COMPARISON OF BOTH TYPES OF TELESCOPING SYSTEMS WITH
EXTENSION RATE $c = 1 \text{ ft/sec}$ - NUMERICAL INTEGRATION.

III. USE OF TELESCOPING SYSTEM FOR DETUMBLING

1. General Considerations

The dynamics of detumbling a randomly spinning spacecraft using externally mounted, movable telescoping appendages are studied both analytically and numerically. The appendages considered are of varying length and could represent extensible booms or a tether connected to the main part of the spacecraft. Two types of telescoping appendages are considered: (a) the case where an end mass is mounted at the end of an assumed massless member (end mass moving) as shown in Fig. 3.1; and (b) where the appendage is assumed to consist of a uniformly distributed, homogeneous mass throughout its length (uniformly distributed mass moving).

The extensible boom type appendages are assumed to originate from the center of the hub along the three principal axes. The desired final states of the system considered are: (1) zero inertial angular velocity vector and (2) a final spin about one of the principal axes. The necessary conditions for asymptotic stability during the detumbling sequences are determined using Lyapunov's second method.

2. End Mass Moving

a. Development of Kinetic Energy

The configuration of the system, where the end masses are assumed to be attached to the end of massless rods along all three principal axes is shown in Fig. 3.1. The end masses are assumed to be identical

(i.e. $m_i = m$). The rotational kinetic energy of the system can be developed as:

$$T = \frac{1}{2} \{ [I_1^* + 2m(\ell_2^2 + \ell_3^2)] \omega_1^2 + [I_2^* + 2m(\ell_3^2 + \ell_1^2)] \omega_2^2 + [I_3^* + 2m(\ell_1^2 + \ell_2^2)] \omega_3^2 + 2m(\dot{\ell}_1^2 + \dot{\ell}_2^2 + \dot{\ell}_3^2) \} \quad (3.1)$$

Defining, $I_1 = I_1^* + 2m(\ell_2^2 + \ell_3^2)$

$$I_2 = I_2^* + 2m(\ell_3^2 + \ell_1^2) \quad (3.2)$$

$$I_3 = I_3^* + 2m(\ell_1^2 + \ell_2^2) ,$$

Eq. (3.1) can be rewritten as:

$$T = \frac{1}{2} [I_1 \omega_1^2 + I_2 \omega_2^2 + I_3 \omega_3^2 + 2m (\dot{\ell}_1^2 + \dot{\ell}_2^2 + \dot{\ell}_3^2)] \quad (3.3)$$

If the extension rates are assumed to be constant, Eq. (3.3) can be expressed:

$$T = \frac{1}{2} [I_1 \omega_1^2 + I_2 \omega_2^2 + I_3 \omega_3^2] + \text{non-negative const.} \quad (3.4)$$

Here the moments of inertia are time varying as the length of the booms varies during extension.

b. Achieve Zero Inertial Angular Rate

1. Lyapunov Function-Kinetic Energy

The desired final state of the system is $\omega_i = 0$. A suitable Lyapunov function, in the state variables ω_1 , ω_2 and ω_3 , is the system

rotational kinetic energy which can be written as:

$$V = T = [I_1\omega_1^2 + I_2\omega_2^2 + I_3\omega_3^2] + \text{non-negative const.} \quad (3.5)$$

The Lyapunov function, V , is positive definite in the state variables selected; for asymptotic stability \dot{V} will now be examined.

Differentiating Eq. (3.5) with respect to time, there results:

$$\dot{V} = \frac{1}{2} (\dot{I}_1\omega_1^2 + \dot{I}_2\omega_2^2 + \dot{I}_3\omega_3^2 + 2I_1\omega_1\dot{\omega}_1 + 2I_2\omega_2\dot{\omega}_2 + 2I_3\omega_3\dot{\omega}_3) \quad (3.6)$$

The equations of motion can be written, from Eq. (2.1), in the following form:

$$\dot{h}_1 = \omega_3 h_2 - \omega_2 h_3 = \dot{I}_1\omega_1 + I_1\dot{\omega}_1 \quad (3.7a)$$

$$\dot{h}_2 = \omega_1 h_3 - \omega_3 h_1 = \dot{I}_2\omega_2 + I_2\dot{\omega}_2 \quad (3.7b)$$

$$\dot{h}_3 = \omega_2 h_1 - \omega_1 h_2 = \dot{I}_3\omega_3 + I_3\dot{\omega}_3 \quad (3.7c)$$

Multiplying Eq. (3.7a) by ω_1 , Eq. (3.7b) by ω_2 , and Eq. (3.7c) by ω_3 , we obtain the following:

$$\begin{aligned} I_1\omega_1\dot{\omega}_1 &= (\omega_3 h_2 - \omega_2 h_3) \omega_1 - \dot{I}_1\omega_1^2 \\ I_2\omega_2\dot{\omega}_2 &= (\omega_1 h_3 - \omega_3 h_1) \omega_2 - \dot{I}_2\omega_2^2 \\ I_3\omega_3\dot{\omega}_3 &= (\omega_2 h_1 - \omega_1 h_2) \omega_3 - \dot{I}_3\omega_3^2 \end{aligned} \quad (3.8)$$

Eqs. (3.8) can be combined to yield:

$$I_1\omega_1\dot{\omega}_1 + I_2\omega_2\dot{\omega}_2 + I_3\omega_3\dot{\omega}_3 = - (\dot{I}_1\omega_1^2 + \dot{I}_2\omega_2^2 + \dot{I}_3\omega_3^2) \quad (3.9)$$

Substituting Eq. (3.9) into Eq. (3.6), we obtain

$$\dot{V} = -\frac{1}{2} (\dot{I}_1 \omega_1^2 + \dot{I}_2 \omega_2^2 + \dot{I}_3 \omega_3^2) \quad (3.10)$$

From (3.10), we conclude that \dot{V} is a negative definite function in the state variables only if $\dot{I}_1, \dot{I}_2, \dot{I}_3 > 0$.

Here it is seen that when the rotational kinetic energy is used as a Lyapunov function expressed in terms of the inertial angular velocity components, that the necessary conditions for asymptotic stability are satisfied for positive constant boom extension rates and three orthogonally mounted sets of booms along the hub principal axes. This means that as time becomes extremely large (and boom lengths become infinite) it would be theoretically possible to de-spin a tumbling spacecraft and achieve a zero inertial angular velocity state. (Of course, such a situation will, in practice, not occur due to finite length appendages, but it will be of interest to simulate how much of a random tumble could be removed by this process. The selection of rotational kinetic energy as a Lyapunov function has also been used by Edwards and Kaplan⁷ for the system treated in Ref. 6.)

2. Analytical Solution

The solutions for the angular momentum of a symmetrical spacecraft ($I_1 = I_2 = I$) during deployment are obtained from Section II.1 as:

$$h_1(t) = q_0^* \cos \left(\int_0^t b(t) dt + \psi_0^* \right) \quad (3.11)$$

$$h_2(t) = q_0^* \sin \left(\int_0^t b(t) dt + \psi_0^* \right) \quad (3.12)$$

$$h_3(t) = h_0 = \text{const} \quad (3.13)$$

$$\text{where } b(t) = \frac{I_3(t) - I(t)}{I(t) I_3(t)} h_0 \quad (3.14)$$

The moments of inertia about the principal axes are given by (Fig. 3.1):

$$\begin{aligned} I_1 &= I^* + 4m\ell^2 = I^* + 2Pt^2 \\ I_2 &= I^* + 4m\ell^2 = I^* + 2Pt^2 \end{aligned} \quad (3.15)$$

$$I_3 = I_3^* + 4m\ell^2 = I_3^* + 2Pt^2$$

Using Eq. (3.15) in Eq. (3.14) we obtain:

$$b(t) = \frac{h_0}{2P} \left\{ \frac{1}{d_1^2 + t^2} - \frac{1}{d_2^2 + t^2} \right\} \quad (3.16)$$

$$\text{where } d_1 = \sqrt{I^*/2P} \quad \text{and} \quad d_2 = \sqrt{I_3^*/2P} \quad (3.17)$$

Introducing Eq. (3.16) in Eqs. (3.11), (3.12), and (3.13) and after performing the integration, the solutions for the angular velocities are obtained as:

$$\omega_1(t) = \frac{q_0^* \cos \left[\frac{h_0}{2P} \left\{ \frac{1}{d_1} \tan^{-1} \frac{t}{d_1} - \frac{1}{d_2} \tan^{-1} \frac{t}{d_2} \right\} + \psi_0^* \right]}{I^* + 2Pt^2} \quad (3.18)$$

$$\omega_2(t) = \frac{q_0^* \sin \left[\frac{h_0}{2p} \left\{ \frac{1}{d_1} \tan^{-1} \frac{t}{d_1} - \frac{1}{d_2} \tan^{-1} \frac{t}{d_2} \right\} + \psi_0^* \right]}{I^* + 2Pt^2} \quad (3.19)$$

$$\omega_3(t) = \frac{I_3^* \omega_3(0)}{I_3^* + 2Pt^2} \quad (3.20)$$

where q_0^* and ψ_0^* are determined from the initial conditions. We observe here for large values of t , the solutions for the angular velocities lead to the form:

$$\omega_i(t) = \text{const}/(I_i^* + 2Pt^2) \quad , \quad i = 1, 2, 3 \quad (3.21)$$

This equation indicates that the magnitudes of the angular velocities decrease during extension of the appendages, with the square of the elapsed time.

3. Numerical Results

A typical detumbling maneuver for an initially slowly tumbling spacecraft is illustrated in Figs. 3.2 and 3.3. In this example because of symmetry the uncontrolled torque-free motion (Fig. 3.2) can be theoretically predicted. With an extension rate of 4 ft/sec after 60 ft. of extension along all three principal axes the angular velocity components have been reduced by more than a factor of 10 and, if 240 ft. of boom could be extended, by a factor of over 300, to a value comparable with the orbital angular rate. Removal of this residual angular velocity could then be achieved by activating on-board

damping devices.

When the initial angular velocity is increased by an order of magnitude the uncontrolled situation (Fig. 3.4) can be recovered as shown in Fig. 3.5. For the same extension rate and end-masses the order of magnitude reduction in the total angular velocity vector is similar to that shown in the slow tumbling case.

The effect of extension rate on detumbling is illustrated in Figs. 3.6(a) - (c). For small extension rates (up to 1 ft/sec) the oscillatory nature of the transverse motion is not removed until after the first cycle; the advantage of considering higher extension rates (at the expense of on-board power) for an initial fast tumbling is apparent. It should be noted that at a given time in these figures different boom lengths are represented according to the extension rate.

Numerical examination of other cases for asymmetrical hubs also verifies the practicality of using movable appendages for the initial detumbling of randomly spinning spacecraft. (Figs. 3.7(a) and (b)). The numerical simulation results for an asymmetrical spacecraft are compared with the closed form solution for a symmetrical extension and it is observed that the closed form solutions are only applicable when the asymmetry is small.

c. Achieve Final Spin About One of the Principal Axes

1. Lyapunov Function-Modified Kinetic Energy

The desired final state of the system is; $\omega_1 = 0$, $\omega_2 = 0$ and $\omega_3 = \omega_{3f} = \Omega$. Using the state variables ω_1 , ω_2 , and $\omega_3 - \Omega$,

the Lyapunov function is defined as the modified rotational kinetic energy, which can be written as:

$$V = \frac{1}{2} [I_1 \omega_1^2 + I_2 \omega_2^2 + I_3 (\omega_3 - \Omega)^2] \quad (3.22)$$

Here V is positive definite in the state variables selected. Differentiating Eq. (3.22) with respect to time, we get

$$\begin{aligned} \dot{V} = \frac{1}{2} [\dot{I}_1 \omega_1^2 + \dot{I}_2 \omega_2^2 + \dot{I}_3 (\omega_3 - \Omega)^2 \\ + 2 I_1 \omega_1 \dot{\omega}_1 + 2 I_2 \omega_2 \dot{\omega}_2 + 2 I_3 (\omega_3 - \Omega) \dot{\omega}_3] \end{aligned} \quad (3.23)$$

Using Eq. (3.9) in Eq. (3.23), we obtain,

$$\dot{V} = -\frac{1}{2} (\dot{I}_1 \omega_1^2 + \dot{I}_2 \omega_2^2 + \dot{I}_3 \omega_3^2) + \frac{1}{2} \Omega^2 \dot{I}_3 - (\dot{I}_3 \omega_3 + I_3 \dot{\omega}_3) \quad (3.24)$$

For symmetry about the '3' axis during extension:

$$\dot{h}_3 = \dot{I}_3 \omega_3 + I_3 \dot{\omega}_3 = 0 \quad (3.25)$$

Eq. (3.25) is used in Eq. (3.24) to obtain:

$$\dot{V} = -\frac{1}{2} [\dot{I}_1 \omega_1^2 + \dot{I}_2 \omega_2^2 + \dot{I}_3 (\omega_3^2 - \Omega^2)] \quad (3.26)$$

After rewriting Eq. (3.26) in terms of the state variables,

$$\dot{V} = -\frac{1}{2} [\dot{I}_1 \omega_1^2 + \dot{I}_2 \omega_2^2 + \dot{I}_3 (\omega_3 - \Omega)^2] - \dot{I}_3 \Omega (\omega_3 - \Omega) \quad (3.27)$$

Also from Eq. (3.25), the solution for $\omega_3(t)$ is given by,

$$\omega_3(t) = I_3^* \omega_3(0) / I_3 \quad (3.28)$$

We conclude from Eq. (3.27) that \dot{V} is negative definite in the state variables

only if $\omega_3 \geq \Omega$, $\dot{I}_1, \dot{I}_2 > 0$, and $\dot{I}_3 > 0$ for $\omega_3 > \Omega$

Thus for the case where a spin about one of the principal axes is a desired final condition, a modified form of the kinetic energy can be used as a Lyapunov function. Here the final state can be achieved by extending all telescoping booms until the desired spin rate is reached and then continuing the extension of the set of booms along the nominal spin axis until the transverse components of angular velocity reach an acceptably small amplitude (within the limitations of boom length). It should be noted that if we allow $\omega_3 < \Omega$ and $\dot{I}_3 \neq 0$, there will be a difference in sign between the third and fourth terms in Eq. (3.27).

2. Analytical Solution

The time at which $\omega_3 = \omega_{3f} = \Omega$ will be denoted by T_{3f} .

At $t = T_{3f}$,

$$\bar{I}_1^* = \bar{I}_2^* = I^* + 2P (T_{3f})^2 \quad (3.29)$$

$$\bar{I}_3^* = I_3^* + 2P (T_{3f})^2 \quad (3.30)$$

For $t \leq T_{3f}$, the solutions for the angular velocities can be obtained from Eqs. (3.18), (3.19) and (3.20).

For $t > T_{3f}$,

$$\bar{I}_3^* = \text{const} = I_3^* + 2P (t_{3f})^2 \quad (3.31)$$

$$\bar{I}^* = I^* + P(T_{3f})^2 + Pt^2 = I_f^* + Pt^2 \quad (3.32)$$

$$\text{where } I_f^* = I^* + P(T_{3f})^2 \quad (3.33)$$

From Eq. (3.14), and using Eqs. (3.31) and (3.33), we obtain

$$b(t) = \omega_{3f} \left\{ \frac{\bar{I}_3^*}{I_f^* + Pt^2} - 1 \right\} \quad (3.34)$$

Introducing Eq. (3.34) into Eqs. (3.11) and (3.12), the solutions for the angular velocities for $t > T_{3f}$ are,

$$\omega_1(t) = \frac{q_0 \cos \left[\omega_{3f} \left[\frac{\bar{I}_3^*}{\sqrt{I_f^*} P} \left\{ \tan^{-1} \left(\frac{t}{\sqrt{I_f^*} P} \right) - \tan^{-1} \left(\frac{T_{3f}}{\sqrt{I_f^*} P} \right) \right\} - t + T_{3f} \right] + \psi_0 \right]}{(I_f^* + Pt^2)} \quad (3.35)$$

$$\omega_2(t) = \frac{q_0 \sin \left[\omega_{3f} \left[\frac{\bar{I}_3^*}{\sqrt{I_f^*} P} \left\{ \tan^{-1} \left(\frac{t}{\sqrt{I_f^*} P} \right) - \tan^{-1} \left(\frac{T_{3f}}{\sqrt{I_f^*} P} \right) \right\} - t + T_{3f} \right] + \psi_0 \right]}{(I_f^* + Pt^2)} \quad (3.36)$$

and from Eq. (3.13),

$$\omega_3(t) = \omega_{3f} = \text{const} \quad (3.37)$$

Here q_0 and ψ_0 are to be determined from Eqs. (3.18) and (3.19) at $t = T_{3f}$ and should not be confused with q_0^* and ψ_0^* which are determined at $t = 0$.

For large values of t , Eqs. (3.35) and (3.36) reduce to the form,

$$\omega_1 = \frac{q_0 \cos (\omega_{3f} \times \text{const} \times t + \text{const})}{I_f^* + Pt^2} \quad (3.38)$$

$$\omega_2 = \frac{q_0 \sin (\omega_{3f} \times \text{const} \times t + \text{const})}{I_f^* + Pt^2} \quad (3.39)$$

The above two equations indicate that the frequency of oscillation approaches a constant value and the magnitude of the oscillation decreases with the square of the elapsed time.

The time $t = T_{3f}$ at which the extension of the booms along '1' and '2' axes are stopped can be determined from $\dot{h}_3 = 0$, yielding the result:

$$T_{3f} = \frac{1}{2c} \sqrt{\frac{I_3^*}{m} \left(\frac{\omega_3(0) - \omega_{3f}}{\omega_{3f}} \right)} \quad (3.40)$$

3. Numerical Results

Figs. 3.8 and 3.9, with extension rates $c = 4$ and $c = 1$ ft/sec, respectively, illustrate a recovery maneuver which would result in a final spin about the '3' body axis with a small transverse residual. The booms are extended so that the modified rotational kinetic energy

is positive definite and its total time derivative is negative definite during the maneuver. All booms are extended until T_{3f} at which time $\omega_3 = \omega_{3f}$. Then, only booms along the \pm '3' axis are extended to reduce the transverse residual components.

A comparison of the recovery maneuver of an asymmetrical spacecraft with that of a symmetrical spacecraft to achieve a final spin along the '3' axis is shown in Figs. 3.10(a) and (b). The calculated T_{3f} for the symmetrical spacecraft is used for stopping the booms along the '1' and '2' axes. It is observed that using this logic the final ω_{3f} reaches a lower value (1.8 rad/sec) when compared with the desired final value (2.0 rad/sec). Also we notice from Fig. 3.10(a), the response of $\omega_1(t)$ for the asymmetrical case differs from that of the symmetrical case. This is due to the increase in the order of the system equations for the asymmetrical extension (i.e. - three first order differential equations must now be considered). It should be pointed out that after T_{3f} , for the asymmetrical case, the time response of ω_3 is not exactly a straight line as apparently indicated in Fig. 3.10(a) but also consists of small amplitude oscillations superimposed about this straight line solution. For larger asymmetries this oscillation would become apparent within the plotting scale shown and the difference between ω_{3f} achieved and desired would also increase using the open loop control logic of switching the extension sequence at a pre-set T_{3f} .

3. Uniformly Distributed Mass Moving

a. Achieve Zero Inertial Angular Rate

1. Analytical Solution

The desired final state of the system is $\omega_i = 0$. The booms considered are assumed to have a uniformly distributed mass along their lengths. The same procedure as adopted in the case of end mass moving can be applied here to obtain the solutions for the angular velocities. Here we present only the final results.

The solutions for the angular velocities are given by:

$$\omega_1(t) = \frac{q_0^* \cos \left\{ \int_0^t b(t) dt + \psi_0^* \right\}}{I^* + \frac{2}{3} Kt^3} \quad (3.41)$$

$$\omega_2(t) = \frac{q_0^* \sin \left\{ \int_0^t b(t) dt + \psi_0^* \right\}}{I^* + \frac{2}{3} Kt^3} \quad (3.42)$$

$$\omega_3(t) = \frac{I_3^* \omega_3(0)}{I_3^* + \frac{2}{3} Kt^3} \quad (3.43)$$

where $\int_0^t b(t) dt = \frac{3h_0}{2K} \left[\frac{1}{6d_3^2} \ln \left\{ \frac{(d_3 + t)^2}{d_3^2 - d_3 t + t^2} \right\} + \frac{1}{d_3^2 \sqrt{3}} \times \right.$

$$\left. \tan^{-1} \left\{ \frac{2t - d_3}{d_3 \sqrt{3}} \right\} - \frac{1}{6d_4^2} \ln \left\{ \frac{(d_4 + t)^2}{d_4^2 - d_4 t + t^2} \right\} - \frac{1}{d_4^2 \sqrt{3}} \tan^{-1} \left\{ \frac{2t - d_4}{d_4 \sqrt{3}} \right\} \right] \quad (3.44)$$

$$d_3^3 = \frac{3I^*}{2K} \quad \text{and} \quad d_4^3 = \frac{3I^*}{2K} \quad (3.45)$$

b. Achieve Final Spin About One of the Principal Axes

1. Analytical Solution

The desired final state of the system is $\omega_1 = 0$, $\omega_2 = 0$ and $\omega_3 = \omega_{3f} = \Omega$. For $t \leq T_{3f}$, the solutions for the angular velocities can be obtained from Eqs. (3.41), (3.42) and (3.43). For $t > T_{3f}$, the solutions for the angular velocities can be obtained as:

$$\omega_1(t) = \frac{q_0 \cos\left\{ \int_{T_{3f}}^t b(t) dt + \psi_0 \right\}}{I_f^* + \frac{1}{3} K t^3} \quad (3.46)$$

$$\omega_2(t) = \frac{q_0 \sin\left\{ \int_{T_{3f}}^t b(t) dt + \psi_0 \right\}}{I_f^* + \frac{1}{3} K t^3} \quad (3.47)$$

$$\omega_3(t) = \omega_{3f} = \text{const} \quad (3.48)$$

$$\text{where: } I_f^* = I^* + \frac{K}{3} (T_{3f})^3 \quad (3.49)$$

$$\int_{T_{3f}}^t b(t) dt = \omega_{3f} \left[\frac{3 \bar{I}_3^*}{K} \left\{ \frac{1}{6d_5^2} \ln \left\{ \frac{(d_5 + t)^2}{d_5^2 - d_5 t + t^2} \right\} \right. \right]$$

$$+ \frac{1}{d_5^2 \sqrt{3}} \tan^{-1} \left\{ \frac{2t - d_5}{d_5 \sqrt{3}} \right\} - t + T_{3f}] \quad (3.50)$$

$$\bar{I}_3^* = I_3^* + \frac{2}{3} K (T_{3f})^3 \quad (3.51)$$

$$d_5^3 = \frac{3 I_f^*}{K} \quad (3.52)$$

The time T_{3f} , at which the booms along the '1' and '2' axes are stopped, can be obtained as:

$$T_{3f} = \left[\frac{3 I_3^*}{2K} \left(\frac{\omega_3(0) - \omega_{3f}}{\omega_{3f}} \right) \right]^{1/3} \quad (3.53)$$

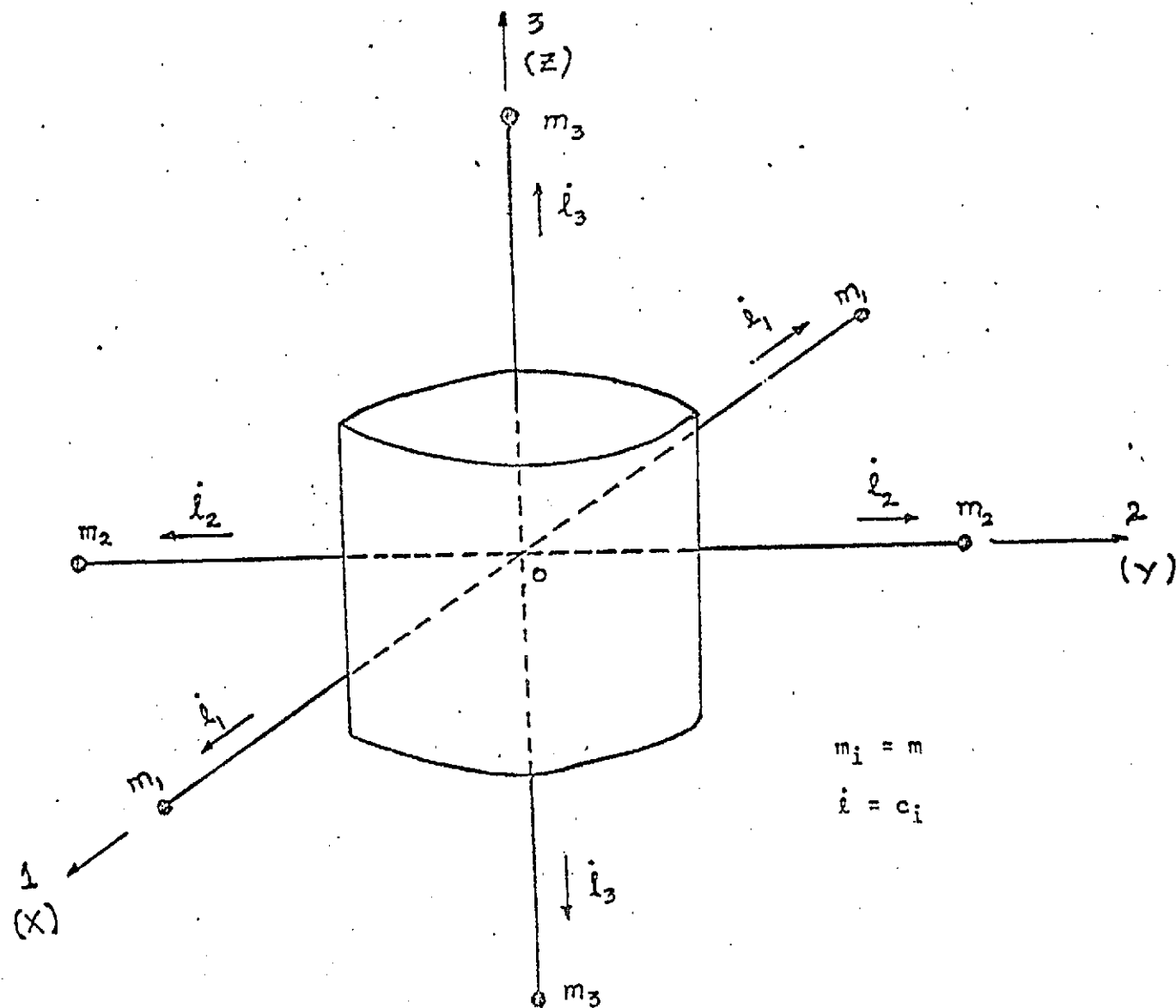


FIG. 3.1. SYSTEM GEOMETRY FOR END MASS EXTENSION MANEUVER USED TO RECOVER A TUMBLING SPACECRAFT.

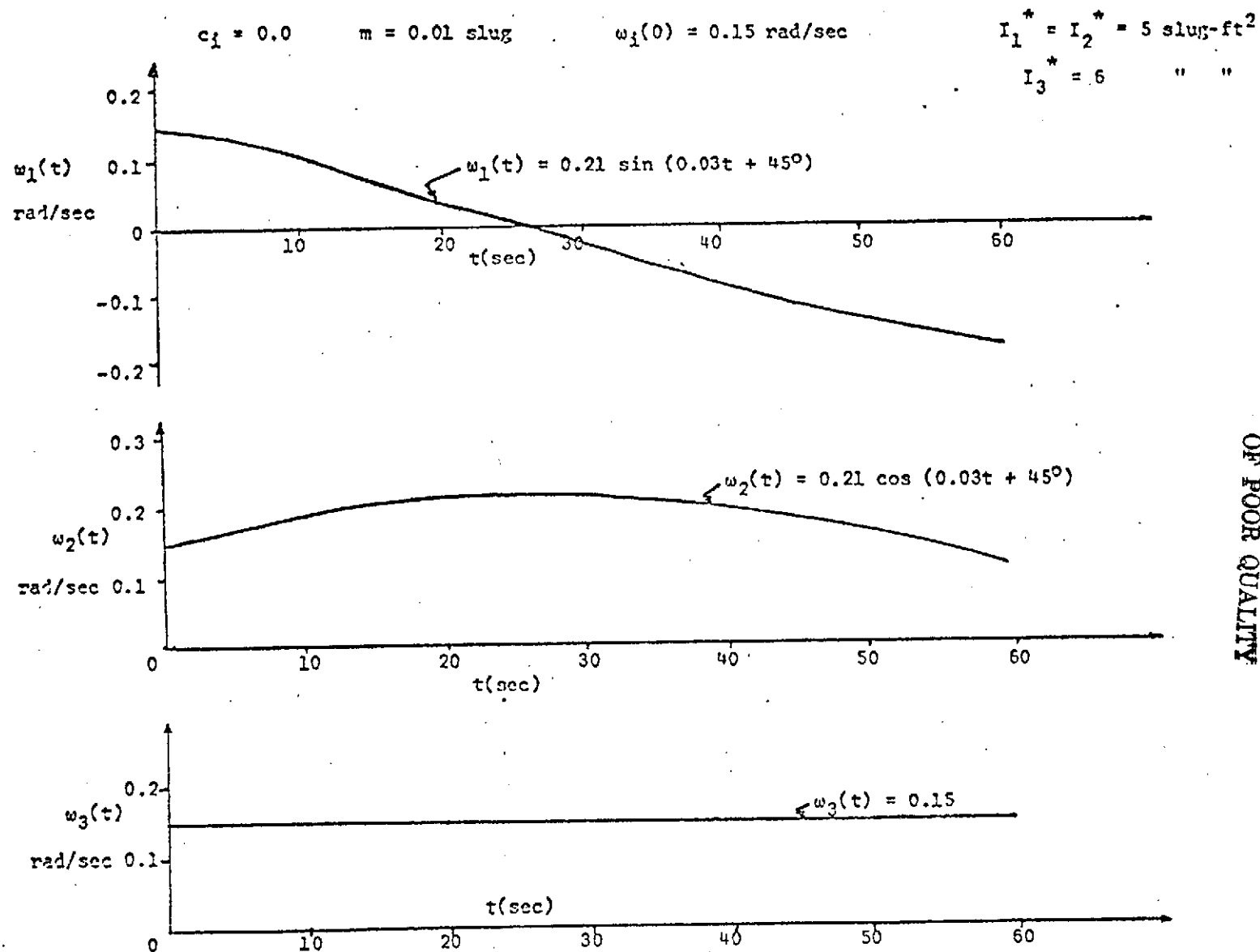


FIG. 3.2. DYNAMICS OF UNCONTROLLED MOTION - SLOW TUMBLING.

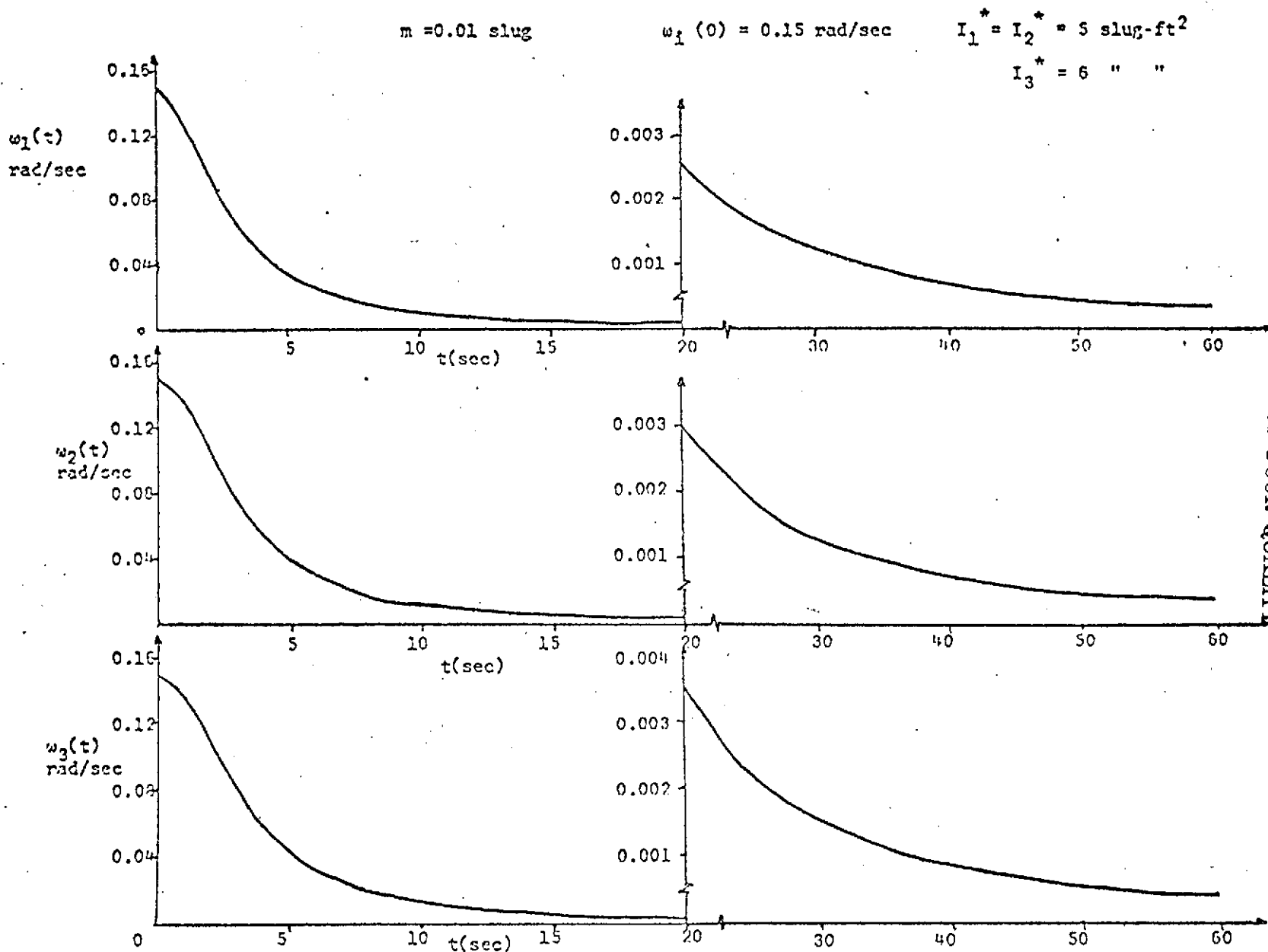

 ORIGINAL PAGE IS
 OF POOR QUALITY

FIG. 3.3. RECOVERY DYNAMICS FOR INITIAL SLOW TUMBLING
 WITH EXTENSION RATE $c_i = 4 \text{ ft/sec}$.

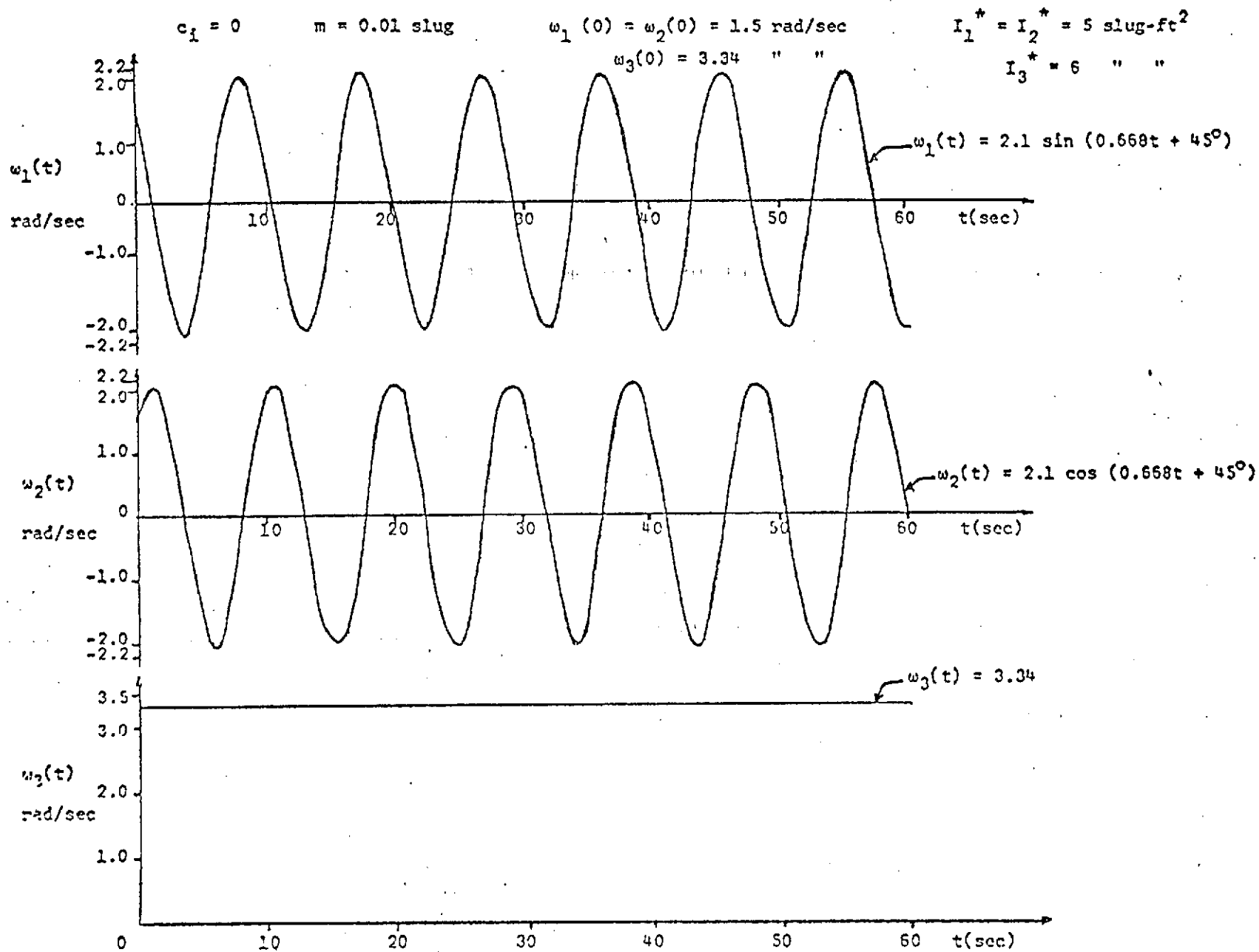


FIG. 3.4. DYNAMICS OF UNCONTROLLED MOTION - FAST TUMBLING.

$m = 0.01$ slug

$\omega_1(0) = \omega_2(0) = 1.5$ rad/sec

$I_1^* = I_2^* = 5$ slug-ft²

$\omega_3(0) = 3.34$ " "

$I_3^* = 6$ " "

57

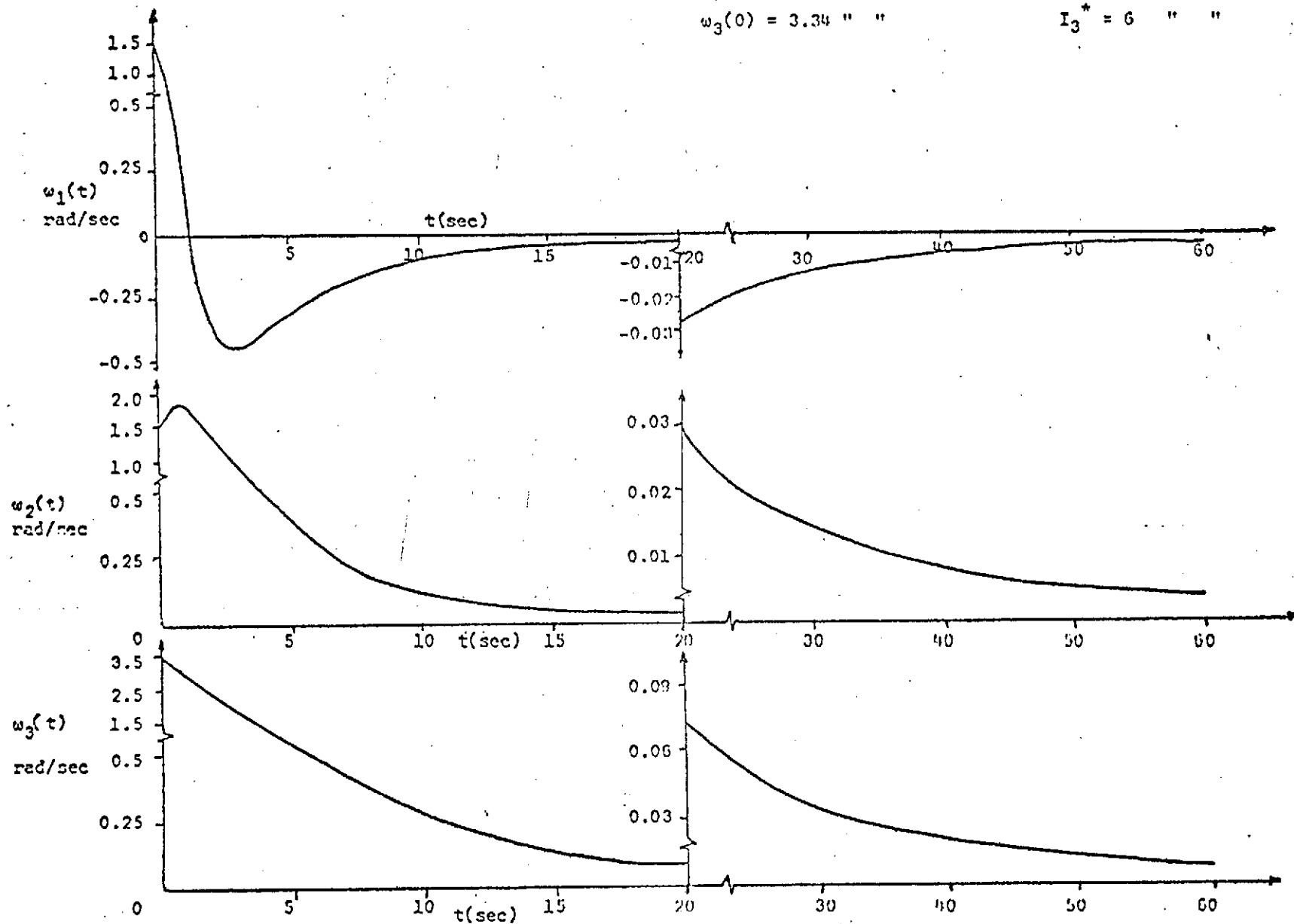


FIG. 3.5. RECOVERY DYNAMICS FOR INITIAL FAST TUMBLING
WITH EXTENSION RATE $c_i = 4$ ft/sec.

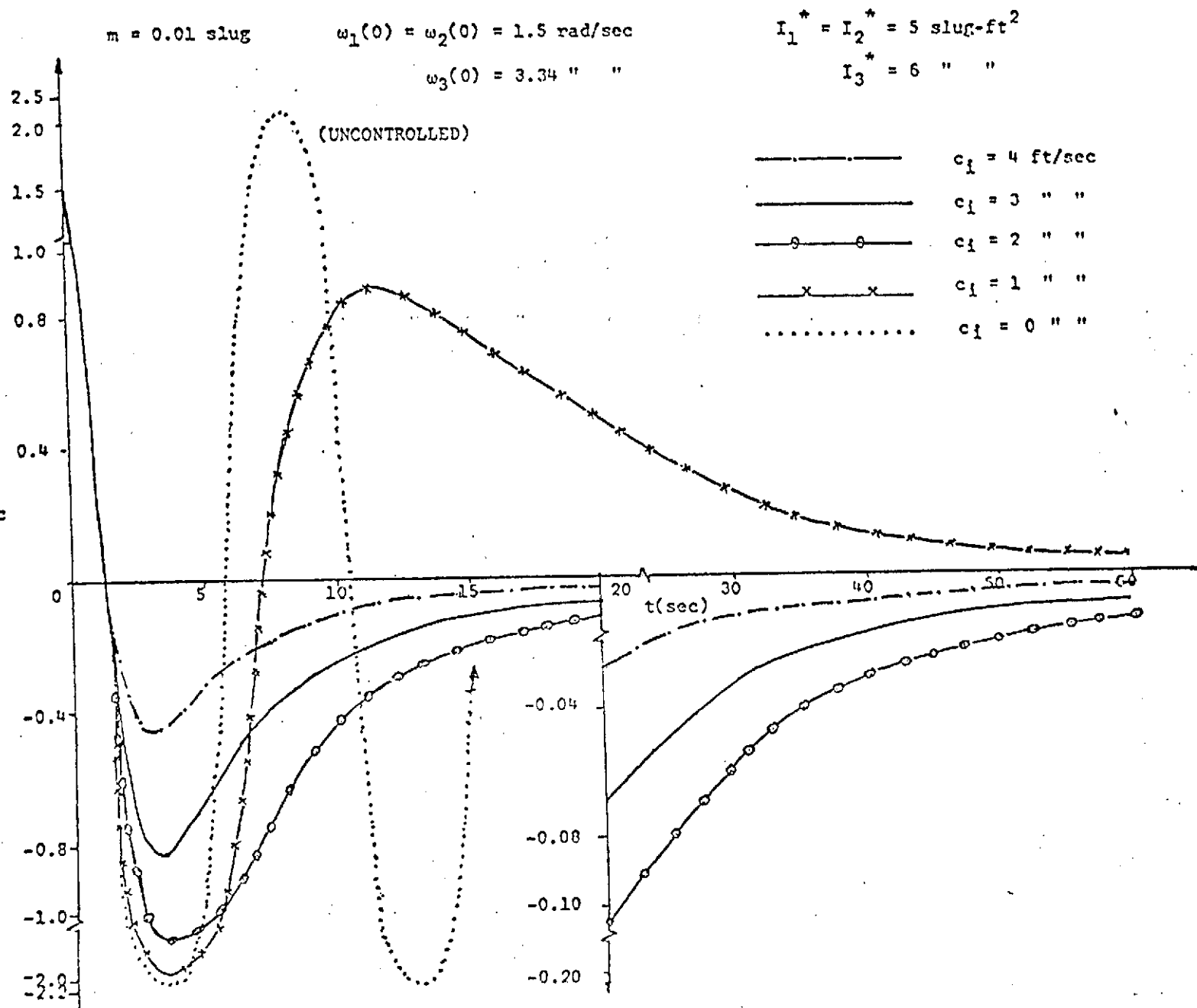


FIG. 3.6(a). EFFECT OF BOOM EXTENSION RATE ON RECOVERY (INITIAL FAST TUMBLING)

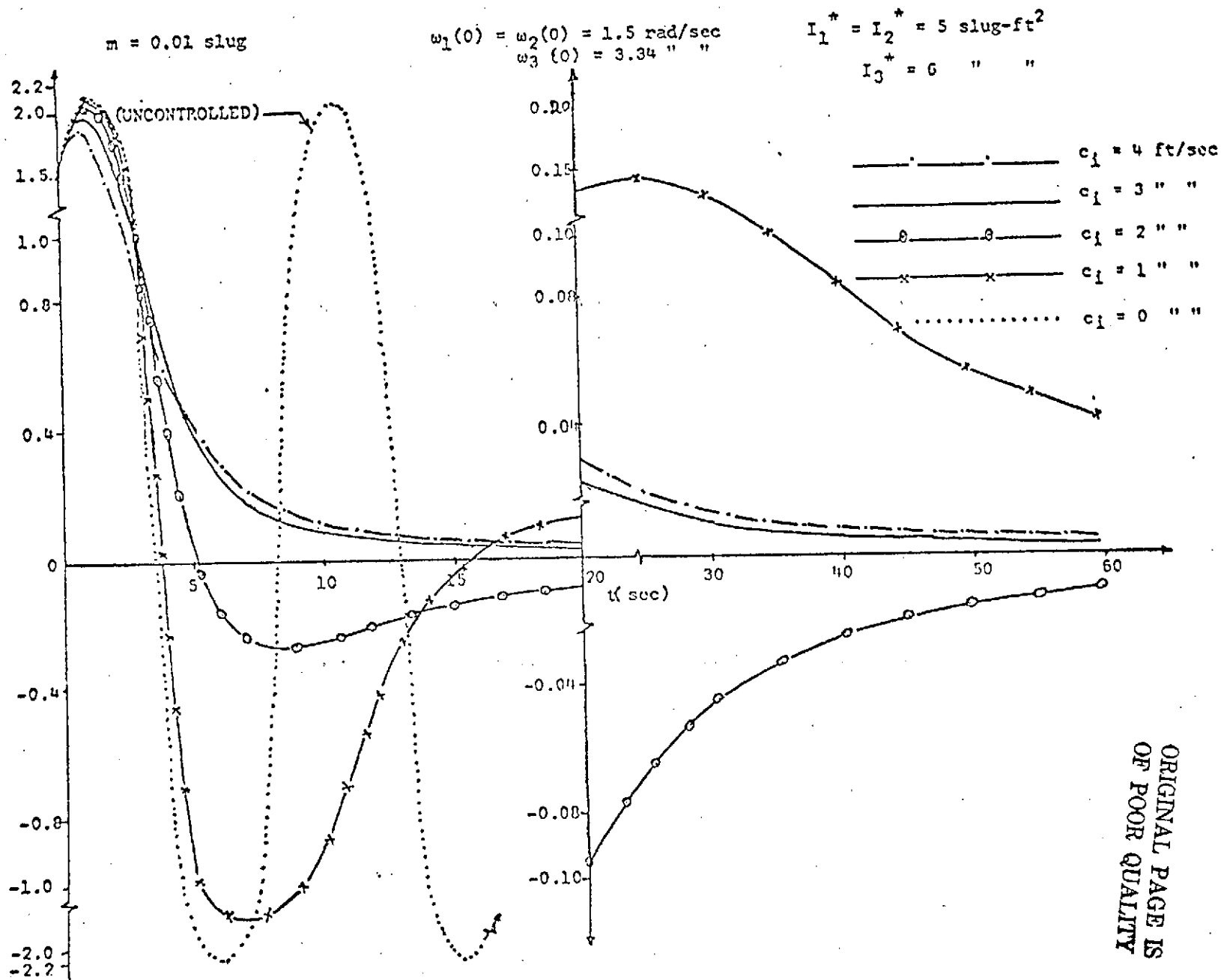


FIG. 3.6(b). EFFECT OF BOOM EXTENSION RATE ON RECOVERY (INITIAL FAST TUMBLING)

 ORIGINAL PAGE IS
 OF POOR QUALITY

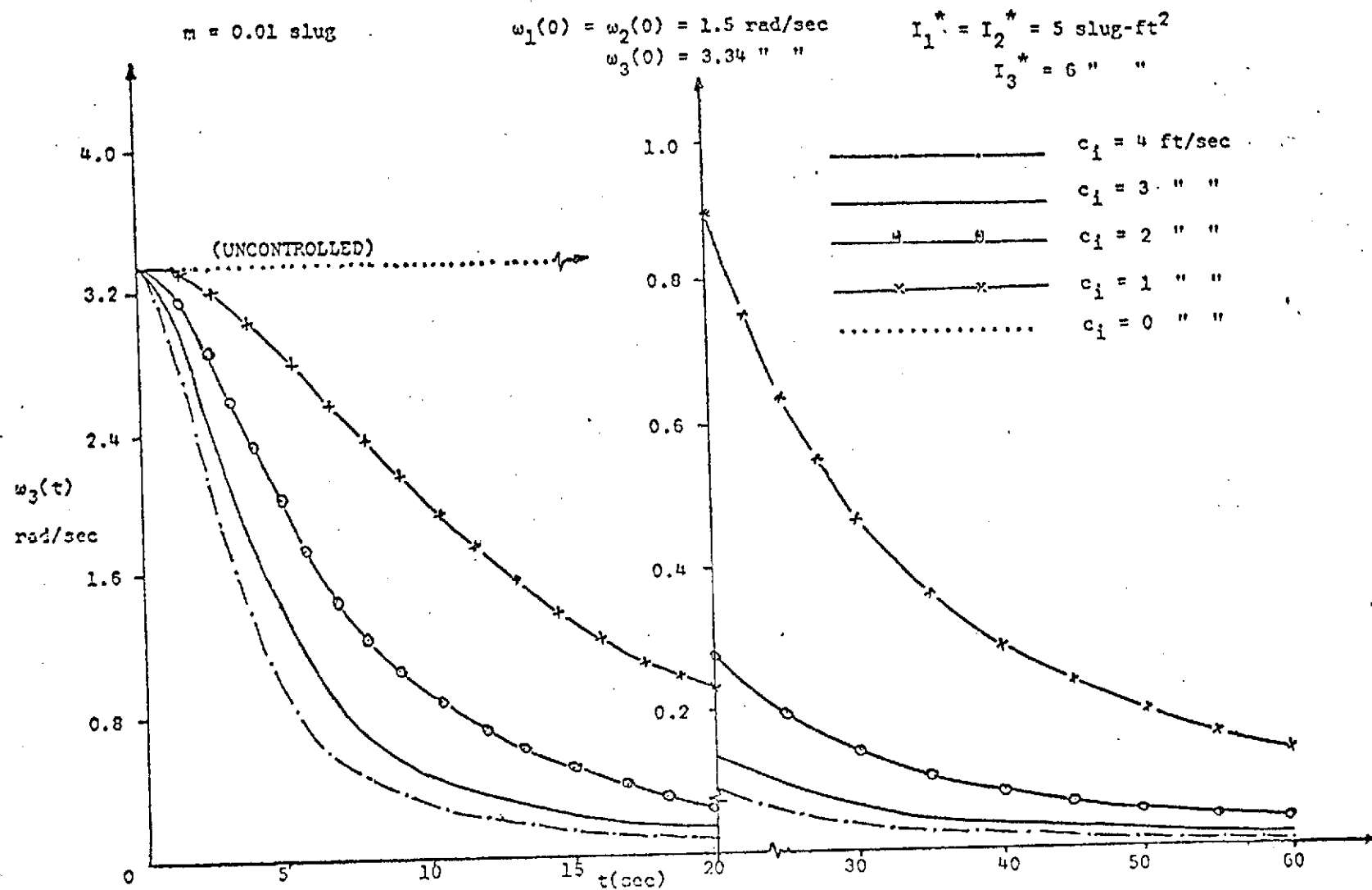


FIG. 3.6(c). EFFECT OF BOOM EXTENSION RATE ON RECOVERY (INITIAL FAST TUMBLING)

$m = 0.01$ slug

$I_1^* = 5.0$ slug-ft²

$I_3^* = 6.0$ " "

$\omega_1(0) = 1.5$ rad/sec

$\omega_2(0) = 1.5$ " "

$\omega_3(0) = 3.34$ " "

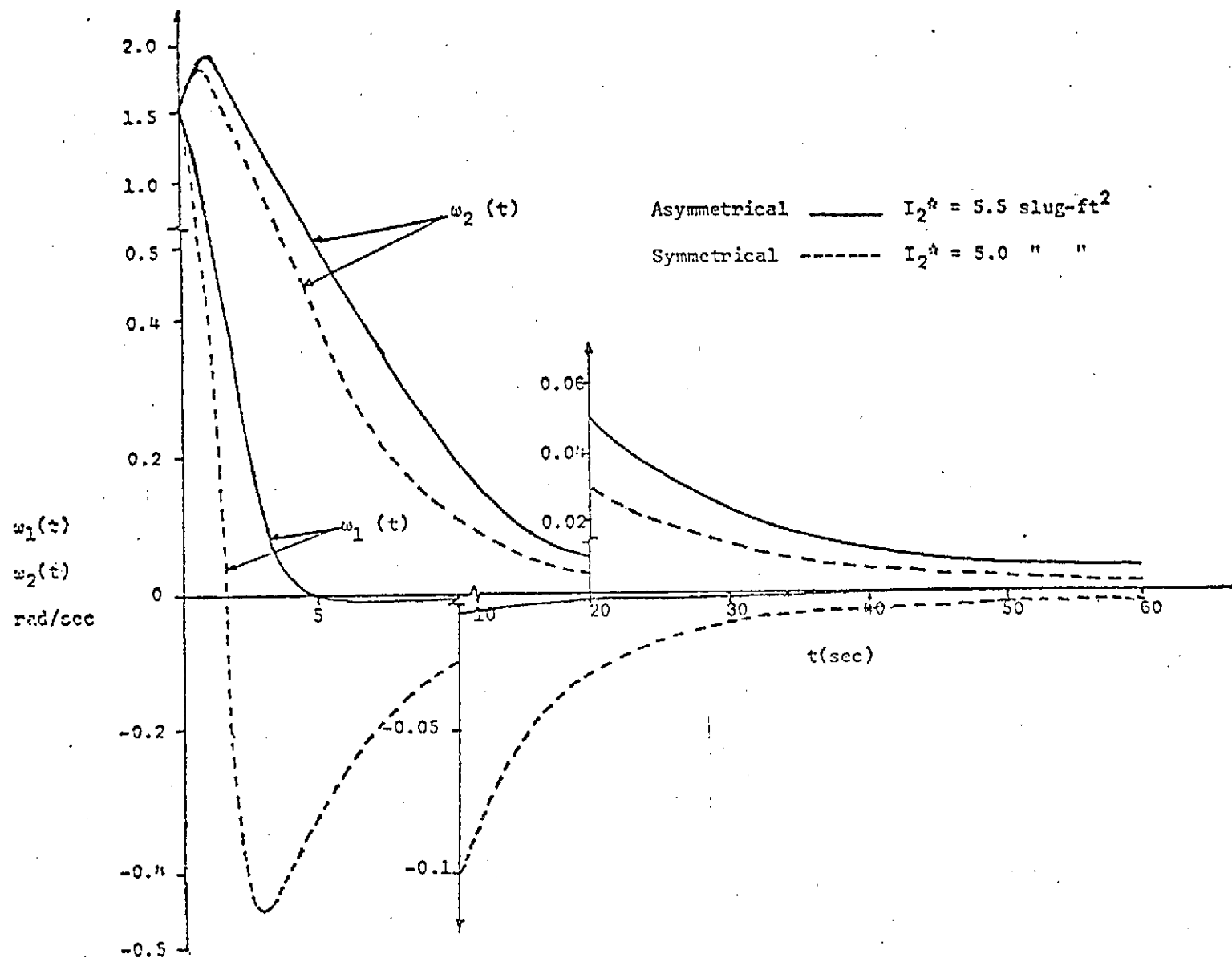


FIG. 3.7(a). COMPARISON OF RECOVERY DYNAMICS OF ASYMMETRICAL SPACECRAFT WITH SYMMETRICAL SPACECRAFT (EXTENSION RATE $\dot{c}_i = 4$ ft/sec).

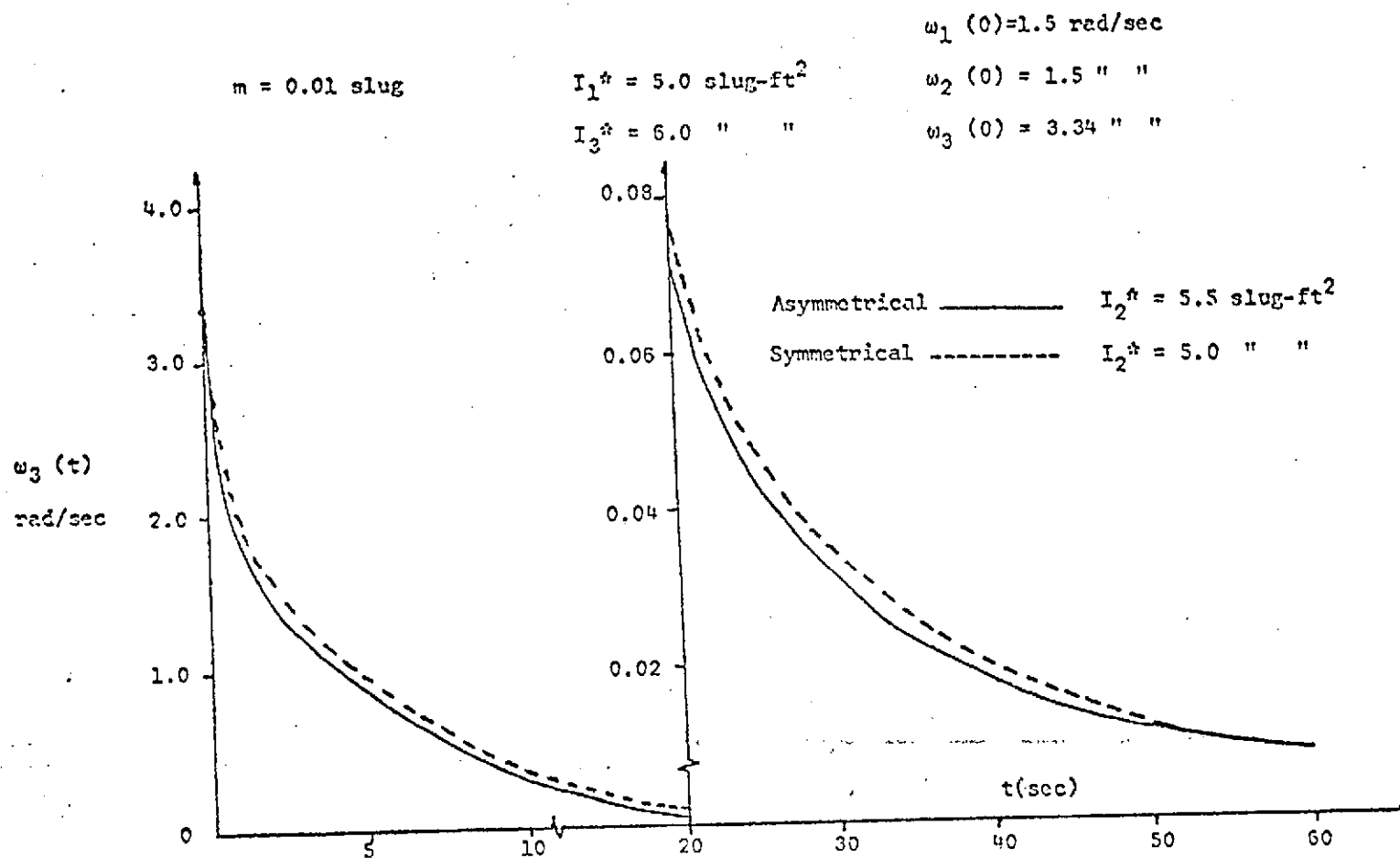


FIG. 3.7(b). COMPARISON OF RECOVERY DYNAMICS OF ASYMMETRICAL SPACECRAFT WITH SYMMETRICAL SPACECRAFT (EXTENSION RATE $c_i = 4 \text{ ft/sec}$).

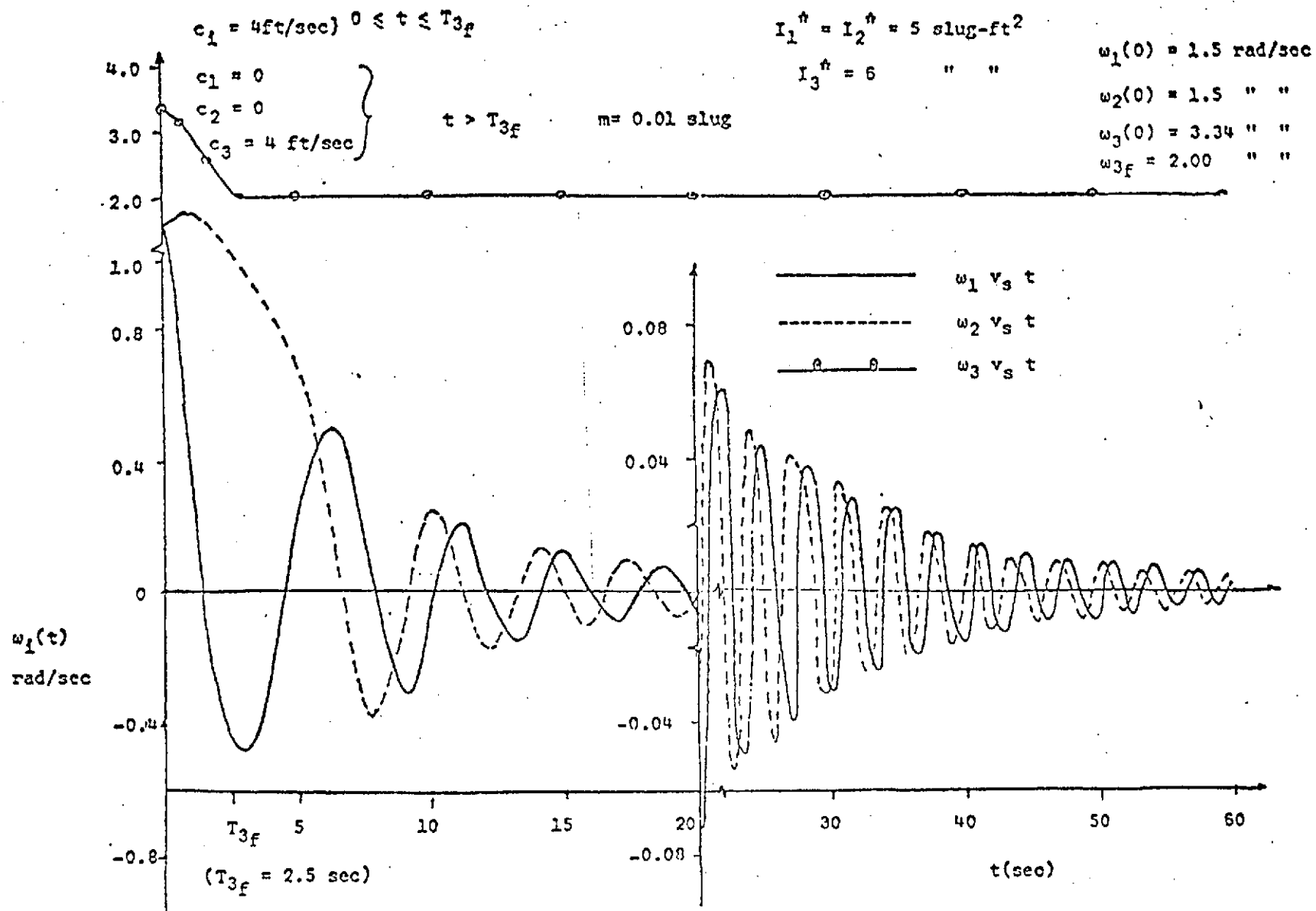


FIG. 3.8. RECOVERY MANEUVER TO ACHIEVE FINAL SPIN ALONG '3' AXIS
WITH EXTENSION RATE $c_i = 4 \text{ ft/sec}$

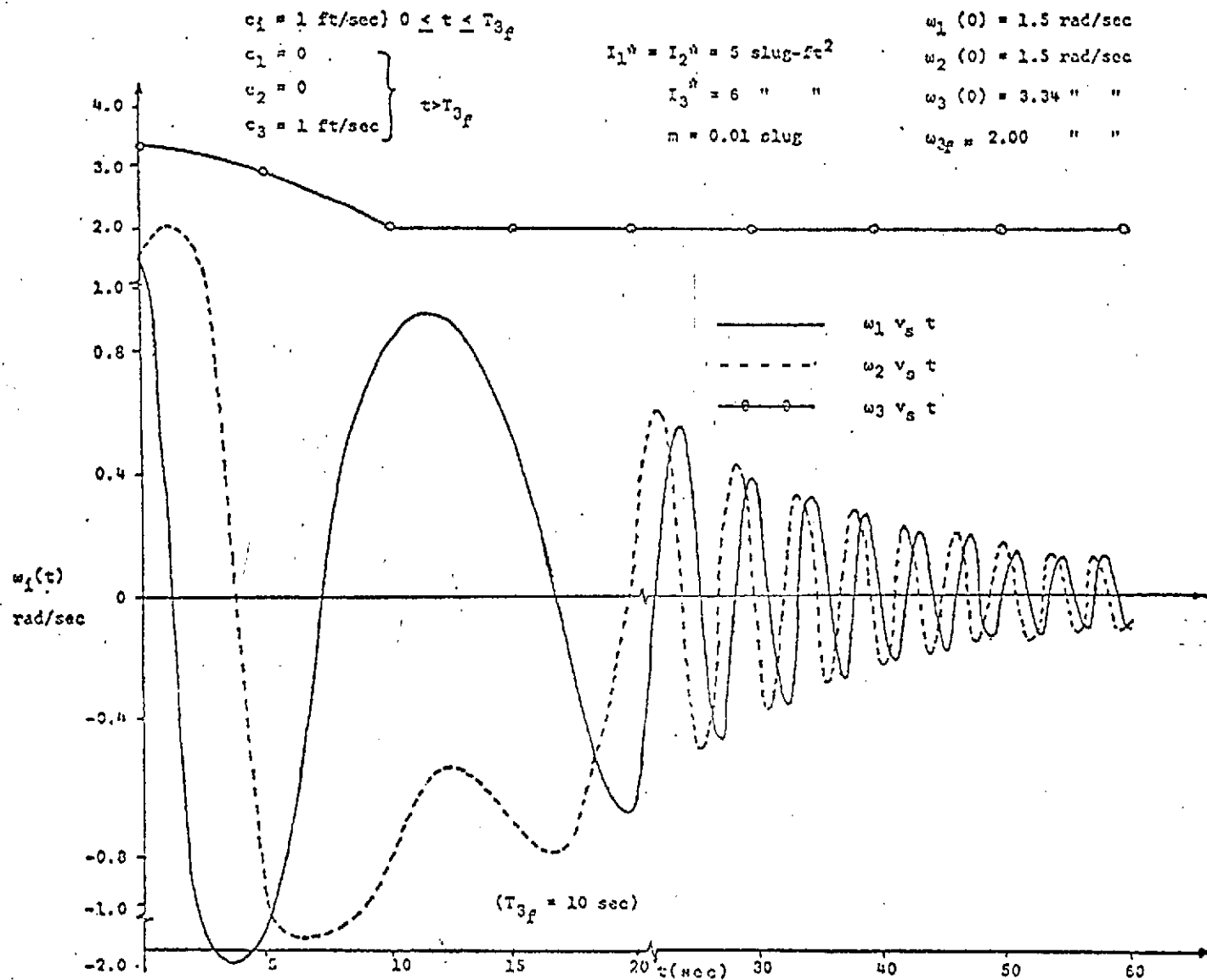


FIG. 3.9. RECOVERY MANEUVER TO ACHIEVE FINAL SPIN ALONG '3' AXIS WITH EXTENSION RATE $c_j = 1 \text{ ft/sec}$.

ORIGINAL PAGE IS
OF POOR QUALITY

$$c_1 = 4 \text{ ft/sec} \quad 0 \leq t \leq T_{3f}$$

$$c_1 = 0$$

$$c_2 = 0$$

$$c_3 = 4 \text{ ft/sec}$$

$$t > T_{3f}$$

$$I_1^* = 5.0 \text{ slug-ft}^2$$

$$I_3^* = 6.0 \text{ " "}$$

$$m = 0.01 \text{ slug}$$

$$\omega_1(0) = 1.5 \text{ rad/sec}$$

$$\omega_2(0) = 1.5 \text{ " "}$$

$$\omega_3(0) = 3.34 \text{ " "}$$

$$\omega_{3f} = 2.00 \text{ " " (desired)}$$

$$\omega_{3f} = 1.8 \text{ (achieved)}$$

$$I_2^* = 5.5 \text{ slug-ft}^2$$

$$I_2^* = 5.0 \text{ " "}$$

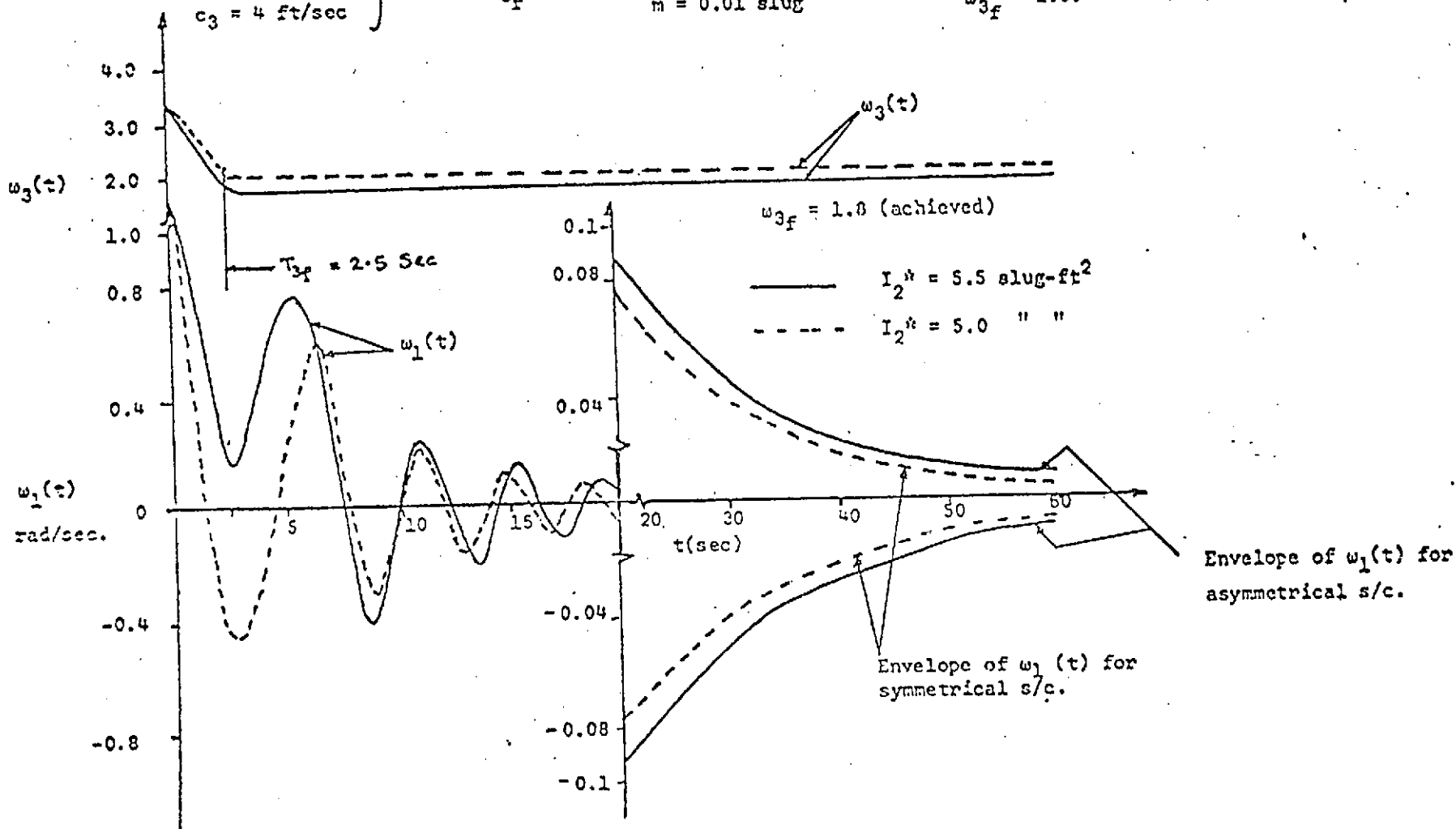


FIG. 3.10(a). COMPARISON OF RECOVERY MANEUVER OF ASYMMETRICAL SPACECRAFT WITH SYMMETRICAL SPACECRAFT TO ACHIEVE FINAL SPIN ALONG '3' AXIS (EXTENSION RATE $c_1 = 4 \text{ ft/sec}$).

$$c_1 = 4 \text{ ft/sec} \quad 0 \leq t \leq T_{3f}$$

$$c_1 = 0$$

$$c_2 = 0$$

$$c_3 = 4 \text{ ft/sec}$$

$$\left. \begin{array}{l} c_1 = 0 \\ c_2 = 0 \\ c_3 = 4 \text{ ft/sec} \end{array} \right\} t > T_{3f}$$

$$I_1^* = 5.0 \text{ slug-ft}^2$$

$$I_2^* = 6.0 \text{ " "}$$

$$m = 0.01 \text{ slug}$$

$$\omega_1(0) = 1.5 \text{ rad/sec}$$

$$\omega_2(0) = 1.5 \text{ " "}$$

$$\omega_3(0) = 3.34 \text{ " "}$$

$$\omega_{3f} = 2.0 \text{ (desired)}$$

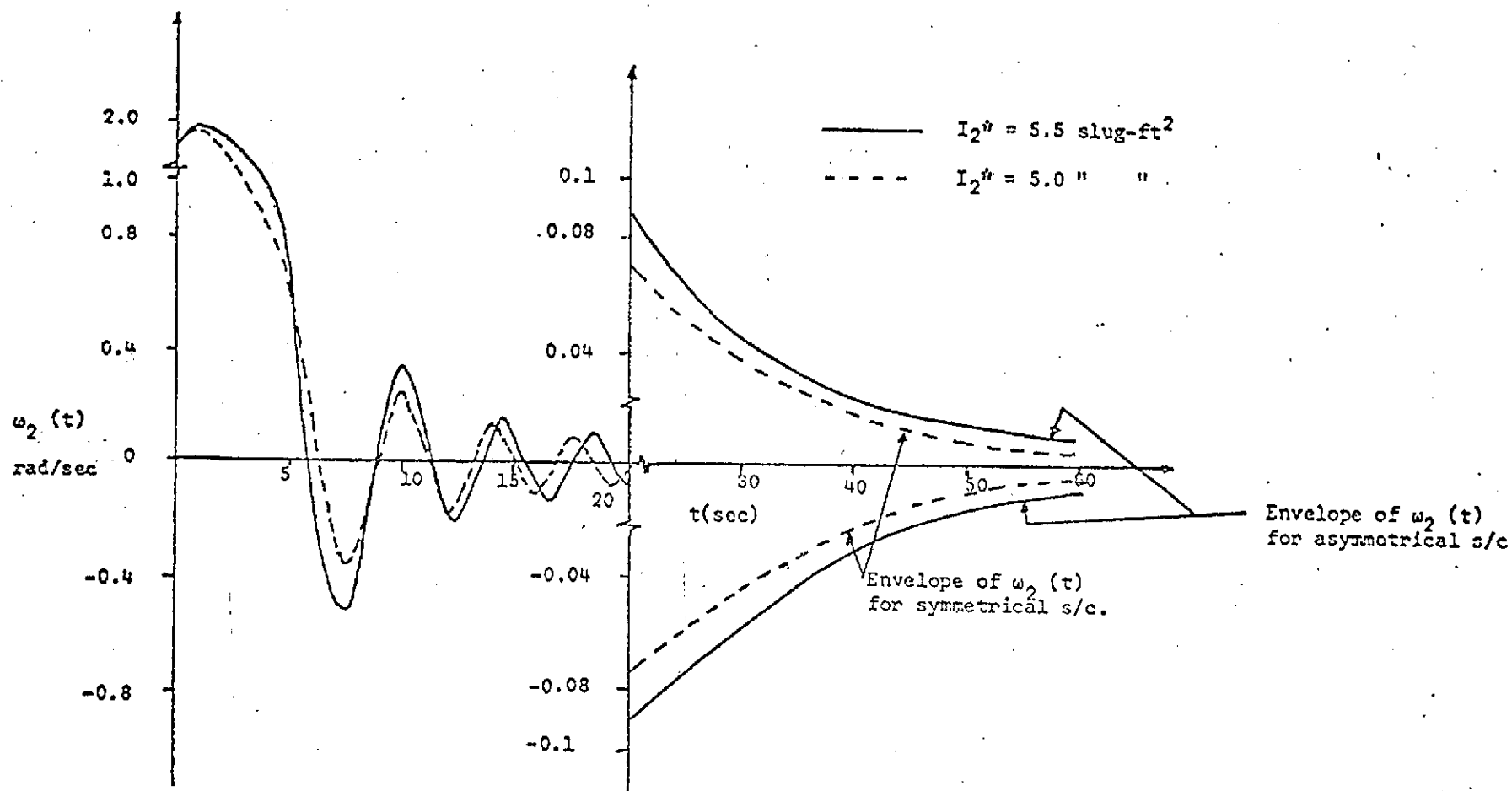


FIG. 3.10(b). COMPARISON OF RECOVERY MANEUVER OF ASYMMETRICAL SPACECRAFT WITH SYMMETRICAL SPACECRAFT TO ACHIEVE FINAL SPIN ALONG '3' AXIS (EXTENSION RATE $c_j=4$ ft/sec).

IV. TIME OPTIMAL CONTROL

1. Combination of Booms and Control Jets (Norm Invariant Principle)

In this section, we shall consider the control of a norm-invariant system which has the property that the Euclidean length of the state vector is constant when the control is zero. Here we state the problem and the control law to achieve the time optimal control of the system from Ref. 9.

Problem:

Given the controllable norm-invariant system

$$\dot{\bar{X}}(t) = g [\bar{X}(t); t] + \bar{u}(t); \bar{X}(0) = \bar{\xi} \quad (4.1)$$

Assume that the dimension of $\bar{u}(t)$ is the same as the dimension of $\bar{X}(t)$ and that $|| \bar{u}(t) || \leq m^*$ for all t . Then determine the control which forces the system (4.1) from the initial state $\bar{\xi}$ to 0 and which minimizes the cost functional

$$J = \int_0^{T_f} dt = T_f, \quad T_f - \text{free} \quad (4.2)$$

Control Law:

The unique time optimal control $\bar{u}^*(t)$ that is, the control which minimizes the cost J of Eq. (4.2) is given by,

$$\bar{u}^*(t) = -m^* \frac{\bar{X}^*(t)}{||\bar{X}^*(t)||} \quad (4.3)$$

where $\bar{X}^*(t)$ is the solution of Eq. (4.1) with $\bar{u}(t) = \bar{u}^*(t)$. The minimum value of J^* of the cost J , that is, the minimum time t^* ,

required to force $\bar{\xi}$ to 0 is given

$$J^* = t^* = \frac{||\bar{\xi}||}{m^*} \quad (4.4)$$

The above theory, which deals with the time optimal control of norm-invariant systems, is applied to the case of an unsymmetrical spacecraft tumbling in torque-free space. The angular momentum equations given by Eqs.(2.1) can be rewritten as:

$$\begin{aligned} \dot{h}_1 &= \left(\frac{1}{I_3} - \frac{1}{I_2}\right) h_2 h_3 \\ \dot{h}_2 &= \left(\frac{1}{I_1} - \frac{1}{I_3}\right) h_3 h_1 \\ \dot{h}_3 &= \left(\frac{1}{I_2} - \frac{1}{I_1}\right) h_1 h_2 \end{aligned} \quad (4.5)$$

$$\text{we find that, } \frac{d}{dt} ||\bar{h}(t)|| = \frac{\langle \dot{\bar{h}}(t), \bar{h}(t) \rangle}{||\bar{h}(t)||} = 0 \quad (4.6)$$

and so the system represented by Eq. (2.1) is norm-invariant.

Eqs.(2.1) describe the motion of the spacecraft in the absence of any applied torques. A torque vector, $\bar{u}(t)$, can be generated by means of gas jets, reaction wheels, gravity-gradient arrangements, etc. At any rate, if $\bar{u}(t)$ is a control torque, whose components are $\tau_i(t)$, $i = 1, 2, 3$, the equations of motion become:

$$\begin{aligned}
\dot{h}_1(t) &= \left[\frac{1}{I_3(t)} - \frac{1}{I_2(t)} \right] h_2(t) h_3(t) + \tau_1(t) \\
\dot{h}_2(t) &= \left[\frac{1}{I_1(t)} - \frac{1}{I_3(t)} \right] h_3(t) h_1(t) + \tau_2(t) \\
\dot{h}_3(t) &= \left[\frac{1}{I_2(t)} - \frac{1}{I_1(t)} \right] h_1(t) h_2(t) + \tau_3(t)
\end{aligned} \tag{4.7}$$

We can immediately conclude that, if the constraints on the control torque $\bar{u}(t)$ are of the form,

$$||\bar{u}(t)|| = \sqrt{\tau_1^2(t) + \tau_2^2(t) + \tau_3^2(t)} \leq m^* \tag{4.8}$$

the torque components for time optimal control are:

$$\begin{aligned}
\tau_1(t) &= - \frac{m^* I_1(t) \omega_1(t)}{||\bar{h}(t)||} \\
\tau_2(t) &= - \frac{m^* I_2(t) \omega_2(t)}{||\bar{h}(t)||} \\
\tau_3(t) &= - \frac{m^* I_3(t) \omega_3(t)}{||\bar{h}(t)||}
\end{aligned} \tag{4.9}$$

where $||\bar{h}(t)||$ is defined as:

$$||\bar{h}(t)|| = \sqrt{I_1^2(t) \omega_1^2(t) + I_2^2(t) \omega_2^2(t) + I_3^2(t) \omega_3^2(t)} \tag{4.10}$$

This means that, in order to reduce the angular momentum vector $\bar{h}(t)$ to zero in the shortest possible time, the torque vector $\bar{u}(t)$ must point in the opposite direction to the angular momentum vector $\bar{h}(t)$

and the torque $\bar{u}(t)$ must be as large as possible.

For the case of symmetrical spacecraft ($I_1(t) = I_2(t)$), the torque components required to reduce the transverse angular momentum to zero are given by:

$$\tau_1(t) = - \frac{m^* \omega_1(t)}{\sqrt{\omega_1^2(t) + \omega_2^2(t)}} \quad (4.11)$$

$$\tau_2(t) = - \frac{m^* \omega_2(t)}{\sqrt{\omega_1^2(t) + \omega_2^2(t)}}$$

$$\text{where } \sqrt{\tau_1^2(t) + \tau_2^2(t)} \leq m^* \quad (4.12)$$

Here we conclude that for a symmetrical spacecraft with $\omega_3 = \text{const}$ and $\tau_3(t) = 0$, the control torques required to reduce the transverse angular momentum are not explicitly dependent on the type of extension. It is doubtful that boom extensions alone could be used to effect time optimal control.

In general, we can say that in the event of control jet failure the booms could certainly be used as a back-up reusable system for de-tumbling (even if they cannot directly implement time optimal recovery).

2. Extension of End Masses

The extension of four end masses, along the symmetry axis of the spacecraft, is shown in Fig. 4.1. This scheme is considered as a possible means of reducing the transverse angular velocities in a time

optimal manner. The end masses are assumed to be equal and they are placed very close to the symmetry axis such that $d/\ell_j \ll 1$. The control variables are the extension rate $\dot{\ell}_1(t)$ and $\dot{\ell}_2(t)$.

The moments of inertia about the principal axes can be written as

$$\begin{aligned} I_1 &= I_2 = I^* + 4m(\ell_1^2 + \ell_2^2) = I \\ I_3 &= I_3^* \end{aligned} \quad (4.13)$$

The equations of motion can be developed, with $\omega_3 = \omega_0 = \text{const}$, as:

$$\begin{aligned} \dot{\omega}_1 &= \frac{(I^* - I_3^*)}{I^*} \omega_0 \omega_2 + \frac{4m}{I^*} (\ell_1^2 + \ell_2^2) (\omega_0 \omega_2 - \dot{\omega}_1) \\ &\quad - \frac{8m}{I^*} (\ell_1 \dot{\ell}_1 + \ell_2 \dot{\ell}_2) \omega_1 \end{aligned} \quad (4.14)$$

$$\begin{aligned} \dot{\omega}_2 &= -\frac{(I^* - I_3^*)}{I^*} \omega_0 \omega_1 - \frac{4m}{I^*} (\ell_1^2 + \ell_2^2) (\omega_0 \omega_1 + \dot{\omega}_2) \\ &\quad - \frac{8m}{I^*} (\ell_1 \dot{\ell}_1 + \ell_2 \dot{\ell}_2) \omega_2 \end{aligned} \quad (4.15)$$

Eqs. (4.14) and (4.15) can be rearranged to yield:

$$\dot{\omega}_1 = \omega \omega_2 + g(t)(\dot{\omega}_1 - \omega_0 \omega_2) + h(t) \omega_1 \quad (4.16)$$

$$\dot{\omega}_2 = -\omega \omega_1 + g(t)(\dot{\omega}_2 + \omega_0 \omega_1) + h(t) \omega_2 \quad (4.17)$$

$$\text{where } \omega = \frac{(I^* - I_3^*)}{I^*} \omega_0 \quad (4.18)$$

$$g(t) = -\frac{4m}{I^*} (\ell_1^2(t) + \ell_2^2(t)) \quad (4.19)$$

$$h(t) = -\frac{8m}{I^*} (\ell_1(t) \dot{\ell}_1(t) + \ell_2(t) \dot{\ell}_2(t)) \quad (4.20)$$

$$\text{and we observe, } h(t) = \dot{g}(t) \quad (4.21)$$

Using the transformation,

$$\begin{bmatrix} \Omega_1 \\ \Omega_2 \end{bmatrix} = \begin{bmatrix} \cos \omega_0 t & -\sin \omega_0 t \\ \sin \omega_0 t & \cos \omega_0 t \end{bmatrix} \begin{bmatrix} \omega_1 \\ \omega_2 \end{bmatrix} \quad (4.22)$$

Eqs. (4.16) and (4.17) become

$$\begin{bmatrix} \dot{\Omega}_1(t) \\ \dot{\Omega}_2(t) \end{bmatrix} = \begin{bmatrix} 0 & (\omega - \omega_0) \\ -(\omega - \omega_0) & 0 \end{bmatrix} \begin{bmatrix} \Omega_1(t) \\ \Omega_2(t) \end{bmatrix} + \frac{d}{dt} \left[g(t) \begin{bmatrix} \Omega_1(t) \\ \Omega_2(t) \end{bmatrix} \right] \quad (4.23)$$

Comparing Eq. (4.23) with the standard form (Ref. 8, p. 599, Eq. (7.378))

$$\begin{bmatrix} \dot{x}_1(t) \\ \dot{x}_2(t) \end{bmatrix} = \begin{bmatrix} 0 & \omega \\ -\omega & 0 \end{bmatrix} \begin{bmatrix} x_1(t) \\ x_2(t) \end{bmatrix} + K \begin{bmatrix} u_1(t) \\ u_2(t) \end{bmatrix} \quad (4.24)$$

we can write,

$$\frac{d}{dt} (g(t) \Omega_1(t)) = K u_1(t) \quad (4.25)$$

$$\frac{d}{dt} (g(t) \Omega_2(t)) = K u_2(t)$$

For time optimal control

$$u_1(t) = \pm 1 \quad (4.26)$$

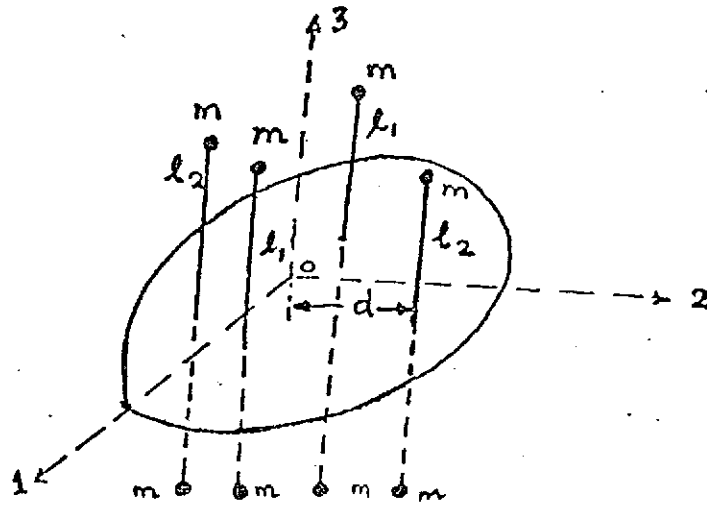
$$u_2(t) = \pm 1$$

Expanding Eq. (4.25), using Eqs. (4.19) and (4.20) with Eq. (4.26), the following result is obtained.

$$-\frac{4m}{I^*} [(\dot{\ell}_1^2(t) + \dot{\ell}_2^2(t))\dot{\Omega}_1(t) + 2(\ell_1(t)\dot{\ell}_1(t) + \ell_2(t)\dot{\ell}_2(t))\Omega_1(t)] = \pm 1 \quad (4.27)$$

$$-\frac{4m}{I^*} [(\dot{\ell}_1^2(t) + \dot{\ell}_2^2(t))\dot{\Omega}_2(t) + 2(\ell_1(t)\dot{\ell}_1(t) + \ell_2(t)\dot{\ell}_2(t))\Omega_2(t)] = \pm 1 \quad (4.28)$$

From the above equations, we observe that the control variables $\dot{\ell}_1(t)$ and $\dot{\ell}_2(t)$ are nonlinearly coupled with the state variables and the solution for $\dot{\ell}_i(t)$ becomes trivial. It can be concluded that the time optimal control of this type of system using only boom extension rates can not be established by analytic means. However it may be possible to consider this problem by using techniques of dynamic programming.



Extension rates: $\dot{l}_1(t)$, $\dot{l}_2(t)$; $\frac{d}{l_i} \ll 1$

Symmetry about '3' axis is maintained

Masses are equal; $m_1 = m_2 = m$

ORIGINAL PAGE IS
OF POOR QUALITY

FIG. 4.1. EXTENSION OF END MASSES ALONG '3' AXIS.

V. HINGED SYSTEM

1. Derivation of Kinetic Energy

The hinged system to be studied is shown schematically in Fig.

5.1. The co-ordinate system representation is shown in Fig. 5.2. The system consists of a spinning spacecraft with masses attached to massless booms of constant length ℓ , which in turn are attached to the main spacecraft at radius r_0 . The end masses are released at $t = t_0$ and thereafter swing out from the spin axis. The angles between the booms and the spin axis are denoted by α_1 and α_2 as shown in Fig. 5.2 and are initially zero. A special case of this type was considered in Ref. 2 (where it was assumed that the transverse angular velocities during deployment remained at zero) but here we consider the general three dimensional deployment dynamics.

The development of the kinetic energy of this type of hinged system from first principles is considered below:

The total kinetic energy of the system, in terms of rotational and translational energies, can be written as,

$$T = T_r + T_t + \text{const. due to (circular) orbit motion} \quad (5.1)$$

$$\text{where } T_r = \frac{1}{2} (I_1 \omega_1^2 + I_2 \omega_2^2 + I_3 \omega_3^2) \quad (5.2)$$

$$T_t = \frac{1}{2} M V_M^2 / \text{cm} + \sum_{i=1}^n m_i V_{mi}^2 / \text{cm} \quad (5.3)$$

(M = mass of main body)

From the definition of center of mass of the system:

$$\bar{r}_{cm/o} = \frac{m \sum_{i=1}^n \bar{r}_{i/o}}{M + \sum_{i=1}^n m_i} \quad (5.4)$$

where point 'o' is the center of coordinate system and the masses are assumed to be equal ($m_i = m$). The velocity of the various components relative to the system center of mass may be expressed:

$$\bar{v}_{m_i/cm} = \bar{v}_{m_i/o} + \bar{v}_{o/cm} \quad (5.5)$$

$$\bar{v}_{M/cm} = \bar{v}_{M/o} + \bar{v}_{o/cm} \quad (5.6)$$

The components appearing in Eqs. (5.5) and (5.6) can be further represented as:

$$\bar{v}_{m_i/o} = \dot{\bar{r}}_i \quad (5.7)$$

$$\bar{v}_{O/M} = 0 \quad (5.8)$$

$$\bar{v}_{o/cm} = -\bar{v}_{cm/o} = -\dot{\bar{r}}_{cm/o} = -\frac{m \sum \dot{\bar{r}}_i}{M + \sum m_i} \quad (5.9)$$

Upon substitution of Eqs. (5.7), (5.8) and (5.9) into Eq. (5.3), the translational energy may be expressed as

$$\begin{aligned} T_t = & \frac{M}{2} |\bar{v}_{o/cm}|^2 + \frac{1}{2} \sum m_i |\bar{v}_{m_i/o}|^2 \\ & + \frac{1}{2} \sum m_i |\bar{v}_{o/cm}|^2 + \sum m_i (\bar{v}_{m_i/o}) \cdot (\bar{v}_{o/cm}) \end{aligned} \quad (5.10)$$

After some algebraic manipulations, we obtain,

$$T_t = \frac{m}{2} \sum (\bar{V}_i \cdot \bar{V}_i) - \frac{m^2}{2\bar{M}} \left(\sum \bar{V}_i \cdot \sum \bar{V}_i \right) \quad (5.11)$$

$$\text{where } \bar{V}_i = \dot{\bar{r}}_i + \bar{\omega} \times \bar{r}_i$$

$$\bar{M} = M + \sum m_i$$

Thus, the total kinetic energy of the system is given by:

$$\begin{aligned} T = & \frac{1}{2} (I_1 \omega_1^2 + I_2 \omega_2^2 + I_3 \omega_3^2) + \frac{m}{2} \sum_{i=1}^n (\bar{V}_i \cdot \bar{V}_i) \\ & - \frac{m^2}{2\bar{M}} \left(\sum_{i=1}^n \bar{V}_i \cdot \sum_{i=1}^n \bar{V}_i \right) + \text{const.} \end{aligned} \quad (5.12)$$

As an example, we consider the case from Ref. 2 where $m = m/2$,

$\alpha_1 = \alpha_2 = \alpha$, $I_3 = I$ and $\omega_3 = \dot{\theta}$. The kinetic energy is then obtained as (neglecting orbital motion)

$$\begin{aligned} T = & \frac{1}{2} I \dot{\theta}^2 + \frac{m}{2} [\ell^2 \dot{\alpha}^2 + \dot{\theta}^2 (r_0 + \ell \sin \alpha)^2] \\ & - \frac{m^2}{2} \frac{\ell^2}{(M + m)} \sin^2 \alpha \dot{\alpha}^2 \end{aligned} \quad (5.13)$$

which corresponds identically with Eq. (18) of Ref. 2, which was presented without development.

Next, a more general case of the hinged deployment system considered is shown in Fig. 5.3. Here there is no restriction on the location of the hinge points. The co-ordinates of the two masses are given by

$$\begin{aligned}
x_1 &= 0 & x_2 &= 0 \\
y_1 &= r_0 + \ell \sin \alpha_1 & y_2 &= -(r_0 + \ell \sin \alpha_2) \\
z_1 &= a_* - \ell \cos \alpha_1 & z_2 &= a_* - \ell \cos \alpha_2
\end{aligned} \tag{5.14}$$

Here ' a_* ' is the offset of the hinge point from the '2' axis. Upon substituting Eqs. (5.14) into Eq. (5.12), and after algebraic simplifications, the resulting equation for kinetic energy is:

$$\begin{aligned}
T &= \frac{1}{2} [I_1 \omega_1^2 + I_2 \omega_2^2 + I_3 \omega_3^2] \\
&+ \frac{m}{2} [\{ 2(r_0^2 + a_*^2 + \ell^2) + 2\ell \{ r_0(\sin \alpha_1 + \sin \alpha_2) - a_*(\cos \alpha_1 + \cos \alpha_2) \} \} \omega_1^2 \\
&+ \{ 2a_*^2 - 2a_*\ell(\cos \alpha_1 + \cos \alpha_2) + \ell^2(\cos^2 \alpha_1 + \cos^2 \alpha_2) \} \omega_2^2 \\
&+ \{ 2r_0^2 + 2r_0\ell(\sin \alpha_1 + \sin \alpha_2) + \ell^2(\sin^2 \alpha_1 + \sin^2 \alpha_2) \} \omega_3^2 \\
&- \{ 2\ell \{ a_*(\sin \alpha_1 - \sin \alpha_2) - r_0(\cos \alpha_1 - \cos \alpha_2) \} \\
&- 2\ell^2(\sin \alpha_1 \cos \alpha_1 - \sin \alpha_2 \cos \alpha_2) \} \omega_2 \omega_3 \\
&+ \{ 2\ell^2(\dot{\alpha}_1 - \dot{\alpha}_2) + 2\ell \{ \dot{\alpha}_1 (r_0 \sin \alpha_1 - a_* \cos \alpha_1) \\
&- \dot{\alpha}_2 (r_0 \sin \alpha_2 - a_* \cos \alpha_2) \} \} \omega_1 + \ell^2 (\dot{\alpha}_1^2 + \dot{\alpha}_2^2)] \\
&- \frac{m^2}{2(M+2m)} [\{ 2(2a_*^2 + \ell^2) + 2\ell^2 \cos(\alpha_1 + \alpha_2) - 4a_*\ell(\cos \alpha_1 + \cos \alpha_2) \} \omega_1^2 \\
&+ \{ 2a_* - \ell(\cos \alpha_1 + \cos \alpha_2) \}^2 \omega_2^2 + \ell^2(\sin \alpha_1 - \sin \alpha_2)^2 \omega_3^2
\end{aligned}$$

$$\begin{aligned}
& -2l(\sin\alpha_1 - \sin\alpha_2) \{2a_* - l(\cos\alpha_1 + \cos\alpha_2)\} \omega_2\omega_3 \\
& + 2l\{l(\ddot{\alpha}_1 - \ddot{\alpha}_2) + l \cos(\alpha_1 + \alpha_2)(\dot{\alpha}_1 - \dot{\alpha}_2) \\
& - 2a_* (\cos\alpha_1 \dot{\alpha}_1 - \cos\alpha_2 \dot{\alpha}_2)\} \omega_1 \\
& + l^2 \{\dot{\alpha}_1^2 + \dot{\alpha}_2^2 - 2\dot{\alpha}_1\dot{\alpha}_2 \cos(\alpha_1 + \alpha_2)\} + \text{const.} \quad (5.15)
\end{aligned}$$

2. Development of Equations of Motion (Neglecting External Torques)

The equations of motion in the five variables $\omega_1, \omega_2, \omega_3, \alpha_1$ and α_2 are developed using the Quasi-Lagrangian formulation¹⁴ for ω_i , $i = 1, 2, 3$ and the general Lagrangian formulation for the variables α_1, α_2 . The equations of motion for this system can be represented by:

$$\frac{d}{dt} \frac{\partial T}{\partial \omega_1} - \omega_3 \frac{\partial T}{\partial \omega_2} + \omega_2 \frac{\partial T}{\partial \omega_3} = 0 \quad (5.16)$$

$$\frac{d}{dt} \frac{\partial T}{\partial \omega_2} - \omega_1 \frac{\partial T}{\partial \omega_3} + \omega_3 \frac{\partial T}{\partial \omega_1} = 0 \quad (5.17)$$

$$\frac{d}{dt} \frac{\partial T}{\partial \omega_3} - \omega_2 \frac{\partial T}{\partial \omega_1} + \omega_1 \frac{\partial T}{\partial \omega_2} = 0 \quad (5.18)$$

$$\frac{d}{dt} \frac{\partial T}{\partial \dot{\alpha}_1} - \frac{\partial T}{\partial \alpha_1} + \frac{\partial F}{\partial \dot{\alpha}_1} = 0 \quad (5.19)$$

$$\frac{d}{dt} \frac{\partial T}{\partial \dot{\alpha}_2} - \frac{\partial T}{\partial \alpha_2} + \frac{\partial F}{\partial \dot{\alpha}_2} = 0 \quad (5.20)$$

where T = Total kinetic energy of the system

F = Rayleigh dissipation function.

Making the approximation: $m^2/\bar{M} \ll m$ or $(m/\bar{M} \ll 1)$ and letting $F = 0$ (for the case of no assumed energy dissipation), the equations of motion are obtained as follows:

$$\begin{aligned}
 I_1 \dot{\omega}_1 - (I_2 - I_3) \omega_2 \omega_3 + m[2(r_0^2 + a_*^2 + \ell^2) + 2\ell\{r_0(s\alpha_1 + s\alpha_2) - a_*(c\alpha_1 + c\alpha_2)\}] \dot{\omega}_1 \\
 - m\{2\dot{a}_*^2 - 2a_*\ell(c\alpha_1 + c\alpha_2) + \ell^2(c^2\alpha_1 + c^2\alpha_2) - 2r_0^2 - 2r_0\ell(s\alpha_1 + s\alpha_2)\} \omega_2 \omega_3 \\
 + 2m\ell\{r_0(c\alpha_1 \dot{\alpha}_1 + c\alpha_2 \dot{\alpha}_2) + a_*(s\alpha_1 \dot{\alpha}_1 + s\alpha_2 \dot{\alpha}_2)\} \omega_1 \\
 + m\ell\{a_*(s\alpha_1 - s\alpha_2) - r_0(c\alpha_1 - c\alpha_2) - \frac{\ell}{2}(s^2\alpha_1 - s^2\alpha_2)\} (\omega_3^2 - \omega_2^2) \\
 + m\ell\{\ell(\ddot{\alpha}_1 - \ddot{\alpha}_2) + (\dot{\alpha}_1)^2(r_0c\alpha_1 + a_*s\alpha_1) + \ddot{\alpha}_1(r_0s\alpha_1 - a_*c\alpha_1) \\
 - (\dot{\alpha}_2)^2(r_0c\alpha_2 + a_*s\alpha_2) - \ddot{\alpha}_2(r_0s\alpha_2 - a_*c\alpha_2)\} = 0 \quad (5.21)
 \end{aligned}$$

$$\begin{aligned}
 I_2 \dot{\omega}_2 - (I_3 - I_1) \omega_3 \omega_1 + m\{2\dot{a}_*^2 - 2a_*\ell(c\alpha_1 + c\alpha_2) + \ell^2(c^2\alpha_1 + c^2\alpha_2)\} \dot{\omega}_2 \\
 - m\ell\{a_*(s\alpha_1 - s\alpha_2) - r_0(c\alpha_1 - c\alpha_2) - \frac{\ell}{2}(s^2\alpha_1 - s^2\alpha_2)\} \dot{\omega}_3 \\
 + m\ell\{a_*(s\alpha_1 - s\alpha_2) - r_0(c\alpha_1 - c\alpha_2) - \frac{\ell}{2}(s^2\alpha_1 - s^2\alpha_2)\} \omega_1 \omega_2 \\
 - m\{\ell^2(s^2\alpha_1 + s^2\alpha_2) - 2(a_*^2 + \ell^2) + 2\ell a_*(c\alpha_1 + c\alpha_2)\} \omega_3 \omega_1
 \end{aligned}$$

$$\begin{aligned}
& + m \{ 2a_* \ell (s\alpha_1 \dot{\alpha}_1 + s\alpha_2 \dot{\alpha}_2) - \ell^2 (s2x_1 \dot{\alpha}_1 + s2\alpha_2 \dot{\alpha}_2) \} \omega_2 \\
& + m \ell \{ \ell (\dot{\alpha}_1 - \dot{\alpha}_2) - 2a_* (c\alpha_1 \dot{\alpha}_1 - c\alpha_2 \dot{\alpha}_2) + \ell (c2x_1 \dot{\alpha}_1 - c2\alpha_2 \dot{\alpha}_2) \} \omega_3 = 0
\end{aligned} \tag{5.22}$$

$$\begin{aligned}
I_3 \dot{\omega}_3 - (I_1 - I_2) \omega_1 \omega_2 + m \{ 2r_0^2 + 2r_0 \ell (s\alpha_1 + s\alpha_2) + \ell^2 (s^2\alpha_1 + s^2\alpha_2) \} \dot{\omega}_3 \\
- m \ell \{ a_* (s\alpha_1 - s\alpha_2) - r_0 (c\alpha_1 - c\alpha_2) - \frac{\ell}{2} (s2x_1 - s2\alpha_2) \} \dot{\omega}_2 \\
- m \{ 2(r_0^2 + \ell^2) + 2\ell r_0 (s\alpha_1 + s\alpha_2) - \ell^2 (c^2\alpha_1 + c^2\alpha_2) \} \omega_1 \omega_2 \\
- m \ell \{ a_* (s\alpha_1 - s\alpha_2) - r_0 (c\alpha_1 - c\alpha_2) - \frac{\ell}{2} (s2x_1 - s2\alpha_2) \} \omega_3 \omega_1 \\
- m \ell \{ 2r_0 (s\alpha_1 \dot{\alpha}_1 - s\alpha_2 \dot{\alpha}_2) - \ell (c2\alpha_1 \dot{\alpha}_1 - c2\alpha_2 \dot{\alpha}_2) + \ell (\dot{\alpha}_1 - \dot{\alpha}_2) \} \omega_2 \\
+ m \{ 2r_0 \ell (c\alpha_1 \dot{\alpha}_1 + c\alpha_2 \dot{\alpha}_2) + \ell^2 (s2x_1 \dot{\alpha}_1 + s2\alpha_2 \dot{\alpha}_2) \} \omega_3 = 0
\end{aligned} \tag{5.23}$$

$$\begin{aligned}
& \ell \ddot{\alpha}_1 + (\ell + s\alpha_1 - a_* c\alpha_1) \dot{\omega}_1 \\
& - (r_0 c\alpha_1 + \frac{\ell}{2} s2\alpha_1) \omega_3^2 - (a_* s\alpha_1 - \frac{\ell}{2} s2\alpha_1) \omega_2^2 \\
& - (r_0 c\alpha_1 + a_* s\alpha_1) \omega_1^2 + (a_* c\alpha_1 + r_0 s\alpha_1 - \ell c2\alpha_1) \omega_3 \omega_2 = 0
\end{aligned} \tag{5.24}$$

$$\begin{aligned}
& \ell \ddot{\alpha}_2 - (\ell + r_0 s\alpha_2 - a_* c\alpha_2) \dot{\omega}_1 \\
& - (r_0 c\alpha_2 + \frac{\ell}{2} s2\alpha_2) \omega_3^2 - (a_* s\alpha_2 - \frac{\ell}{2} s2\alpha_2) \omega_2^2 \\
& - (r_0 c\alpha_2 + a_* s\alpha_2) \omega_1^2 - (a_* c\alpha_2 + r_0 s\alpha_2 - \ell c2\alpha_2) \omega_3 \omega_2 = 0 \quad (5.25)
\end{aligned}$$

where $s\alpha_j \equiv \sin\alpha_j$ and $c\alpha_j \equiv \cos\alpha_j$

3. Numerical Results

The five nonlinear equations of motion for the hinged system are used to study the torque free motion of the system. The equations have been coded for computer simulation and the results are expected in the near future.

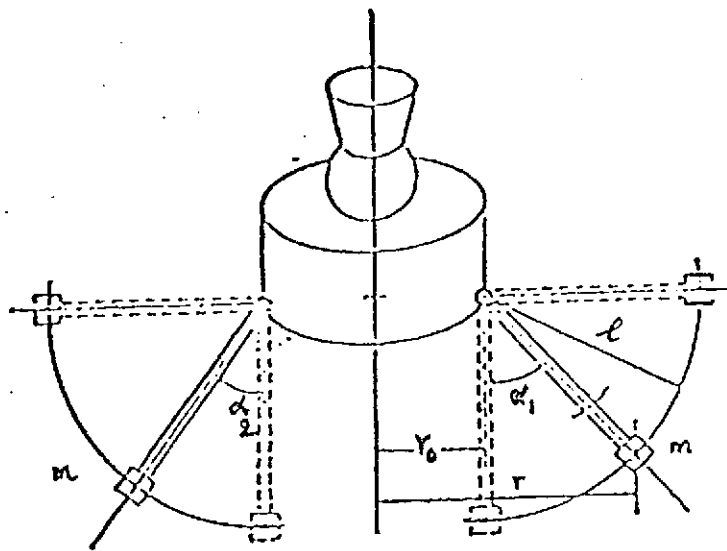


FIG. 5.1. HINGED DEPLOYMENT SYSTEM.

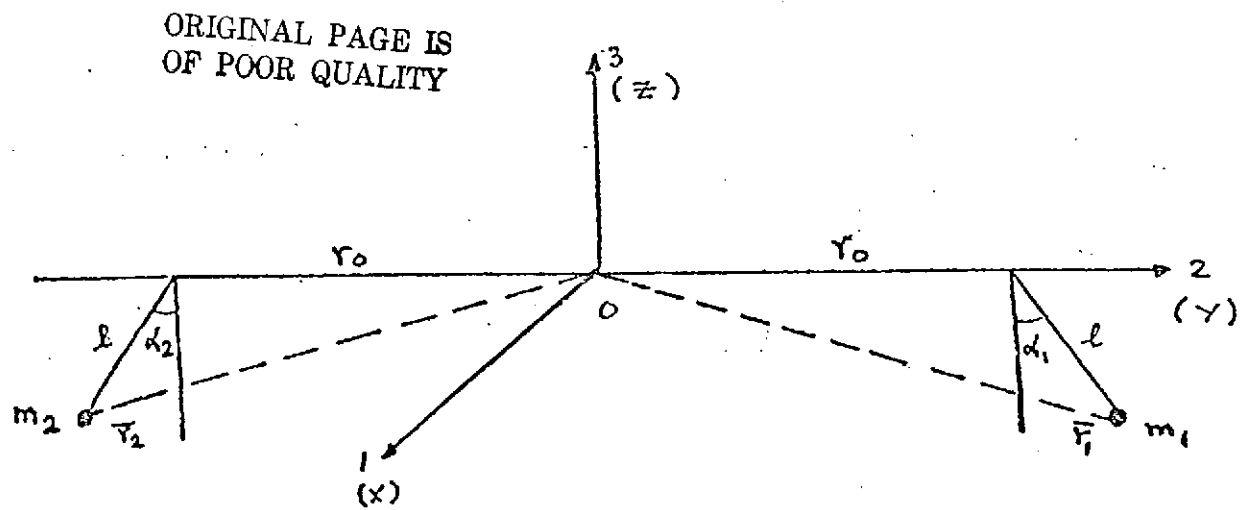
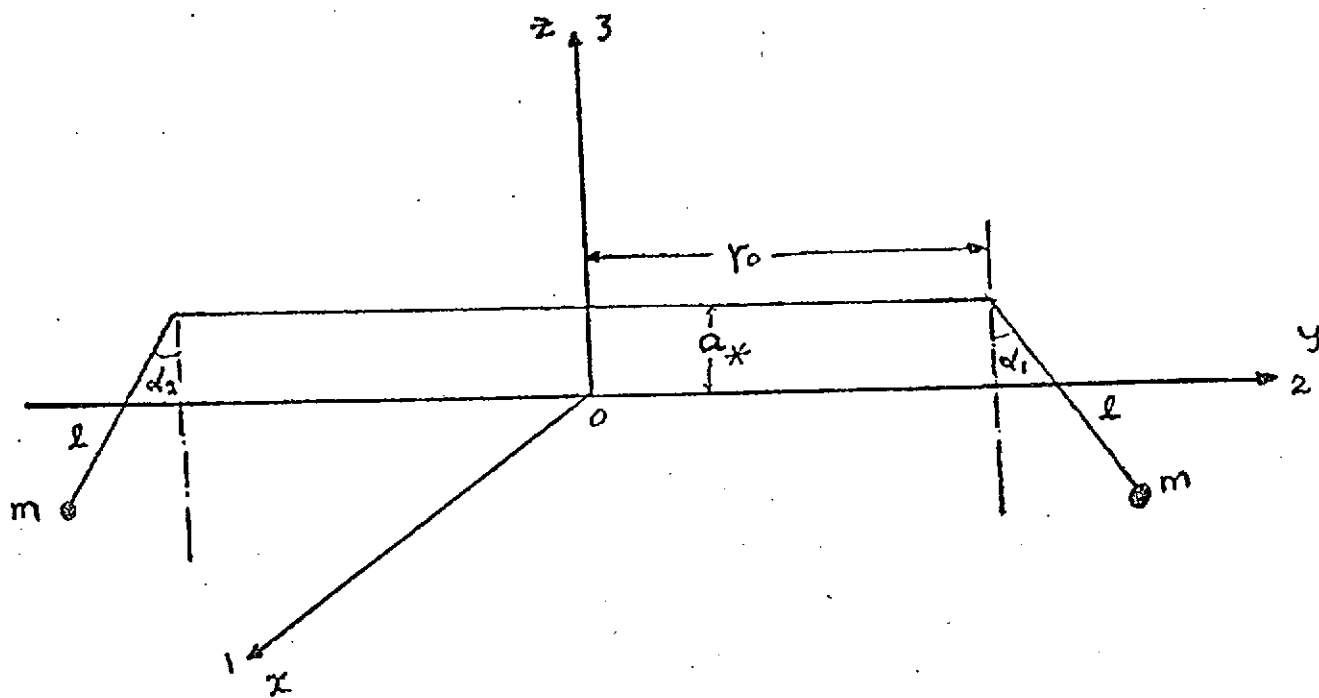


FIG. 5.2. COORDINATE SYSTEM FOR FIG. 5.1.



$$x_1 = 0$$

$$x_2 = 0$$

$$y_1 = r_0 + l \sin \alpha_1$$

$$y_2 = -(r_0 + l \sin \alpha_2)$$

$$z_1 = a_* - l \cos \alpha_1$$

$$z_2 = a_* - l \cos \alpha_2$$

FIG. 5.3. MORE GENERAL CASE OF HINGED DEPLOYMENT SYSTEM.

VI. CONCLUDING COMMENTS

As a result of the present analysis and numerical results, the following conclusions can be made:

1. For both types of telescoping systems, closed form analytical solutions for the transverse components of angular velocities as a function of time are obtained for the special case where the spacecraft hub (main part) has a nearly spherical mass distribution and where the telescoping system is assumed to originate from the hub mass center along one of the transverse axes only.

2. When the telescoping system is assumed to consist of two identical sets of two orthogonally mounted booms in a plane normal to the spin axis, the spin axis remains an axis of mass symmetry and, for this special case, the analytical solutions are identical to those obtained previously.³ For this special situation it is seen that the amplitudes of the transverse components of the angular momentum remain constant (but at an accelerating frequency) during deployment.

3. For the more general case where the hub is not spherical a series solution is obtained about $t = 0$, an ordinary point of the time dependent coefficients, in the differential equations of the rotational motion of the telescoping system. However, the radius of convergence of such a solution is limited due to the other singular points in the coefficients.

4. The approximate analytical solution for the nearly spherical hub and the series solution for the general case are compared with

numerical integration results. It is observed that the analytical solution corresponds more closely with numerical integration results when the extension rate is increased. The series solution can be used only in the initial part of the extension where the analytical solution also gives essentially the same result.

5. With fast extension rates and large end masses, the numerical study shows that the oscillatory nature of the responses of the transverse angular velocity components can be reduced rapidly.

6. As an application for spacecraft rescue and recovery, when booms are extended along all the principal axes to detumble a symmetrical spacecraft, exact closed form analytical solutions are obtained for all three angular velocities of the spacecraft.

7. The necessary conditions for asymptotic stability during the detumbling sequences can be obtained using Lyapunov's second method. The conclusions are that: (1) as time becomes extremely large (and boom lengths become infinite) it would be theoretically possible to despin a tumbling spacecraft and achieve a zero inertial angular velocity state (of course, such a situation will, in practice, not occur due to finite length booms); (2) the final spin about one of the principal axes can be achieved by extending all telescoping booms until the desired spin rate is reached and then continuing the extension of the set of booms along the nominal spin axis until the transverse components of angular velocity reach an acceptably small amplitude.

8. Numerical examination of other cases for asymmetrical hubs

also verifies the practicality of using movable appendages for the initial detumbling of randomly spinning spacecraft.

9. Simple boom extension maneuvers alone can not be used to detumble a randomly spinning spacecraft to achieve a desired final state in a time optimal manner.

10. The constraints on the telescoping system as used for detumbling are: (1) the limitations on the extension rate, size of end mass masses and the length of booms that are practicable; (2) the limitations on the rate of initiabile tumble that could be handled by the system without compromising its structural integrity.

VII. FUTURE WORK - PART II

It is proposed that this effort will be a continuation of the research accomplished during the first year (May 1974-May 1975) on the dynamics of spin stabilized spacecraft with movable appendages. Part I concentrated on the analysis of the motion of a spinning spacecraft during the deployment of two types of movable appendages - the telescoping rod type of varying length during deployment and fixed length appendages whose orientation with respect to the main hub can vary. In addition the use of these appendages to detumble a spacecraft with a random spin to achieve final states of (1) close to zero inertial angular rate and (2) a final spin rate about one of the principal axis was also considered. In the effort proposed for Part II the following will be treated: effect of energy dissipation during deployment; use of appendages to detumble spacecraft when the appendages may not be deployed along principal body axis of inertia; examination of linear optimal control theory as applied to the deployment maneuver by selecting different integrand functions in the cost functional; and an examination of the effects of first order perturbations such as due to solar pressure, gravity-gradient, and small amplitude flexibility of the appendages.

With reference to Table I, the items denoted by an asterisk were not treated during the first year, Part I. This Plan of Study has been modified slightly in accordance with technical discussions held at NASA-Langley. The proposed items for future study, as indicated

by asterisks will now be discussed.

The effect of damping during deployment can be studied by incorporating additional degrees of freedom in the mathematical model of both types of appendage systems. For example, a pendulous type of nutation damping mechanism on the main hub could be considered and the Lagrangian equations of motion for the hinged system modified directly to include generalized coordinate(s) associated with the damper motion. The Eulerian equations of motion as derived for the telescoping system would also require appropriate redevelopment since the center of the spacecraft hub would no longer be the instantaneous system center of mass. The effect of energy dissipation during a general deployment maneuver could be evaluated using numerical integration techniques. For deployment with a small nutation angle - i.e., transverse momentum components small when compared with the total momentum, approximate analytical approximations such as energy sink will be studied.

In the area of detumbling (a randomly spinning spacecraft) the use of telescoping appendages offset from the principal axes will be considered. An attempt will be made to reformulate a modified Lyapunov function, either in terms of cross products of inertia using the original hub symmetry axes system or in terms of the instantaneous principal moments of inertia. Numerical simulation of this more complicated system will be performed and results compared with those for the simpler system. In addition the use of the hinged type system in conjunction with a pair of telescoping booms along the "3" axis could be examined.

The difficulty in determining a control sequence of extension rates for different pairs of telescoping booms which would yield a time-optimal recovery of a tumbling spacecraft is seen in Section IV. The problem has been that when the equations are written in standard state form--e.g. for a case of two sets of booms parallel to the spin axis - (where symmetry about this axis is maintained during extension), the control function (two different extension rates) is non-linearly coupled with the state variables.

Instead of considering only time optimal control of a tumbling spacecraft, it was suggested at NASA-Langley that linear optimal control theory might be applied where now the integrand function in the cost functional would contain a quadratic form in the state variables plus some function of the control. After appropriate linearization of the system an attempt will be made using the matrix Riccati equation to yield solutions for boom extension rates.

A time optimal control solution for this problem can be obtained numerically using the techniques of dynamic programming (gradient techniques). This approach was recently employed by Kunciw¹³ in analyzing the optimal detumbling of the system treated in Ref. 7. A dynamic programming solution as applied to the present problem will be considered, especially if the application of linear optimal control techniques does not yield meaningful physical results.

As time permits at the end of the study, it is planned to briefly examine the effect of such perturbations as gravity-gradient torques,

solar pressure, and first order flexibility. It is hoped that this effort would establish limits on the rate of tumble that could be handled by extendible appendages without compromising their structural integrity.

It is felt that by analyzing the dynamics, control and perturbations of such types of systems with various types of appendages, a valuable insight into the dynamical behavior of more complex systems can be obtained.

TABLE I - TWO YEAR PLAN OF STUDY

THE DYNAMICS OF SPIN STABILIZED SPACECRAFT WITH MOVABLE APPENDAGES

CONTENTS

A. MOTION DURING DEPLOYMENT

Spinning spacecraft - small transverse momentum

1. Hinged Type

- development of equations of motion

2. Telescopic Type

a. End mass moving b. Uniformly distributed mass moving

- Analytical solution for spherical Hub

- Series solution for non-spherical Hub

*3. Effect of Dampers

B. USE OF APPENDAGES TO DETUMBLE SPACECRAFT

1. Telescopic Type

- derivation of kinetic energy

a. Achieve zero inertial angular rate

- Lyapunov Function - Kinetic Energy

b. Achieve spin about principal axis

- Lyapunov function - Modified kinetic energy

*2. Telescoping appendages offset from hub principal axes

*3. Appendages + "3" axis boom

C. OPTIMAL CONTROL

*1. Application of linear optimal

control theory using different performance indices

*2. Use of gradient technique

D. EFFECT OF PETURBATIONS

- *1. Gravity-gradient
- *2. Solar pressure
- *3. Flexibility with small amplitude

*Proposed for study in second year (Part II)

REFERENCES

1. Vigneron, F., "Stability of a Freely Spinning Satellite of Crossed-Dipole Configuration," CASI Trans. Vol. 3, No. 1, 1970, pp. 8-19.
2. Lang, W. and Honeycutt, G.H., "Simulation of Deployment Dynamics of Spinning Spacecraft," NASA-TN-D-4074, August 1967.
3. Hughes, P.C., "Dynamics of a Spin-Stabilized Satellite During Extension of Rigid Booms," CASI Trans. Vol. 5, No. 1, March 1972, pp. 11-14.
4. Sherman, B.C. and Graham, J.D., "Coming Motion of a Spinning Rigid Body with Slowly Varying Inertias," AIAA Journal, Vol. 4, No. 8, 1966, pp. 1467-1469.
5. Barba, P.M., Furumoto, N., and Leliakov, I.P., "Techniques for Flat-Spin Recovery of Spinning Satellites," AIAA Guidance and Control Conference, Key Biscayne, Fla., August 20-22, 1973, Paper No. 73-859.
6. Kaplan, M.H., "Techniques for Detumbling a Disabled Space Base," 24th Congress of the International Astronautical Federation, Baku, U.S.S.R., October 7-13, 1973.
7. Edwards, T.L. and Kaplan, M.H., "Automatic Spacecraft Detumbling by Internal Mass Motion," AIAA Journal, Vol. 12, No. 4, 1974, pp. 496-502.
8. Athans, M. and Falb, P.L., Optimal Control--An Introduction to the Theory and its Applications, McGraw-Hill, 1966, pp. 595-601.
9. Athans, M. Falb, P.L. and Lacoss, R.T., "Time-Fuel-and Energy-Optimal Control of Nonlinear Norm-Invariant Systems," IEEE Transactions on Automatic Control, Vol. AC-8, July 1963, pp. 196-202.
10. Sen, S. and Bainum, P.M., "Motion of a Dual-Spin Satellite During Momentum Wheel Spin-Up," Journal of Spacecraft and Rockets, Vol. 10, No. 12, Dec. 1973, pp. 760-766.
11. Puri, V. and Bainum, P.M., "Planar Librational Motion of a Gravity-Gradient Satellite During Deployment," Astronautical Research 1971, D. Reidel Publishing Co., Dordrecht, Holland, 1973, pp. 63-80.

REFERENCES

12. IBM 1130 Scientific Subroutine Package Programmer's Manual, IBM Technical Publications Department, White Plains, N.Y.; pp. 92-94.
13. Kunciw, B.G., "Optimal Detumbling of Large Manned Spacecraft Using an Internal Moving Mass," Ph.D. Thesis, Dept. of Aerospace Engrg., The Pennsylvania State University, June 1973.
14. Meirovitch, L., Methods of Analytical Dynamics, McGraw-Hill Book Co., 1970, pp. 157-160.

COMPUTER PROGRAMS

1. End Mass Moving - Numerical Integration

```

C      PROGRAM FOR GEN. EULERIAN FORMULATION
C      TELESCOPIC TYPE A. END MASS MOVING
      SUBROUTINE RGS01(T,W,DW)
      DIMENSION W(3),DW(3)
      REAL      I1,I2,I3,L1,L2,L3,I10,I20,I30,M1,M2,M3
      COMMON    I1,I2,I3,I10,I20,I30,M1,M2,M3,C1,C2,C3

```

```

C
C
C
      L1=C1*T
      L2=C2*T
      L3=C3*T
      DL1=C1
      DL2=C2
      DL3=C3
      A1=M1*L1*L1
      A2=M2*L2*L2
      A3=M3*L3*L3
      I1=I10+2.0*(A2+A3)
      I2=I20+2.0*(A3+A1)
      I3=I30+2.0*(A1+A2)
      B1=M1*L1*DL1
      B2=M2*L2*DL2
      B3=M3*L3*DL3
      D11=4.0*(B2+B3)
      D12=4.0*(B3+B1)
      D13=4.0*(B1+B2)
      DW(1)=((I2-I3)*W(2)*W(3)-D11*W(1))/I1
      DW(2)=((I3-I1)*W(3)*W(1)-D12*W(2))/I2
      DW(3)=((I1-I2)*W(1)*W(2)-D13*W(3))/I3
      RETURN
      END

```

```

      SUBROUTINE RGS02(T,W,DW,IHLF,N,P)
      DIMENSION W(3),DW(3),DUMMY(3)
      REAL      I1,I2,I3
      COMMON    I1,I2,I3
      DATA     DEG/57.2957795/
      CALL      RGS01(T,W,DUMMY)
      H1=I1*W(1)
      H2=I2*W(2)
      H3=I3*W(3)
      THETA=ATN2(SQRT(H1*H1+H2*H2),H3)*DEG
      TP=T+0.00005
      WRITE(5,1) TP,W,THETA,DW,IHLF
      RETURN

```

1 FORMAT (1X,F9.4,7F13.7,110)

C

END

EXTERNAL RGS01,RGS02

DIMENSION PARM(5),W(3),DW(3),SIZE(3),WORK(8,3)

DATA N/3/

REAL I1,I2,I3,I10,I20,I30,M1,M2,M3

COMMON I1,I2,I3,I10,I20,I30,M1,M2,M3,C1,C2,C3

C

C

C

DATA CARDS -- 10 COLUMNS FOR EACH VALUE

C

1- TMAX,INITIAL STEP, TOLERANCE

C

2- MASSES

C

3- INITIAL I'S

C

4- C'S

C

5- INITIAL W'S

C

6- TYPICAL SIZES OF W'S

C

READ(2,91) TMAX,STEP,TOL

READ(2,91) M1,M2,M3

READ(2,91) I10,I20,I30

READ(2,91) C1,C2,C3

READ(2,91) W

READ(2,91) SIZE

WRITE(5,92) TMAX,STEP,TOL

WRITE(5,93) M1,M2,M3

WRITE(5,94) I10,I20,I30

WRITE(5,95) C1,C2,C3

WRITE(5,96) W

WRITE(5,97) SIZE

WRITE(5,98)

PARM(1)=0.0

PARM(2)=TMAX

PARM(3)=STEP

CALL RKSC(LN,SIZE,DW,TOL,PARM)

CALL RKGS(PARM,W,DW,N,IHLF,RGS01,RGS02,WORK)

WRITE(5,99)IHLF

CALL EXIT

C

91 FORMAT(8F10.0)

92 FORMAT('1TMAX=',F8.2,10X,'STEP=',F8.4,10X,'TOL=',F8.6)

93 FORMAT('0MASSES',3F10.6)

94 FORMAT('0INIT I',3F10.6)

95 FORMAT('0C',3F10.6)

96 FORMAT('0W',3F10.6)

97 FORMAT('0SIZE',3F10.6)

98 FORMAT('1',T6,'T',T17,'W1',T30,'W2',T43,'W3',

2T55,'THETA',T69,'DW1',T81,'DW2',

3T94,'DW3',T108,'IHLF',/)

99 FORMAT('0IHLF=',I3)

C

END

2. End Mass Moving - Analytical Solution

```

C      ANALY. CAL. W1,W2.  A. END MASS MOVING
      REAL IO,M
      READ(2,51) W10,W20
      READ(2,51) DW10,DW20
      READ(2,51) IO,M,C
51     FORMAT(5F16.0)
      WRITE(5,52) W10,W20
      WRITE(5,53) DW10,DW20
      WRITE(5,54) IO,M,C
52     FORMAT('1W10=',F15.6,10X,'W20=',F15.6)
53     FORMAT('0DW10=',F15.6,10X,'DW20=',F15.6)
54     FORMAT('0IO=',F8.4,10X,'M=',F8.4,10X,'C=',F8.4)
      WRITE(5,5)
5     FORMAT('1',T6,'1',I17,'W1',T30,'W2')
      T=0.0
      STEP=1.0
15    P=2.0*I1*C*C
      A1=SQRT(2.0*IO/P)
      B1=SQRT(0.5*IO/P)
      C1=T/A1
      D1=ATAN(C1)
      E1=B1*D1
      F1=P/IO
      G1=1.0+F1*T*T
      W1=(W10+2.0*DW10*(T-E1))/G1
      A2=SQRT(IO/P)
      B2=IO/P
      C2=T/A2
      D2=ATAN(C2)
      E2=D2/A2
      F2=T*T+B2
      G2=T/F2
      W2=W20+0.5*DW20*B2*(G2+E2)
      WRITE(5,10) T,W1,W2
10    FORMAT(1X,F9.4,2F13.7)
      T=T+STEP
      IF(T-60.0) 15,15,20
20    CONTINUE
      CALL EXIT
      END

```

3. End Mass Moving - Series Solution

```

C   SERIES SOLN. CAL. W1,W2. A. END MASS MOVING
REAL I10,I20,I30,I1,I2,M
READ(2,21) I10,I20,I30,M,C,TF
READ(2,21) W10,W20,DW10,DW20,H0
21 FORMAT(8F10.0)
WRITE(5,51) I10,I20,I30,M,C,TF
WRITE(5,51) W10,W20,DW10,DW20,H0
51 FORMAT(8F10.6)

C   P=2.0*M*C*C

C   CONSTANTS FOR H1(T)
AD1=I10*I20*I30*I30*(I20+I30)
AE1=I20*(I30*I30*(I10+I20+I30)+2.0*I10*I30*(I20+I30))*P
AF1=I20*(I30*I30+I10*(I20+I30))*P*P
AG1=I20*(I10+I20+3.0*I30)*(P**3.0)
AH1=I20*(P**4.0)
AI1=2.0*I10*I30*I20*I20*P
AJ1=2.0*(I10+I30)*I20*I20*P*P
AK1=2.0*(I20*I20)*(P**3.0)
AL1=(I30-I10)*(I30*I30-I20*I20)*H0*H0
AM1=2.0*I30*(I30-I10)*P*H0*H0
AN1=(I30-I10)*P*P*H0*H0

C   A1=-(AL1)/(AD1*2.0*1.0)
A2=-(2.0*1.0*AE1-2.0*AI1+AL1)/(AD1*4.0*3.0)
A3=-AM1/(AD1*4.0*3.0)
A4=-(4.0*3.0*AE1-4.0*AI1+AL1)/(AD1*6.0*5.0)
A5=-(2.0*1.0*AF1-2.0*AJ1+AM1)/(AD1*6.0*5.0)
A6=-AN1/(AD1*6.0*5.0)
A7=-(6.0*5.0*AE1-6.0*AI1+AL1)/(AD1*8.0*7.0)
A8=-(4.0*3.0*AF1-4.0*AJ1+AM1)/(AD1*8.0*7.0)
A9=-(2.0*1.0*AG1-2.0*AK1+AN1)/(AD1*8.0*7.0)
A10=-(8.0*7.0*AE1-8.0*AI1+AL1)/(AD1*10.0*9.0)
A11=(6.0*5.0*AF1-6.0*AJ1+AM1)/(AD1*10.0*9.0)
A12=(4.0*3.0*AG1-4.0*AK1+AN1)/(AD1*10.0*9.0)
A13=(2.0*1.0*AH1)/(AD1*10.0*9.0)

C   B1=-(-AI1+AL1)/(AD1*3.0*2.0)
B2=-(3.0*2.0*AE1-3.0*AI1+AL1)/(AD1*5.0*4.0)
B3=-(-AJ1+AM1)/(AD1*5.0*4.0)
B4=-(5.0*4.0*AE1-5.0*AI1+AL1)/(AD1*7.0*6.0)
B5=-(3.0*2.0*AF1-3.0*AJ1+AM1)/(AD1*7.0*6.0)
B6=-(-AK1+AN1)/(AD1*7.0*6.0)
B7=-(7.0*6.0*AE1-7.0*AI1+AL1)/(AD1*8.0*7.0)

```

```

B8=-(5.0*4.0*AF1-5.0*AJ1+AM1)/(AD1*8.0*7.0)
B9=-(3.0*2.0*AG1-3.0*AK1+AN1)/(AD1*9.0*8.0)

```

C

```

WRITE(5,5)
5 FORMAT('11',T6,'T',T17,'W1',T30,'W2')
T=0.0
STEP=1.0
A10=I10*W10
A11=I10*DW10
15 AA12=A1*(T**2.0)
AA13=(A2*A1+A3)*(T**4.0)
AA14=(A4*(A2*A1+A3)+A5*A1+A6)*(T**6.0)
A151=A7*A4*(A2*A1+A3)+A7*A5*A1+A7*A6
A152=A8*(A2*A1+A3)+A9*A1
AA15=(A151+A152)*(T**8.0)
A161=A10*A7*(A4*A2*A1+A3*A4)+A10*A7*A5*A1
A162=A10*A7*A6+A11*(A4*A2*A1+A4*A3+A5*A1+A6)
A163=A12*(A2*A1+A3)+A13
AA16=(A161+A162+A163)*(T**10.0)
A17=1.0+AA12+AA13+AA14+AA15+AA16

```

C

```

B11=B1*(T**2.0)
B12=(B2*B1+B3)*(T**4.0)
B13=(B4*(B2*B1+B3)+B5*B1+B6)*(T**6.0)
B141=B7*B4*(B2*B1+B3)+B7*B5*B1+B7*B6
B142=B8*(B2*B1+B3)+B9*B1
B14=(B141+B142)*(T**8.0)
B15=1.0+B11+B12+B13+B14

```

C

```

H1=A10*A17+A11*T*B15
I1=I10+P*T*T
W1=H1/I1

```

C

C

```

CONSTANTS FOR H2(T)
AD2=I10*I20*I30*I30
AE2=(2.0*I10*I20*I30+I20*I30*I30)*P
AF2=I20*(I10+2.0*I30)*P*P
AG2=I20*(P**3.0)
AH2=2.0*(I10+I30)*I20*I30*P
AI2=2.0*(I10+3.0*I30)*I20*P*P
AJ2=4.0*I20*(P**3.0)
AK2=(I30-I10)*(I30-I20)*H0*H0
AL2=(I30-I10)*P*H0*H0

```

C

```

C1=-AK2/(AD2*2.0*1.0)
C2=-(2.0*1.0*AF2+2.0*AH2+AK2)/(AD2*4.0*3.0)
C3=-(AL2)/(AD2*4.0*3.0)
C4=-(4.0*3.0*AE2+4.0*AH2+AK2)/(AD2*6.0*5.0)
C5=-(2.0*1.0*AF2+2.0*AI2+AL2)/(AD2*6.0*5.0)
C6=-(6.0*5.0*AE2+6.0*AH2+AK2)/(AD2*8.0*7.0)
C7=-(4.0*3.0*AF2+4.0*AI2+AL2)/(AD2*8.0*7.0)
C8=-(2.0*1.0*AG2+2.0*AJ2)/(AD2*8.0*7.0)

```

C

```

D1=-(AH2+AK2)/(AD2*3.0*2.0)
D2=-(3.0*2.0*AE2+3.0*AH2+AK2)/(AD2*5.0*4.0)
D3=-(AI2+AL2)/(AD2*5.0*4.0)
D4=-(5.0*4.0*AE2+5.0*AH2+AK2)/(AD2*7.0*6.0)

```

```

D5=-(3.0*2.0*AF2+3.0*AI2+AL2)/(AD2*7.0*6.0)
D6=-AJ2/(AD2*7.0*6.0)

```

C

```

A20=I20*W20
A21=I20*DW20

```

C

```

C12=C1*(T**2.0)
C13=(C2*C1+C3)*(T**4.0)
C14=(C4*(C2*C1+C3)+C5*C1)*(T**6.0)
C151=C6*C4*(C2*C1+C3)+C6*C5*C1
C152=C7*(C2*C1+C3)+C8*C1
C15=(C151+C152)*(T**8.0)
C16=1.0+C12+C13+C14+C15

```

C

```

D11=C1*(T**2.0)
D12=(D2*D1+D3)*(T**4.0)
D13=(D4*(D2*D1+D3)+D5*D1+D6)*(T**6.0)
D14=1.0+D11+D12+D13

```

C

```

H2=A20*C16+A21*T*D14
I2=I20
W2=H2/I2

```

C

```

WRITE(5,10) T,W1,W2
10 FORMAT(1X,F9.4,2F13.7)
T=T+STEP
IF(T-TF) 15,15,20
20 CONTINUE
CALL EXIT
END

```

ORIGINAL PAGE IS
OF POOR QUALITY

4. Uniformly Distributed Mass Moving - Numerical Integration

```

C PROGRAM FOR GEN. EULERIAN FORMULATION
C UNIFORMLY DIST MASS MOVING - NUMERICAL
SUBROUTINE RGS01(T,W,DW)
  DIMENSION W(3),CW(3)
  REAL I1,I2,I3,L,LF,I10,I20,I30
  COMMON I1,I2,I3,I10,I20,I30,A,DEN,C,L,LF
  L=C*T
  AA=(2.0/3.C)*DEN*((A+L)**3-A**3)+2.C*DEN*(LF-L)*A**2
  BB=2.C*DEN*C*((A+L)**2-A**2)
  I1=I10+AA
  I2=I20
  I3=I30+AA
  C11=BB
  C12=C.C
  C13=BB
  CW(1)=((I2-I3)*W(2)*W(3)-C11*W(1))/I1
  CW(2)=((I3-I1)*W(3)*W(1)-C12*W(2))/I2
  CW(3)=((I1-I2)*W(1)*W(2)-C13*W(3))/I3
  RETURN

```

C
C

END

```

SUBROUTINE RGS02(T,W,DW,IHLF,N,P)
  DIMENSION W(3),CW(3),DUMMY(3)
  REAL I1,I2,I3
  COMMON I1,I2,I3
  DATA DEG/57.2957795/

```

C
C

```

  CALL RGS01(T,W,DUMMY)
  F1=I1*W(1)
  F2=I2*W(2)
  F3=I3*W(3)
  THETA=ATAN2(SCRAT(H1*H1+H2*F2),F3)*DEG
  TP=T+C.OCCCC5
  WRITE(5,1) TP,W,THETA,CW,IHLF
  RETURN

```

C
C

1 FORMAT (1X,F9.4,7F13.7,I10)

C

END

ORIGINAL PAGE IS
OF POOR QUALITY

```

EXTERNAL RGS01,RGS02
DIMENSION PARM(5),W(3),DW(3),SIZE(3),WCRK(8,3)
DATA N/3/
REAL 11,12,13,11C,12C,13C,L,LF
COMMON 11,12,13,11C,12C,13C,A,DEN,C,L,LF

```

```

C
C
C DATA CARDS -- 10 COLUMNS FOR EACH VALUE
C 1- TMAX,INITIAL STEP, TOLERANCE
C 2- DENSITY, A(RADIUS OF SATELLITE)
C 3- INITIAL I'S
C 4- C,LF
C 5- INITIAL W'S
C 6- TYPICAL SIZES OF W'S
READ(2,91) TMAX,STEP,TOL
READ(2,91) DEN,A
READ(2,91) 11C,12C,13C
READ(2,91) C,LF
READ(2,91) W
READ(2,91) SIZE
WRITE(5,92) TMAX,STEP,TOL
WRITE(5,93) DEN,A
WRITE(5,94) 11C,12C,13C
WRITE(5,95) C,LF
WRITE(5,96) W
WRITE(5,97) SIZE
WRITE(5,98)
PARM(1)=0.C
PARM(2)=TMAX
PARM(3)=STEP
CALL RKSC1(N,SIZE,DW,TOL,PARM)
CALL RKGS(PARM,W,DW,N,IHLF,RGS01,RGS02,WCRK)
WRITE(5,99)IHLF
CALL EXIT

```

```

C
91 FORMAT( 8F10.0 )
92 FORMAT( 11TMAX= ',F8.2,10X,'STEP= ',F8.4,10X,'TOL= ',F8.6)
93 FORMAT( 10DEN= ',F8.4,10X,'A= ',F8.4)
94 FORMAT( 10INIT 1',3F10.6)
95 FORMAT( 10C= ',F8.2,10X,'LF= ',F8.4)
96 FORMAT( 10W ',3F10.6)
97 FORMAT( 10SIZE ',3F10.6)
98 FORMAT( 11',T6,'T1',T17,'W1',T30,'W2',T43,'W3',
2T55,'THETA',T69,'CW1',T81,'CW2',
3T94,'CW3',T108,'IHLF',/)
99 FORMAT( 10IHLF= ',13)

```

END

ORIGINAL PAGE IS
OF POOR QUALITY

5. Uniformly Distributed Mass Moving - Analytical Solution

```

C      ANALY CAL. W1,W2. E.UNIFORM. DIST. MASS MOVING
      REAL IC
      READ(2,51) W1C,W2C
      READ(2,51) CW1C,CW2C
      READ(2,51) IC,C,C,TF
51  FORMAT(5F16.6)
C      DENSITY OF PCCM
      WRITE(5,52) W1C,W2C
      WRITE(5,53) CW1C,CW2C
      WRITE(5,54) IC,C,C,TF
52  FORMAT('W1C=',F15.6,10X,'W2C=',F15.6)
53  FORMAT('CW1C=',F15.6,10X,'CW2C=',F15.6)
54  FORMAT('CIC=',F8.4,10X,'C=',F8.4,10X,'C=',F8.4,10X,'TF=',F8.4)
      WRITE(5,5)
5  FORMAT('I',I6,'T',T17,'W1',W1C,'W2',W2C)
      T=C.C
      STEP=1.C
      E=((1.5*IC/C)**(1.C/3.0))/C
      WRITE(5,61)E
61  FORMAT(1X,F9.4)
15  W1=W1C/((1.C+T**3.C/E**3.0)
C      EXTRA TERMS WITH RI ARE LEFT
      B1=((E**3.C)*T)/(E**2.0+T**3.C)
      F=((P+T)**2.0)/(B**2.0-E*T+T**2.0)
      C1=(B/3.C)**ALOG(F)
      C=22.C/42.C
      C1=(2.C*T-E)/(1.732*E)
      C2=ATAN(C1)+C
      C3=(2.0*B)/1.732
      C4=C3*C2
      E1=CW2C/3.C
      W2=W2C+E1*(B1+C1+C4)
      WRITE(5,10) T,W1,W2
10  FORMAT(1X,F9.4,2F13.7)
      T=T+STEP
      IF(T-TF)15,15,20
20  CONTINUE
      CALL EXIT
      END

```

6. Detumbling--To Achieve Final Spin Along One of the Principal Axes (End Mass Moving - Numerical Integration)

```

:      EXTERNAL RGS01,RGS02
:      DIMENSION PARM(5),W(3),DW(3),SIZE(3),WORK(8,3)
:      REAL      11,12,13,110,120,130,M1,M2,M3
:      COMMON    11,12,13,110,120,130,M1,M2,M3,C1,C2,C3
:
: C
: C
: C      DATA CARDS -- 10 COLUMNS FOR EACH VALUE
: C      1- TMAX,INITIAL STEP, TOLERANCE
: C      2- MASSES
: C      3- INITIAL I'S
: C      4- C'S
: C      5- INITIAL W'S
: C      6- TYPICAL SIZES OF W'S
: C
:      CALL INOUT(2,5)
:      N= 3
:      TYPE 'RKGS JOB'
:      READ(2,91) TMAX,STEP,TOL
:      READ(2,91) M1,M2,M3
:      READ(2,91) 110,120,130
:      READ(2,91) C1,C2,C3
:      READ(2,91) W
:      READ(2,91) SIZE
:      WRITE(5,92) TMAX,STEP,TOL
:      WRITE(5,93) M1,M2,M3
:      WRITE(5,94) 110,120,130
:      WRITE(5,95) C1,C2,C3
:      WRITE(5,96) W
:      WRITE(5,97) SIZE
:      PARM(1)=0.0
:      PARM(2)=TMAX
:      PARM(3)=STEP
:      CALL RKSC(N,SIZE,DW,TOL,PARM)
:      WRITE(5,98)
:      CALL RKGS(PARM,W,DW,N,1HLF,RGS01,RGS02,WORK)
:      WRITE(5,99)1HLF
:      CALL EXIT
:
: C
: 91 FORMAT( 8F10.0 )
: 92 FORMAT( '1TMAX=',F8.2,10X,'STEP=',F8.4,10X,'TOL=',F8.6)
: 93 FORMAT('0MASSES',3F10.6)
: 94 FORMAT('0INIT I',3F10.6)
: 95 FORMAT('0C      ',3F10.6)
: 96 FORMAT('0W      ',3F10.6)
: 97 FORMAT('0SIZE   ',3F10.6)
: 98 FORMAT('1',T6,'T',T17,'W1',T30,'W2',T43,'W3',
: 2T55,'THETA',T69,'DW1',T81,'DW2',
: 3T94,'DW3',T108,'1HLF',/)
: 99 FORMAT('01HLF=',I3)
:
: C
:      END

```

```

; C   PROGRAM FOR GEN. EULERIAN FORMULATION
; C   TELESCOPIC TYPE A. END MASS MOVING DETUMBLING
;     SUBROUTINE RGS01(T,U,DW)
;       DIMENSION W(3),DW(3)
;       REAL    11,12,13,L1,L2,L3,I10,I20,I30,M1,M2,M3
;       COMMON  11,12,13,I10,I20,I30,M1,M2,M3,C1,C2,C3
; C
; C
;       IF(T.GT.2.5) GO TO 20
;       L1=C1*T
;       L2=C2*T
;       DL1=C1
;       DL2=C2
;       GO TO 30
; C
; 20  L1=C1*2.5
;       L2=C2*2.5
;       DL1=0.0
;       DL2=0.0
; 30  CONTINUE
;       L3=C3*T
;       DL3=C3
;       A1=M1*L1*L1
;       A2=M2*L2*L2
;       A3=M3*L3*L3
;       I1=I10+2.0*(A2+A3)
;       I2=I20+2.0*(A3+A1)
;       I3=I30+2.0*(A1+A2)
;       B1=M1*L1*DL1
;       B2=M2*L2*DL2
;       B3=M3*L3*DL3
;       D11=4.0*(B2+B3)
;       D12=4.0*(B3+B1)
;       D13=4.0*(B1+B2)
;       DW(1)=((I2-I3)*W(2)*W(3)-D11*W(1))/I1
;       DW(2)=((I3-I1)*W(3)*W(1)-D12*W(2))/I2
;       DW(3)=((I1-I2)*W(1)*W(2)-D13*W(3))/I3
;       RETURN
;       END
;
;     PARAMETER DEG=57.2957795
;     SUBROUTINE RGS02(T,W,DW,IHLF,N,P)
;       DIMENSION W(3),DW(3),DUMMY(3)
;       REAL    11,12,13
;       COMMON  11,12,13
; C
; C
;       CALL RGS01(T,W,DUMMY)
;       H1=11*W(1)
;       H2=12*W(2)
;       H3=13*W(3)
;       THETA=ATAN2(SQRT(H1*H1+H2*H2),H3)*DEG
;       TP=T+0.00005
;       WRITE(5,1) TP,W,THETA,DW,IHLF
;       RETURN
; 1  FORMAT (1X,F9.4,7F13.7,110)
;       END

```

7. Subroutine RKSCL

```
SUBROUTINE RKSCL(NU, UMAG, DU, TOL, P)  
  REAL UMAG(1), DU(1), P(4)
```

C
C
C

```
  N = NU  
  UNORM = 0.0  
  DO 1 I=1, N  
    UNORM = UNORM + 1.0/UMAG(I)  
1  CONTINUE  
  UNORM = 1.0/UNORM  
  DO 2 I=1, N  
    DU(I) = UNORM/UMAG(I)  
2  CONTINUE  
  P(4) = N*UNORM*TOL/15.0  
  RETURN
```

C
C

```
  END
```

8. Subroutine RKGS

	SUBROUTINE RKGS(PRMT,Y,DERY,NDIM,IHLF,FCT,OUTP,AUX)	RKGS 1
	DIMENSION Y(1),DERY(1),AUX(8,1),A(4),B(4),C(4),PRMT(5)	RKGS 101
	DO 1 I=1,NDIM	RKGS 3
1	AUX(8,1)=.06666667*DERY(1)	RKGS 4
	X=PRMT(1)	RKGS 5
	XEND=PRMT(2)	RKGS 6
	H=PRMT(3)	RKGS 7
	PRMT(5)=0.	RKGS 8
	CALL FCT(X,Y,DERY)	RKGS 9
C	ERROR TEST	RKGS 10
	IF (H*(XEND-X))38.37,2	RKGS 11
C	PREPARATIONS FOR RUNGE-KUTTA METHOD	RKGS 12
2	A(1)=.5	RKGS 13
	A(2)=.2928932	RKGS 14
	A(3)=1.787107	RKGS 15
	A(4)=.1666667	RKGS 16
	B(1)=2.	RKGS 17
	B(2)=1.	RKGS 18
	B(3)=1.	RKGS 19
	B(4)=2.	RKGS 20
	C(1)=.5	RKGS 21
	C(2)=.2928932	RKGS 22
	C(3)=1.787107	RKGS 23
	C(4)=.5	RKGS 24
C	PREPARATIONS OF FIRST RUNGE-KUTTA STEP	RKGS 25
	DO 3 I=1,NDIM	RKGS 26
	AUX(1,1)=Y(1)	RKGS 27
	AUX(2,1)=DERY(1)	RKGS 28
	AUX(3,1)=0.	RKGS 29
3	AUX(6,1)=0.	RKGS 30
	IREC=0	RKGS 31
	H=H+H	RKGS 32
	IHLF=-1	RKGS 33
	ISTEP=0	RKGS 34
	IEND=0	RKGS 35
C	START OF A RUNGE-KUTTA STEP	RKGS 36
4	IF ((X+H-XEND)*H)7,6,5	RKGS 37
5	H=XEND-X	RKGS 38
6	IEND=1	RKGS 39
C	RECORDING OF INITIAL VALUES OF THIS STEP	RKGS 40
7	CALL OUTP(X,Y,DERY,IREC,NDIM,PRMT)	RKGS 41
	IF (PRMT(5))40,8,40	RKGS 42
8	ITEST=0	RKGS 43
9	ISTEP=ISTEP+1	RKGS 44
C	START OF INNERMOST RUNGE-KUTTA LOOP	RKGS 45
	J=1	RKGS 46

10	AJ=A(J)	RKGS	47
	BJ=B(J)	RKGS	48
	CJ=C(J)	RKGS	49
	DO 11 I=1,NDIM	RKGS	50
	R1=H*DERY(I)	RKGS	51
	R2=AJ*(R1-BJ*AUX(6,I))	RKGS	52
	Y(I)=Y(I)+R2	RKGS	53
	R2=R2+R2+R2	RKGS	54
11	AUX(6,I)=AUX(6,I)+R2-CJ*R1	RKGS	55
	IF(J-4)12,15,15	RKGS	56
12	J=J+1	RKGS	57
	IF(J-3)13,14,13	RKGS	58
13	X=X+.5*H	RKGS	59
14	CALL FCT(X,Y,DERY)	RKGS	60
	GOTO 10	RKGS	61
C	END OF INNERMOST RUNGE-KUTTA LOOP	RKGS	62
C	TEST OF ACCURACY	RKGS	63
15	IF(ITEST)16,16,20	RKGS	64
C	IN CASE ITEST=0 THERE IS NO POSSIBILITY FOR TESTING OF ACCURACY	RKGS	65
16	DO 17 I=1,NDIM	RKGS	66
17	AUX(4,I)=Y(I)	RKGS	67
	ITEST=1	RKGS	68
	ISTEP=ISTEP+ISTEP-2	RKGS	69
18	IHLF=IHLF+1	RKGS	70
	X=X-H	RKGS	71
	H=.5*H	RKGS	72
	DO 19 I=1,NDIM	RKGS	73
	Y(I)=AUX(1,I)	RKGS	74
	DERY(I)=AUX(2,I)	RKGS	75
19	AUX(6,I)=AUX(3,I)	RKGS	76
	GOTO 9	RKGS	77
C	IN CASE ITEST=1 TESTING OF ACCURACY IS POSSIBLE	RKGS	78
20	IMOD=ISTEP/2	RKGS	79
	IF(ISTEP-IMOD-IMOD)21,23,21	RKGS	80
21	CALL FCT(X,Y,DERY)	RKGS	81
	DO 22 I=1,NDIM	RKGS	82
	AUX(5,I)=Y(I)	RKGS	83
22	AUX(7,I)=DERY(I)	RKGS	84
	GOTO 9	RKGS	85
C	COMPUTATION OF TEST VALUE DELT	RKGS	86
23	DELT=0.	RKGS	87
	DO 24 I=1,NDIM	RKGS	88
24	DELT=DELT+AUX(8,I)*ABS(AUX(4,I)-Y(I))	RKGS	89
	IF(DELT-PRMT(4))28,28,25	RKGS	90
C	ERROR IS TOO GREAT	RKGS	91
25	IF(IHLF-10)26,36,36	RKGS	92
26	DO 27 I=1,NDIM	RKGS	93
27	AUX(4,I)=AUX(5,I)	RKGS	94
	ISTEP=ISTEP+ISTEP-4	RKGS	95
	X=X-H	RKGS	96
	IEND=0	RKGS	97
	GOTO 18	RKGS	98
C	RESULT VALUES ARE GOOD	RKGS	99
28	CALL FCT(X,Y,DERY)	RKGS	100

DO 29 I=1,NDIM	RKGS 101
AUX(1,I)=Y(I)	RKGS 102
AUX(2,I)=DERY(I)	RKGS 103
AUX(3,I)=AUX(6,I)	RKGS 104
Y(I)=AUX(5,I)	RKGS 105
29 DERY(I)=AUX(7,I)	RKGS 106
CALL OUTP(X,H,Y,DERY,IHLF,NDIM,PRMT)	RKGS 107
IF (PRMT(5)) 40,30,40	RKGS 108
30 DO 31 I=1,NDIM	RKGS 109
Y(I)=AUX(1,I)	RKGS 110
31 DERY(I)=AUX(2,I)	RKGS 111
IREC=IHLF	RKGS 112
IF (IEND) 32,32,39	RKGS 113
C INCREMENT GETS DOUBLED	RKGS 114
32 IHLF=IHLF-1	RKGS 115
ISTEP=ISTEP/2	RKGS 116
H=H+H	RKGS 117
IF (IHLF) 4,33,33	RKGS 118
33 IMOD=ISTEP/2	RKGS 119
IF (ISTEP-IMOD-IMOD) 4,34,4	RKGS 120
34 IF (DELT-.02*PRMT(4)) 35,35,4	RKGS 121
35 IHLF=IHLF-1	RKGS 122
ISTEP=ISTEP/2	RKGS 123
H=H+H	RKGS 124
GOTO 4	RKGS 125
C RETURNS TO CALLING PROGRAM	RKGS 126
36 IHLF=11	RKGS 127
CALL FCT(X,Y,DERY)	RKGS 128
GOTO 39	RKGS 129
37 IHLF=12	RKGS 130
GOTO 39	RKGS 131
38 IHLF=13	RKGS 132
39 CALL OUTP(X,Y,DERY,IHLF,NDIM,PRMT)	RKGS 133
40 RETURN	RKGS 134
END	RKGS 135